Master Thesis

Substrate acceptance and activity of the alkane monooxygenase from *Marinobacter sp.*

Handed in by

Christine Kaiserer, BSc.

Matr. Nr.: 11722220

December 2024

Supervisors	Robert Kourist, Univ.-Prof. Dr.rer.nat.,
	Jelena Spasic, Dr.rer.nat. Dipl. biol. Mast. biol.
	Andrea Nigl, Dipl. Ing.
Institution	Graz University of Technology,
	Institute of Molecular Biotechnology

AFFIDAVIT

I declare that I have authored this thesis independently, that I have not used other than the declared sources/resources, and that I have explicitly indicated all material which has been quoted either literally or by content from the sources used. The text document uploaded to TUGRAZonline is identical to the present master's thesis.

_____

Date, Signature

Acknowledgements

First and foremost, I want to express my sincere gratitude towards Professor Kourist, who gave me the opportunity to join his research group and who provided me with solutions when any obstacles would arise. When we first met in person for an exam, I did not expect that it would go so well, that I would be offered a position as a student research assistant. Happily, I accepted the offer as I was eager to gain more experience in the laboratory and it allowed me to grow my independence and self-confidence, which helped me throughout the journey of my master thesis.

I am deeply thankful for my supervisors Jelena Spasic and Andrea Nigl, whose expertise proved invaluable during my work. Untiringly, they assisted me during seemingly endless days in the laboratory and always had an open ear for me whenever I had questions. I appreciate everything they taught me along the way and their guidance was essential in order bring this thesis into its final form.

Furthermore, I would like to thank the GC-Team for their support in case any questions on practicalities or result interpretation arose, which posed a challenge at times.

Each colleague of the Kourist group, who would always kindly offer a helping hand or honest advice if needed, made a big contribution to create a team spirit, which is key to make work more enjoyable each day.

I want to thank my parents, Hermann and Birgitte, who unconditionally supported me from the very first day and who enabled me to pursue my education in molecular biotechnology, so that I will be able to work in the field of my biggest interest. Thank you also to my little brother, Nicolai, who would never hesitate to make me laugh when I took myself too seriously.

Last but not least, I am incredibly grateful for my boyfriend, Christian, who would always be there for me with open arms, even when times were challenging, and who helped me to never forget my reason to smile.

Abstract

For a sustainable production of polymers, the controlled functionalization of simple organic precursors is a key aspect, where highly selective enzymes are envisioned to replace energy intensive chemical reactions. The transmembrane alkane monooxygenase AlkB from *P. putida* GPo1 is one promising candidate, which hydroxylates terminal methyl groups in a broad range of substrates with high selectivity for hydroxylation of the ω-position. AlkB has been reported to functionalize medium chain fatty acid methyl esters (FAMEs) with even higher rates than its natural substrate *n*-octane, which makes it especially interesting for the synthesis of bifunctional hydroxy fatty acids, as precursors of lactones and polymers. This work focuses on AlkB from *Marinobacter sp.*, a homologous monooxygenase identified in a marine metagenomic sample. AlkB from *Msp* was heterologously expressed in *E. coli* and its acceptance of FAMEs and alcohol acetates was evaluated in whole-cell biotransformation experiments. To elucidate the role of selected amino acids affecting the substrate scope of the membrane enzyme, single and double mutants of the monooxygenase were created in a rational enzyme engineering approach and compared regarding their relative activities. The active site residue F169 turned out to be a particularly interesting target for mutation, as the variant F169L led to an up to 1.8-fold improved activity towards methyl nonanoate compared to the wild type, while F169I and F169V showed higher tendencies for hydroxylation and parallel overoxidation. Likewise, with I238V the activity improved 1.7-fold compared to the wild type. A combination of both mutants F169L/I238V did however not lead to increased activities compared to the single mutants. Another outstanding variant is W60S, which was the only variant that allowed for the determination of specific hydroxylation rate towards the long chain ester dodecyl acetate. The findings of this work, provide a basis for future enzyme engineering projects and can serve as inspiration for the design of novel variants of alkane monooxygenases, optimised for the synthesis of key precursors of fine chemicals.

Zusammenfassung

Für die nachhaltige Produktion von Polymeren, ist eine kontrollierte Hydroxylierung von einfachen organischen Molekülen ein zentraler Schritt, um energieintensive chemische Reaktionen durch hochselektive Enzyme zu ersetzen, welche unter milden Reaktionsbedingungen arbeiten können. Die in der Zellmembran integrierte Alkan-Monooxygenase AlkB von *P. putida* GPo1 ist ein vielversprechender Kandidat, da es mit herausragender Selektivität die terminale Methylgruppe einer Reihe verschiedener Substrate hydroxylieren kann. In mehreren Publikationen wurde gezeigt, dass AlkB mittellange Fettsäure-Methylester sogar mit höherer Aktivität zu den terminalen Alkoholen funktionalisiert als das natürliches Substrat *n*-Octan. Dadurch wird das Enzym besonders für die Synthese von bifunktionellen Hydroxy-Fettsäuren interessant, welche als Vorläufermoleküle für Laktone und Polymere dienen können. In der vorliegenden Arbeit liegt der Fokus auf AlkB von *Marinobacter sp.,* einer homologen Monooxygenase, welche bei einer metagnomischen Analyse einer marinen Wasserprobe erstmals identifiziert wurde. AlkB von *Msp* wurde heterolog in *E. coli* exprimiert und die Umsetzung von Fettsäure-Methylestern sowie Alkoholacetaten wurde experimentell im Rahmen von Ganzzell-Biotransformationen evaluiert. Um auch den Einfluss ausgewählter Aminosäuren auf das Substratspektrum des Membranenzyms zu untersuchen, wurden durch rationales Enzym Engineering Einzel- oder Doppelmutanten der Monooxygenase hergestellt und deren relative Aktivitäten jeweils quantifiziert und zueinander in Relation gesetzt. Die Aminosäure F169 im aktiven Zentrum erwies sich als besonders interessante Position für Mutationen, denn die Variante F169L setzte Methylnonanoat mit der 1.8-fachen Aktivität um als der Wildtyp, während F169I und F169V dazu tendierten, gleichzeitig Hydroxylierungen und Überoxidationen zu katalysieren. I238V zeigte ebenfalls eine 1.7-fach verbesserte Aktivität als der Wildtyp. Durch die Kombination der Mutationen F169L/I238V konnte die Aktivität jedoch nicht über die der Einzelmutanten hinaus erhöht werden. Darüber hinaus konnte gezeigt werden, dass ausschließlich die Variante W60S in der Lage war, das langkettige Dodecylacetat mit ausreichender Aktivität zu hydroxylieren, sodass spezifische Umsetzungsraten bestimmt werden konnten. Die Ergebnisse dieser Arbeit bieten eine Grundlage für weitere Enzyme Engineering Projekte und können auch als Inspiration dienen für das Design optimierter Alkan-Monooxygenase Varianten, die in der Synthese von zentralen Vorläufermolekülen von Feinchemikalien einsetzbar sind.

Table of contents

1 Introduction

Alkanes and represent basic starting compounds for the synthesis of more complex molecules. Especially for the synthesis of organic molecules not found in nature or only scarcely available, it is desired to modify precursor molecules in a controlled way. Amino-, carboxy-, hydroxy- and keto-groups for example show high reactivity, but C-H bonds are inert and therefore targeted C-H functionalization reactions are challenging. The controlled hydroxylation of organic molecules is gaining increasing importance in the chemical industry. One application of this reaction is the synthesis of alternative biobased and biodegradable polymers to replace conventional petroleum-based ones. Both chemical and biocatalytic approaches exist for hydroxylation of hydrocarbons. Chemical routes often require metal catalysts and solvents that are toxic for the environment, while yielding low regio- and stereoselectivity. Therefore, enzymes have gained recognition for their outstanding selectivity and their potential for industrial applications.[1] As they are also well adapted to convert substrates from natural sources, they represent an interesting alternative to petrochemical synthesis and can help to drive the chemical industry toward a more sustainable and circular economy.

Monooxygenases belong to a sub-group (EC 1.13.x.x. and EC 1.14.x.x.) within the class of oxidoreductases and they catalyse the cleavage of molecular oxygen to integrate one oxygen atom into their organic substrate, while reducing the other oxygen atom to water.[2] In nature there can be found a vast diversity of oxygenases and based on their cofactor requirements in the active site they are further categorized into cofactor-free-, haem CYP450-, flavin-, non-haem iron-, copper- or multicenter oxygenases.[3] In general, haem-dependent CYP450 monooxygenases are the most studied enzymes for hydroxylation reactions also on larger scale.[2,4] However, they frequently prefer long chain alkanes[5] or tend to hydroxylate sub-terminal positions in linear substrates with low regioselectivity.[6] The regioselectivity of selected CYP450 enzymes could be shifted through enzyme engineering, but the hydroxylation of off-target positions could not be avoided completely.[7,8,9]

As an alternative biocatalyst the non-haem iron dependent monooxygenase AlkB from *Pseudomonas putida* (*Pp*) GPo1 gained interest. It is one of the most well studied monooxygenases of its kind, as it catalyses terminal hydroxylation with an outstanding regioselectivity[10] and was successfully expressed in *E. coli* as a heterologous host.[11] AlkB accepts a broad scope of different substrates including linear, branched and circular alkanes as well as substituted aromatics and medium chain esters.[12,5,13,14] For the synthesis of platform chemicals the (bi)functionalisation of naturally abundant alkanes or fatty acids are of great interest as they represent reactive precursors for the production of biofuels, lactones or polymers.[13,15,16,5] For their biocatalytic production, AlkB was the subject of engineering[8,14] and scale-up projects[17,18,19], but its large-scale applications are still limited. However, thousands of other annotated homologs of *Pp* AlkB exist of which the biocatalytic potential is still unexplored.[20]

1.1 The alkane oxidation system of *Pseudomonas putida*

In 1940, a new bacterial species of *Pseudomonas* was described. It was found to be the predominant microorganism thriving in water-oil emulsions used in the cutting industry and causing their spoilage. Referring to its ability to use the hydrocarbons in mineral oil as sole energy source, the bacterium was initially named "*Pseudomonas oleovorans*"[21], nowadays it is known as *Pseudomonas putida* GPo1 (*Pp* Gpo1).[22]

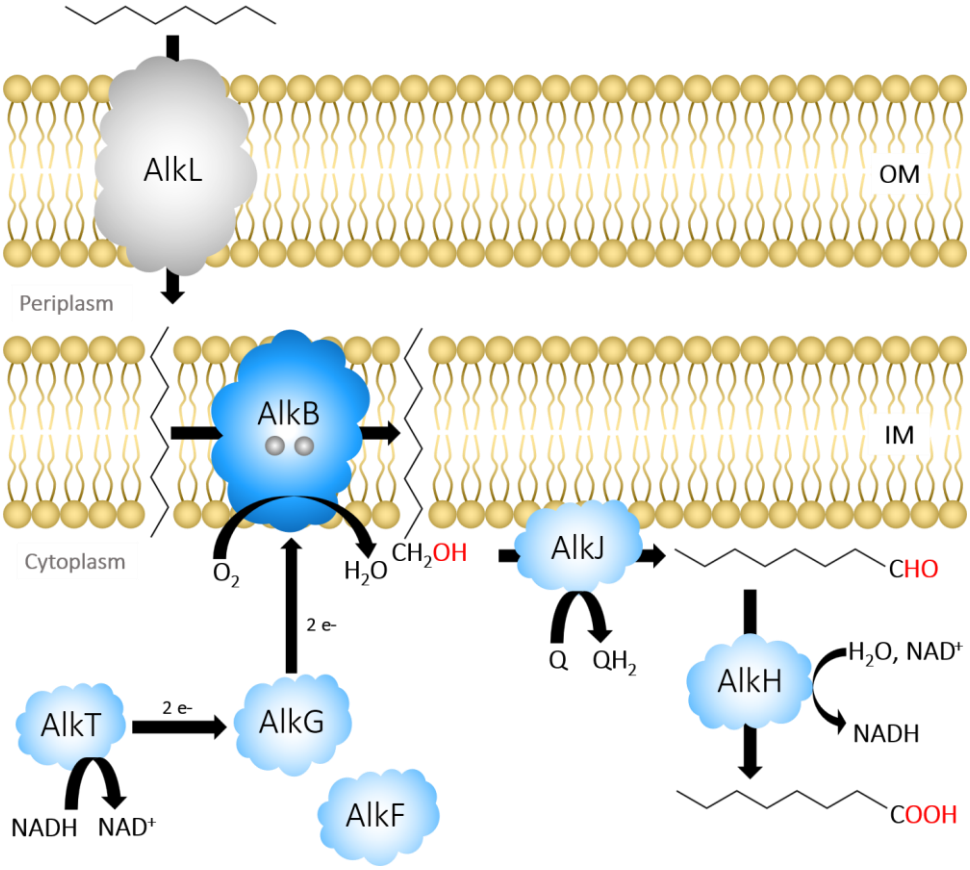

Figure 1 - Alkane degradation pathway catalysed by the enzymes AlkBFGHJKL_T in P. putida (adapted from Van Beilen 2001[22]).

Later it was shown that the preferred substrate for growth of *P. putida* was *n*-octane, but also alkanes ranging from C_5-C_{13} were found to support the growth.[23] The genes required for metabolizing alkanes are encoded on an extrachromosomal plasmid[24], clustered into two gene loci coding for soluble and membrane-bound proteins of the alkane hydroxylase pathway (Figure 1). One operon harbours the coding sequences for seven proteins, of which AlkB, AlkF, AlkG, AlkH, AlkJ and AlkK are involved in alkane metabolism[25,26] and *alkL* codes for an outer membrane protein.[27] Expression of *alkBFGHJKL* is under the regulatory control of the second operon, strictly required for expression of the previous.[11] It comprises the gene sequences for the rubredoxin reductase AlkT and the regulatory protein AlkS, which is involved in inducer binding and transcription activation.[28] Together, these enzymes constitute a multi-enzyme system for the degradation of hydrocarbons. In the presence of certain alkanes, alkanols or other organic inducers[29], AlkS upregulates expression of the AlkBFGHJKL enzymes.[30] At the

initial step, the rubredoxin reductase AlkT transfers two electrons from NADH to the rubredoxin AlkG (and AlkF) which then in turn reduces the iron atoms in the active site of AlkB.[31,23,32] In its reduced state, AlkB splits molecular oxygen, reducing one oxygen atom to water, and inserts the other one into its substrates, leading to their terminal hydroxylation.[23] The alcohol group can be further oxidized to an aldehyde by the alcohol dehydrogenase AlkJ[33], while the aldehyde dehydrogenase AlkH[26] oxidizes the aldehyde to the corresponding fatty acid. However, these oxidations can be catalysed by AlkB as well, as it was found to be capable of over-oxidising its alcohol product. Thereby AlkB itself can further convert the alcohol to the corresponding aldehyde and fatty acid.[34] Finally, the Acyl-CoA synthetase AlkK can functionalize the fatty acid to its corresponding CoA derivative, which enters the β-oxidation pathway.[27] A second rubredoxin is encoded by *alkF*, which seems to be partly a product of gene duplication from *alkG*.[26] However, it is assumed to be inactive as it was not found to be required for alkane utilization or any other activity, so far.[26,35] The outer membrane protein AlkL was shown to facilitate the uptake of hydrophobic substrates and seems to be essential for import of medium chain alkanes (C_{12}-C_{16}).[34]

1.2 Structure and mechanism of AlkB

Due to the challenges associated with the structure determination of integral membrane proteins, the exact structure of AlkB and the key residues involved in catalysis were not known for a long time. In the 1970s, cell lysis and fractionation experiments by Benson et al. indicated that the hydroxylase and alcohol dehydrogenase activities were coming from enzymes connected to or embedded into the lipid bilayer of the cytoplasmic membrane.[36,37] Later, AlkB was identified as a single polypeptide chain of 41 kDa.[25] Conducting protein-fusion experiments, Van Beilen et al. provided a general idea of the overall topology of the enzyme, comprising eight hydrophobic segments, six of which form membrane-spanning alpha helices. Other parts of the enzyme were found to reach into the cytosol, mostly the C-terminal domain, a short stretch of the N-terminus and two loops (Figure 2).[38] Further spectroscopy studies shed light on the architecture of the active site, which harbours two iron atoms without being bound to a haem molecule as in CYP450 enzymes. Instead, a "nitrogen-rich" center was identified, containing several histidine residues.[39] These were found to be part of four sequence motifs (HELGH – HNKGHH – NYIEH – HSDHH) that contain nine histidine residues which are widely conserved in related alkane monooxygenases.[40,41,42,43] Alanine-scanning studies on a related fatty acid desaturase, containing three of these sequence motifs, revealed that at least eight of these histidine residues are also required for catalytic activity.[40] This was supported by recent cryo-EM structure elucidation of a related homolog from *Fontimonas thermophila* (*Ft* AlkB),

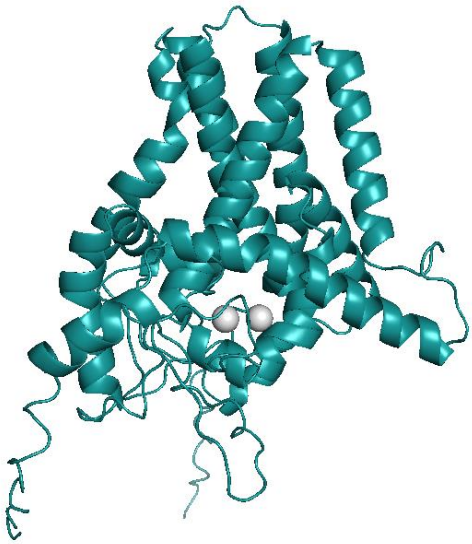

Figure 2 – AlphaFold 2 genereated model of the 3D structure of Pp GPo1 AlkB with two iron atoms (depicted in grey) in the active site.

in which nine conserved histidine residues were identified, five of which coordinate iron one, while the second iron is coordinated by four histidine plus one glutamate residue.[41,43]

In a study on the 2D-structure elucidation revealed that AlkB forms trimers when isolated with weak detergents and reconstituted in a lipid bilayer. When the enzyme assembly of individual monomers was perturbed, the activity was lost, which suggests that the monooxygenase might require oligomerisation for its functional state.[44] The same authors then also proposed a 3D-model of the membrane-spanning part of the enzyme, based on computational *ab initio* modelling. According to the model, the six transmembrane helices form a hydrophobic cavity from the transmembrane region opening towards the cytosol, thus, predicting that the active site faces the cytoplasmatic side. This was also supported by a suicide inhibitor experiment with 1-octyne, that led to the covalent binding of nucleophilic residues, and all of them were located on the cytoplasmatic side. Also the N-terminus and a C-terminal loop are on the cytoplasmatic side were hypothesized to form a channel for substrate entrance or exit.[45]

More recently, two groups reported two 3D cryo-EM structures of related alkane monooxygenases from *Ft* AlkB, one of them having a sequence similarity of 62 % compared to *Pp* AlkB. Their results also indicate that the six transmembrane helices are arranged in a slightly cone-like shape, opening towards the cytosol. Inside there is a hydrophobic tunnel that leads from the membrane-embedded portion and down to the active site located within the part that extends into the cytosol. The location of the iron centre at the very end of the substrate tunnel and the proper positioning of the substrates' terminal methyl group just next to the two irons explains the high selectivity for terminal oxidations.[41,43]

However, they found that the hydrophobic tunnel is mainly formed by transmembrane helices 2, -4 and -6. Among those three, helix 2 seemed to be more loosely arranged, forming a vertical gap of the tunnel, which is blocked by two horizontal helices. This arrangement was hypothesised to allow controlled passage of substrates or products between the lipid bilayer and the enzyme´s hydrophobic cavity.[41] Even though the structure was determined from a homolog enzyme, this interpretation is in contrast to the previous results mentioned above by Alonso et al., rather indicating substrate entrance from the cytosol.[45] Therefore, the exact mechanisms of substrate entry and product release remain to be elucidated. It could be hypothesised though, that there exist two routes, where hydrophobic substrates enter from the lipid bilayer and the hydroxylated products are released into the cytosol.

1.2.1 Reaction mechanism

As a non-haem[46], di-iron monooxygenase, AlkB harbours two iron atoms in its active site, that are coordinated by nine conserved histidine residues.[40,41,42] This feature makes AlkB unique compared to other alkane hydroxylases, which harbour carboxylate groups in the active site to coordinate the iron cluster.[41] This also raised the question, if AlkB catalyses the reaction by a different mechanism. Early investigations of the reaction mechanism of AlkB suggested that the hydroxylation occurs via the oxygen-rebound mechanism.[10,47] First, the two iron atoms are reduced by a pair of electrons. Binding of molecular oxygen to the iron cluster, then leads to heterolytic cleavage of the O_2 molecule. One

oxygen atom is released as H_2O, while the other one forms a reactive Fe=O species. This allows to abstract one hydrogen atom from the substrate, forming one iron-bound hydroxy radical and one radical of the substrate. In the final step, the hydroxy radical attacks the substrate, yielding the hydroxylated product alcohol, which is then released.[10,48]

The most recent cryo-EM structure determination of the homolog *Ft* AlkB unexpectedly revealed that, in contrast to other known alkane monooxygenases, the iron atoms in the active site are further apart (around 5.4 instead of 3 Å). Also, they do not coordinate a bridging ligand, which could hint at a different reaction mechanism. The authors suggested distinct functions for each iron atom, with atom 1 binding H_2O and atom 2 binding O_2 and proposed a catalytic mechanism. From atom 1, electrons would be transferred via proton-coupled electron transfer to atom 2, which causes O_2 cleavage and the release of one oxygen as water. The other one stays bound as Fe(V)=O being involved in catalysis. In the presence of the substrate, it donates one hydrogen to Fe=O on atom 1, forming Fe-OH and the substrate radical. The hydroxyl-group is then introduced to the substrate, leading to the hydroxylated product. However, they also highlight that other mechanisms are possible.[41]

1.2.2 Substrate scope

Among the group of alkane hydroxylases that generally convert substrates with C_5-C_{16}, most members prefer substrates longer than C_{10}, but AlkB represents one of a few that oxidises substrates even in lower range including C_5-C_{12}.[49] The substrate specificity is primarily determined by AlkB, while the enzymes further downstream the pathway were shown to be replaceable by others.[36] Regarding the shape and dimensions of the hydrophobic substrate channel, AlkB is well adapted for accommodating linear alkanes ideally with a length of around eight carbon atoms. That is also reflected in the activity maxima observed with *n*-octane and -nonane in comparison with other linear alkanes, but substrates in the range of C_5-C_{16} were found to be oxidised too.[12,50,34] For the conversion of longer substrates C_{12}-C_{16} in whole-cell biotransformations, the outer membrane protein AlkL is increasingly important to ensure substrate availability in the cell.[34] Unsaturated hydrocarbons are another type of substrate that were demonstrated to be oxidised by AlkB. Terminal double bonds in unsaturated alkanes of e.g. 1-octene or 1,7-octadiene are oxidised to the corresponding epoxides in a stereoselective way, which is another feature that makes AlkB a promising candidate for fine chemical production.[50]

Despite the structural complementarity of the substrate tunnel to linear substrates, AlkB was shown to be sufficiently flexible to also accept more bulky substrates.[12] In whole-cell and *in vitro* assays it was demonstrated that AlkB can hydroxylate fatty acids[31], fatty acid esters[13], branched- and small alicyclic alkanes, and substituted benzenes to the respective alcohols.[12] Depending on the substrate, mostly no or neglectable oxidation of non-terminal positions was found.[12,8,51]

One of the natural substrates of *Pp* AlkB, *n*-octane, is converted with an initial rate of up to 30-65 U g_{CDW}^{-1}.[12,52] Interestingly, it was reported that the non-natural substrate methyl nonanoate can be oxidised by the *alkBGT* system at even higher rates ranging from 84-104 U g_{CDW}^{-1} [13,51], hinting that

esters could be a promising substrate for biocatalytic conversions on larger scale. Other methyl esters with alkyl chains between C_5-C_{12} were tested as well, however, substrates with either longer or shorter chain lengths relative to methyl nonanoate led to lower activities.[13] Van Nuland and co-workers reported comparable rates for the terminal hydroxylation of esters from C_6-C_{10} acids and C_2-C_4 alkyl chains, with butyl hexanoate yielding the highest rate of around 82 U g_{CDW}^{-1}.[51] Also, they reported the selective terminal oxidation of acetate esters of fatty alcohols.[5]

Taken together, the broad substrate scope of AlkB offers a valuable basis for further development of biocatalytic synthesis reactions. Nevertheless, the preference for medium chain lengths still poses a limitation. Therefore, the natural substrate scope of AlkB was targeted by several engineering projects, which showed successful tuning of its acceptance towards substrates of different lengths.[8,14] It is believed, that the size of the hydrophobic residues in the substrate tunnel is the main factor decisive for the substrate specificity regarding chain length[41], which will be discussed in section 1.4.

1.3 A homolog monooxygenase from *Marinobacter sp.*

Apart from *P. putida* many more bacterial species with the ability to metabolize hydrocarbons were discovered in all possible habitats, including soil, surface and deep sea water.[53–56] The increasing pollution through anthropogenic activities worldwide, has raised concerns about the impact on the environment, which motivated the examination of affected ecosystems. Metagenomic analyses found genes encoding hydrocarbon-degrading enzymes naturally found in both uncontaminated as well as contaminated areas, although the abundance of such genes or species is significantly higher in sites contaminated with petroleum-based [56,57]

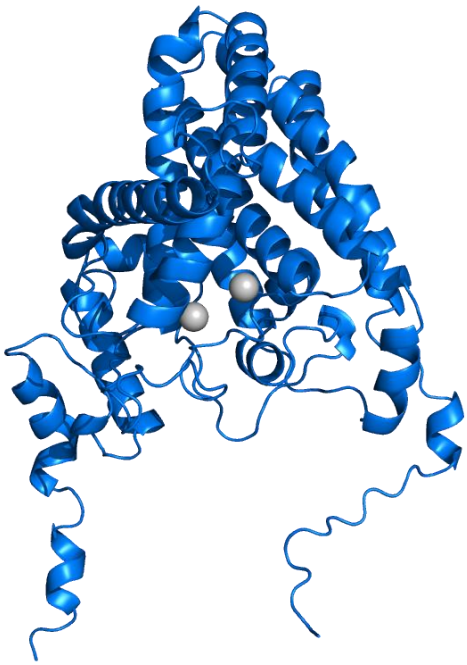

Figure 3 – AlphaFold generated model of the 3D structure of Msp AlkB with two iron atoms in the active site (depicted in grey).

Some of the most predominant bacteria in polluted sea water and able to degrade and grow on alkanes as single carbon source belong to the genus of *Marinobacter*.[58] The first member of this genus was *Marinobacter hydrocarbonoclasticus,* described by Gauthier et al., who reported growth of this bacterium on linear C_{12}-C_{20} alkanes.[59] Later on, other species were isolated and their hydrocarbon degrading ability was shown either by growth experiments[58,60] and/or supported by sequencing of genomic DNA of plankton in marine water samples.[61] Through genetic analysis and comparison with genomic databases, it was discovered that several species of *Marinobacter* contain genes homologous to *Pp* AlkB[49,61], as well as accessory proteins for electron transfer, similar to the system in *P. putida*.[62] As mentioned previously, most homologues of *Pp* AlkB, that were heterologously

expressed and tested in growth experiments, show a preference for ≥ C_{10} substrates.[60] This finding is also reflected in the inability of many bacteria to grow on ≤ C_8 n-alkanes at all.[63] One exception is *M. hydrocarbonoclasticus* strain NI9, which showed higher growth rates on n-alkanes with C_6-C_8, compared to ≥ C_8 n-alkanes and it was reported to harbour two or more genes encoding AlkB homologues.[64,65] Inspired by this finding, our group also identified an alkane-1-monooxygenase from a *Marinobacter sp.* (*Msp*) (Figure 3) which has a sequence identity of 78 % compared to *Pp* AlkB and shares the four characteristic histidine motifs (Figure 4). The sequence similarity and conservation of the essential histidine sequence motifs in both *Pp* AlkB and *Msp* AlkB, indicate their evolutionary relationship. The parent species of the enzyme is, however, not known exactly as the protein sequence was derived from a metagenomic sample.

```
Pp AlkB   -----MLEKHRVLDSAPEYVDKKKYLWILSTLWPATPMIGIWLANETGWGIFYGLVLLVW   55
Msp AlkB  MSENVLTESLQRDPGAENYVDRKRHLWILSVLWPATPLIGLYLVAQTGWSIWYGLVLILW   60

Pp AlkB   YGALPLLDAMFGEDFNNPPEEVVPKLEKERYYRVLTYLTVPMHYAALIVSAWWVGTQPMS   115
Msp AlkB  YGAVPLIDAMFGEDFSNPPESAVPRLEQDRYYRVLTYLTVPIHYAALIVSAWWVSTQPMS   120

Pp AlkB   WLEIGALALSLGIVNGLALNTGHELGHKKETFDRWMAKIVLAVVGYGHFFIEHNKGHHRD   175
Msp AlkB  VFEFLALALSLGIVNGLALNTGHELGHKKETFDRWMAKLVLAVVGYGHFFIEHNKGHHRD   180

Pp AlkB   VATPMDPATSRMGESIYKFSIREIPGAFIRAWGLEEQRLSRRGQSVWSFDNEILQPMIIT   235
Msp AlkB  VATPMDPATSRMGESIYSFSLREIPGAFKRAWDLEEQRLSRCGKSVWSLENEVLQPMILT   240

Pp AlkB   VILYAVLLALFGPKMLVFLPIQMAFGWWQLTSANYIEHYGLLRQKMEDGRYEHQKPHHSW   295
Msp AlkB  AVLYAGLLAFFGPLMLIFLPIQMAFGWWQLTSANYIEHYGLLREKMSDGRYERQQPHHSW   300

Pp AlkB   NSNHIVSNLVLFHLQRHSDHHAHPTRSYQSLRDFPGLPALPTGYPGAFLMAMIPQWFRSV   355
Msp AlkB  NSNHIMSNLILFHLQRHSDHHAHPTRSYQSLRDFKDLPSLPSGYPGMFLAAMFPSWFRSI   360

Pp AlkB   MDPKVVDWAGGDLNKIQIDDSMRETYLKKFGTSSAGHSSSTSAVAS               401
Msp AlkB  MDHRVLDWAKGDLDKIQIQPGKREFYVRKFGGTDSESVDTAASK--               404
```

Figure 4 – Sequence alignment of Pp GPo1 AlkB (GenBank Accession: CAB54050.1) and Msp AlkB (GenBank Accession: MAB50652.1). The four conserved sequence motifs are highlighted in light grey, and the nine conserved histidine residues are highlighted in dark grey. The four positions targeted by single site mutagenesis are highlighted in blue and bold.

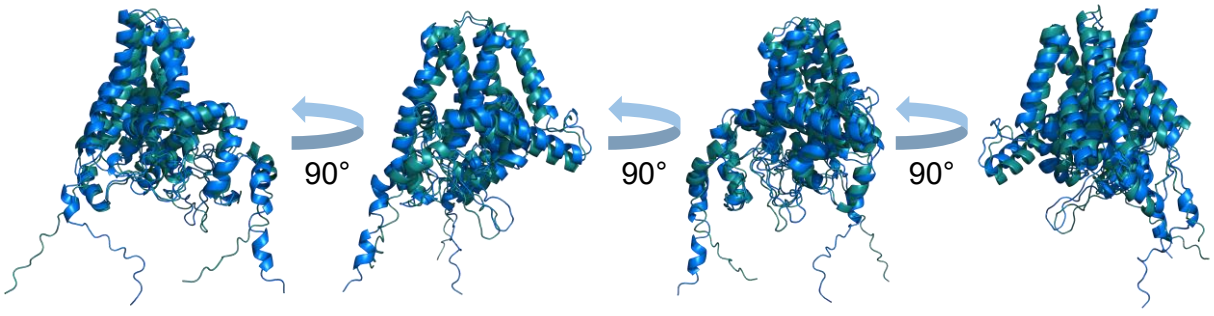

Figure 5 – Structural comparison of the overlapped protein fold of Pp AlkB (green) and Msp AlkB (blue, shown from four angles.

While both enzymes share a clear structural similarity (Figure 5), models of *Msp* AlkB predicted by AlphaFold 2 show a rather loose fold (Figure 6). This raised the question of whether its substrate scope is more flexible than in *Pp* AlkB. As published recently, it was demonstrated that the wild type of *Msp*

AlkB showed two times higher activity towards *n*-octane and isoprenyl acetate. Furthermore, it was used and engineered successfully for the terminal hydroxylation of isoprenyl acetate, which is only 6 carbon atoms in length.[66] So far, this was the first report on a *Pp* AlkB homolog from *Marinobacter* that was studied in detail on a biocatalytic level. To learn more about the substrate scope of this monooxygenase, this work focused on the characterisation of *Msp* AlkB regarding its substrate acceptance of methyl and acetate esters with alkyl moieties of C_5, C_9 and C_{12} in length. Moreover, the evaluation of selected single site mutants of *Msp* AlkB provides a better understanding of the role of these residues in determining substrate specificity and activity, even across homologs.

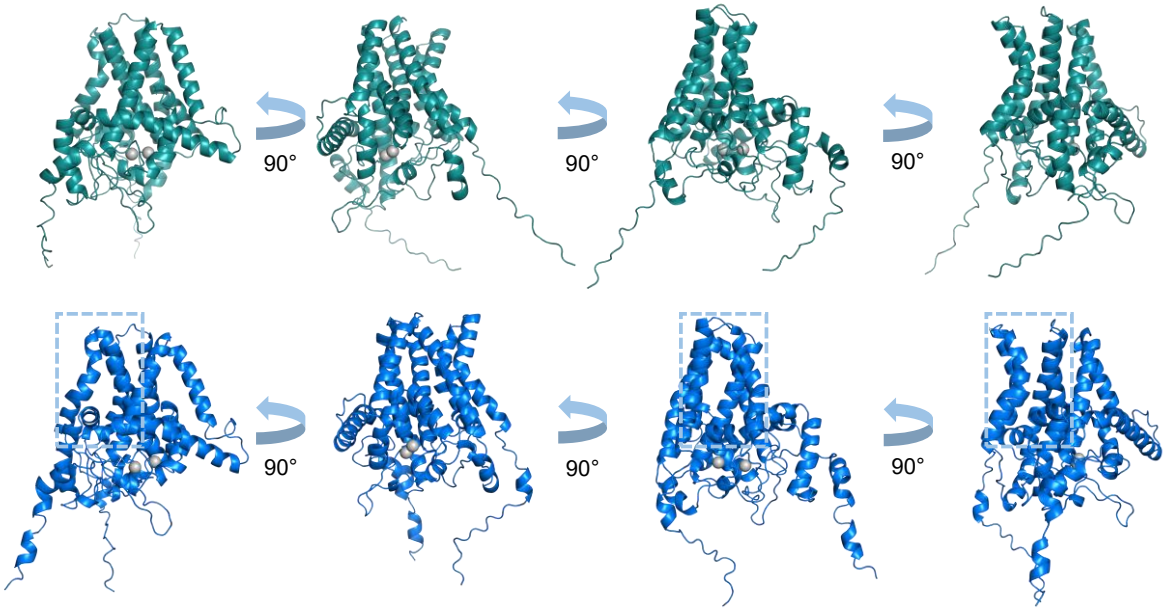

Figure 6 – Structural comparison of the protein fold of Pp AlkB (green) and Msp AlkB (blue), shown from four angles. The helices forming the hypothesized hydrophobic substrate binding pocket in Msp AlkB are marked by a light blue rectangle. Comparing this domain with the Pp AlkB shows that the same helices are more loosely arranged in Msp AlkB.

1.4 Single site mutations

In several publications the modification of substrate specificities and conversion rates towards selected substrates in *Pp* AlkB was reported.[8,66,14] As described in a section 1.2, many of the hydrophobic residues in the substrate channel were found to be decisive for substrate scope. For example, the mutation of residue W55 to smaller residues like serine or cysteine was identified by a growth selection assay. It allowed to exceed the limit of C_{13} substrates so that C_{14} and C_{16} alkanes could be oxidised.[14,8] According to structural studies, this residue is located in the middle of the substrate tunnel and might be involved in stabilizing the opposite end of the substrate, but also poses a steric hindrance for substrates longer than C_{11}.[45,41] In a similar experiment, the mutation L132V led to a shift in the preference towards shorter substrates like butane, while V129M and I233V improved the overall efficiency indicated by increased growth rates.[8] The authors located the residue I233 in helix 6 close to the periplasm (based on the structure proposed by van Beilen[14]), while Alonso et al. reported that the same residue belongs to those lining the hydrophobic cavity.[45] In the models of *Pp* AlkB and *Msp* AlkB that were generated by AlphaFold 2 (Figure 7 and Figure 8), I233 faces outward towards the lipid bilayer. These differences

in the proposed positioning of I233 residue highlight that there are open questions regarding the structure of membrane-bound enzymes. This makes interpretations difficult and the function of position 233 is still not known.

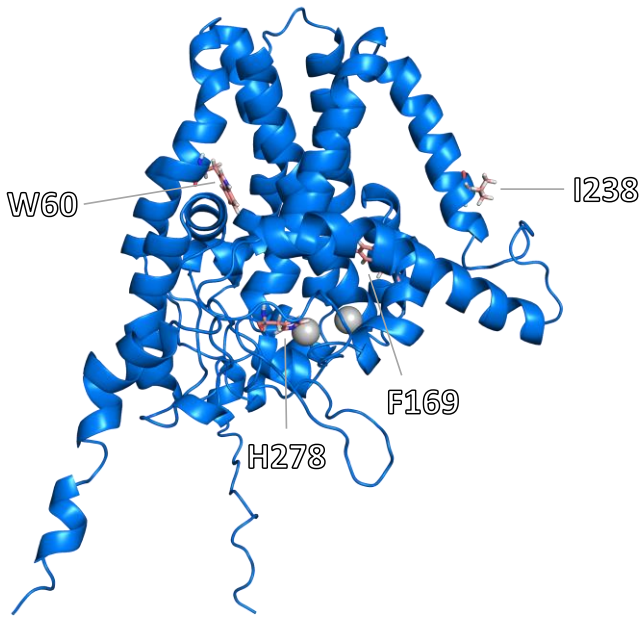

Figure 7 – AlphaFold 2 generated structure of Msp AlkB with the wild-type residues targeted for single site mutagenesis in this work are indicated as sticks in pink. The identity of the amino acids and their position in the WT sequence is indicated.

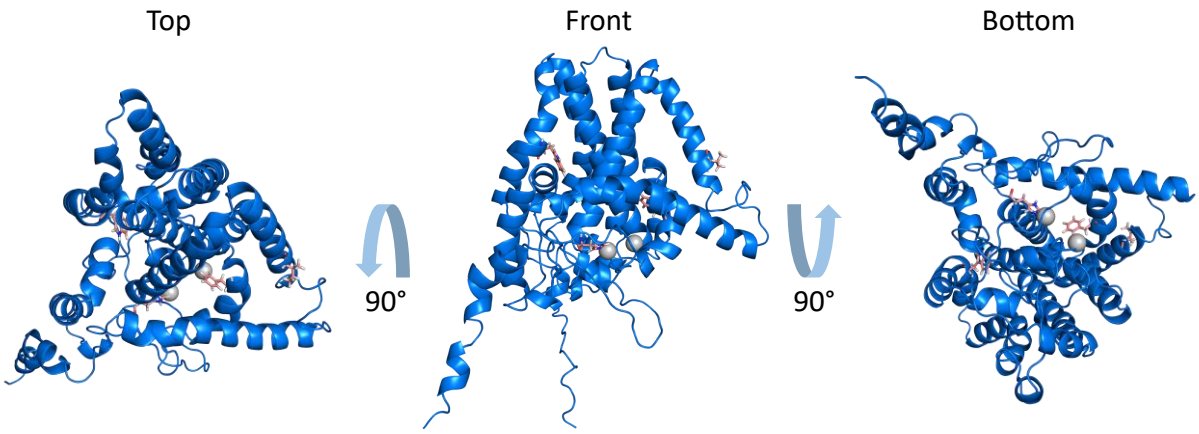

Figure 8 – 3D Structure of Msp AlkB from three different angles. The front view shows the approximate orientation of the enzyme within the inner membrane, with the C- and N-termini facing the cytosol and the loops facing the periplasm. The amino acids mutated for this work are indicated as pink sticks.

The residues V129, L132 and T136 are suspected to be involved in enzyme-substrate interaction and the mutation T136A might lead to increased activity in *Pp* AlkB.[67] The position H273 is known to be

one of the essential histidine residues coordinating the iron atoms in the active site, required for catalysis.[45] An exchange to an alanine renders the enzyme inactive.[14]

In an enzyme engineering project of our group new targets for improvement in *Pp*- and *Msp* AlkB were identified by modelling and docking experiments with isoprenyl acetate (by Veronica Delsoglio, working group Oberdorfer, TU Graz). The results suggested an amino acid exchange of the active site residue F164 (in *Pp* AlkB) with leucine. The improved activity of the mutation F164L towards isoprenyl acetate was proven by findings of our group as reported by Nigl et al., in a recent pre-print.[66] Interestingly, the exchange of F164 to similar amino acids isoleucine and valine did not lead to increased activities. In the docking studies of *n*-octane in *Msp* AlkB (by Veronica Delsoglio), also G136M, G136V and I204L were identified as possible mutations for a more stable protein-substrate interaction. To complement the modelling and support the choice of mutations, 3DM analyses were carried out as well. 3DM is an online meta-database that can extract various types of data available from other databases. It also creates a three-dimensional multiple sequence alignments of all known sequences and structures of a specific protein class, whereof valuable information on the conservation of specific structures, sequences, motifs or single residues can be derived.[68] In accordance with the mutation in position I233V in *Pp* AlkB reported in literature[8], the corresponding site in *Msp* AlkB showed to be frequently occupied by an alanine instead of isoleucine, suggesting I238A as a possible substitution (3DM results see Figure 27, Appendix).

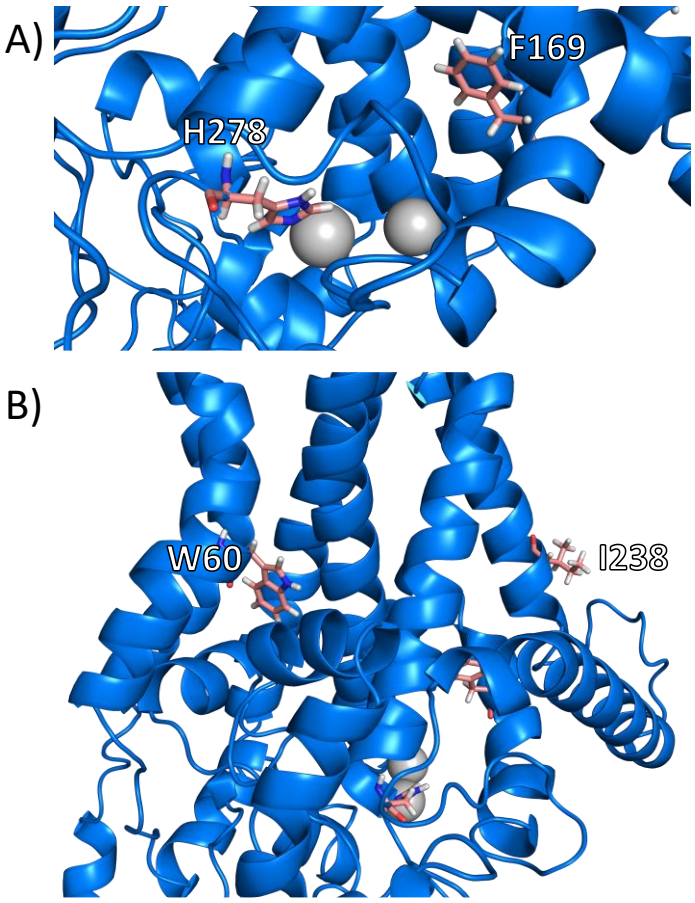

Figure 9 – AlphaFold Structure of Msp AlkB. Closer view of the positions of the wild type residues that were targeted for single site mutagenesis (highlighted in pink) in the active site (A) and in the periphery (B). The identity of the amino acids and their position in the primary sequence is indicated.

For this work, the mutations known from analyses or reports on *Pp GPo1* AlkB were introduced into *Msp* AlkB in the corresponding positions being I238V, W60S, H278A, F169L, F169I, F169V (Figure 9). For follow-up experiments, five more single site mutants were prepared which are G136M, G136V, I204L, I238A, and I238F.

1.5 Substrates – Fatty acid methyl esters and alkyl acetates

The choice of substrates used for this work is based on two factors: firstly, it was already reported that fatty acid methyl esters (FAMEs) and alcohol acetates (AAs) are well accepted by *Pp* AlkB and represent suitable substrates for biotransformations[13,5,51] ; secondly, because alkanes, fatty acids and esters thereof can be derived from abundant and renewable resources such as fermentation of sugars[69], organic waste[70] or lignocellulose.[71] Through specific functionalisation, they can be transformed into valuable precursors of polymer building blocks. While many routes exist to synthesise these monomers, some chemical reactions involve the utilization of hazardous oxidants and/or yield only low regioselectivity.[72]

Therefore, the biotechnological field aims to provide alternative catalysts for more sustainable synthetic routes. As reviewed by Stadler et al., some of the compounds with great importance for the polymer industry are dicarboxylic acids for the production of polyesters and polyamides, diols for polyesters or polyurethanes, as well as hydroxy acids or -esters, and lactones for biodegradable polyesters.[72] Using the AlkB system, precursors of these molecules can be synthesised from FAMEs or AAs of fatty alcohols by terminal hydroxylation or overoxidation to the terminal carboxyl group (Figure 10). The utilisation of esters is advantageous, since the esterified hydroxy- or carboxy groups are protected against further oxidation or other modifications. Moreover, the polarity of that terminus is reduced compared to the free hydroxy- or carboxy groups, which significantly facilitates the interaction with AlkB, as it favours hydrophobic substrates. This allows for the synthesis of di-terminally functionalised hydroxy-acids, diacids or diols, as shown by Van Nuland and colleagues.[5]

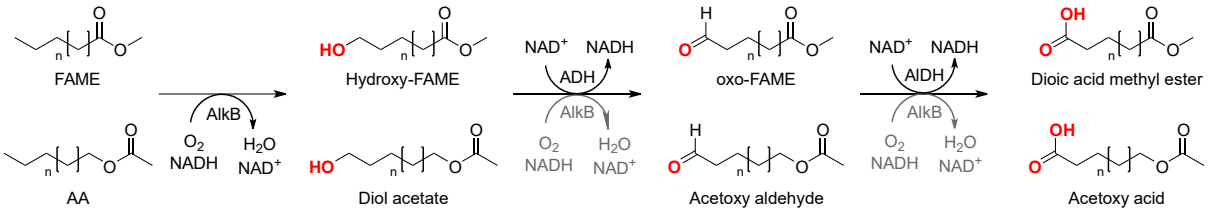

Figure 10 – Reaction scheme showing the terminal oxidation of FAMEs with n = 3, 7, or 10 or AAs with n = 4, 8 or 11, leading to the corresponding alcohols or over-oxidised aldehydes and acids (adapted from van Nuland et al.[73]).

Following the functionalisation, the esters can be hydrolysed, or "deprotected", which is usually done chemically under alkaline conditions.[74,75] The free hydroxyl- and carboxylic groups in hydroxy-acids, or between diols and diacids, can be polymerised in a polycondensation reaction, but the length of the polymers obtained from polycondensation is frequently limited.[76,77]

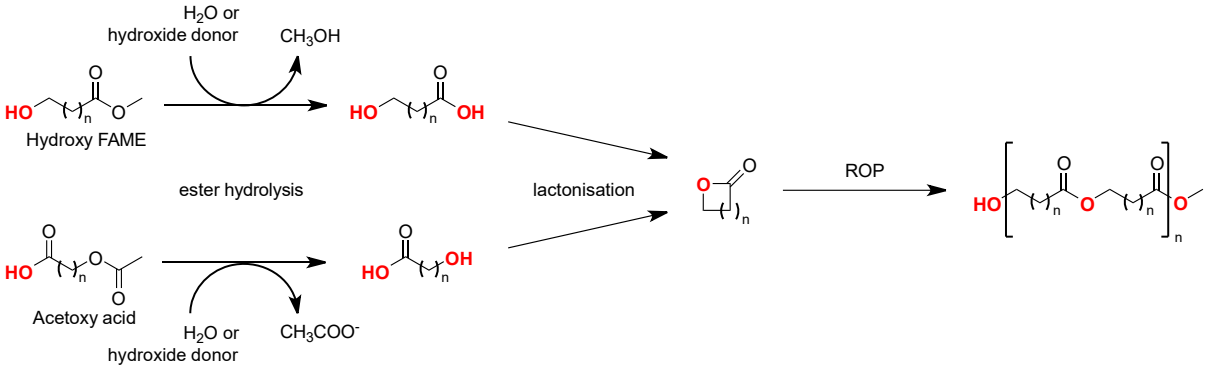

Figure 11 – Simplified reaction scheme showing the hydrolysis of an oxy-functionalised FAME (n = 1 – 14) or AA (n=4 – 6). Upon hydrolysis the hydroxy and the carboxy groups are free to react with other to form the lactone through internal esterification. Ring-opening polymerisation (ROP) of the lactone yields polyesters.

Alternatively, the di-terminally functionalised molecules can intermediately cyclise to lactones, either through intramolecular esterification of C_3[78]-C_{16}[79,80] hydroxy fatty acids, or through oxidative- or dehydrogenative lactonization[81,82] of C_4-C_6 diols.[83] These can serve as precursors for the so-called ring opening polymerisation (ROP) (Figure 11), which is more widely employed as it yields polymers of higher molecular weight than polycondensation. ROP can be achieved both by various chemical and enzymatic routes. Since the chemical pathways require metal catalysts, there might be residual metals in the final polymer which is not desired for the application in e.g. biological or electronic environment. Therefore, and aiming at a more sustainable production process, the enzyme catalysed ROP, "eROP", is intensively investigated, for which lipases can be employed as alternative catalysts[76,77], such as *Candida antarctica* Lipase B.[84] It was shown that, depending on the individual lipase, lactones of different sizes ranging from only four- up to even 17-membered rings can be used as substrate in eROP for the synthesis of polyesters.[85] However, mostly smaller rings consisting of four to seven atoms are considered suitable for polymerization and (bio-)degradation.[86] One of the most frequently used monomers in polylactones is ε-caprolactone, a seven-membered ring which can constitute the only building block in a polymer or be combined with others in heteropolymers to modify the characteristics of the material.[87] In general polylactones have gained increased attention due to their biodegradability and biocompatibility. Their features make them not only attractive for the production of environmentally friendly packaging materials[88,89], but also applicable in medicinal products such as sutures, implantable wound dressings and fibres, or for delayed drug delivery from nanoparticles.[90,91,92]

In summary, the FAMEs and AAs chosen as substrates for this work represent simple precursors that can be converted to valuable fine chemicals for the polymer industry with versatile applications. The biocatalytic oxyfunctionalization of this type of esters by *Pp* AlkB has been demonstrated in several publications already.[5,13,73] Therefore, these were regarded as suitable compounds for studying and engineering a homolog thereof, namely an alkane-1-monooxygenase from *Marinobacter sp.* (*Msp*), which has not been characterised in detail so far. This thesis focusses on the determination of the substrate acceptance and activity towards the selected FAMEs and AAs with varying chain length in whole-cell biocatalytic reactions. The different lengths of the alkyl chains (C_5, C_9 and C_{12}) allows

determination of the enzyme´s substrate preference. The introduction of selected single site mutations (SSMs), in the substrate tunnel, the active site and the membrane-enzyme interface and their influence on the substrate acceptance and conversion was evaluated. Combined, the results of this work aim to better understand the role of each residue in terms of substrate acceptance and catalytic activity.

2 Materials and methods

2.1 Chemicals

The compounds used as substrates, standards or for induction, were purchased in highest purity from Tokyo Chemical Industries, Sigma Aldrich, Ambeed, BLD Pharmatech GmbH, and Merck (Table 8, Appendix)

2.2 Media and culture conditions

For cell cultivation LB (lysogeny broth)- and $M9^{N2x}$ minimal medium were used, all supplemented with Kanamycin (40 µl mL^{-1}). During preparation, the components for LB media (liquid or solid) were combined, dissolved in ddH_2O, and sterilized by autoclaving. The components of the $M9^{N2x}$ minimal medium were dissolved in ddH_2O individually, sterilized and combined just before use. Antibiotics, inducer, and substrate solutions were added separately to each culture medium or buffer for biotransformation. The concentration of each component and composition of the complete media are shown in Table 1.

LB-agar plates were incubated at 37 °C overnight. Liquid over-night cultures (ONCs) were prepared by inoculating 4 mL of sterile LB medium with a single colony and incubated at 37 °C and with 120 rpm overnight in an orbital shaker. Pre- and main cultures in $M9^{N2x}$ were incubated at 30°C in an orbital shaker with 120 rpm.

Table 1 – Media and aqueous solutions used for cultivation, expression, and biotransformation reaction.

Medium	Final concentration	Components
LB (liquid)	20 g L^{-1}	LB (lysogeny broth)
	40 µg mL^{-1}	Kanamycin
LB (solid)	20 g L^{-1}	LB
	15 g L^{-1}	Agar
	40 µg mL^{-1}	Kanamycin
SOC	20 g L^{-1}	Tryptone
	5 g L^{-1}	yeast extract
	4.8 g L^{-1}	$MgSO_4$
	3.6 g L^{-1}	Glucose
	0.5 g L^{-1}	NaCl
	0.186 g L^{-1}	KCl (1 M)
$M9^{N2x}$ minimal medium	1x	M9 minimal salts^{N2x} (5 x)
	5 g L^{-1}	D(+)-Glucose
	2 mM	$MgSO_4$
	1 mL L^{-1}	Trace element solution US^{Fe}, stock (1000 x)
	1 mL L^{-1}	Thiamine*HCl, stock (1000 x)
	50 µl L^{-1}	Biotin, stock (20.000 x)
	40 µg mL^{-1}	Kanamycin, stock (1000 x)
5 x $M9^{N2x}$ minimal salts	15 g L^{-1}	KH_2PO_4
	2.5 g L^{-1}	NaCl
	33.9 g L^{-1}	Na_2HPO_4
	10 g L^{-1}	NH_4Cl

$MgSO_4$	1 M	$MgSO_4$*7H_2O
Glucose	200 g L^{-1}	D(+)-Glucose
1.000 x Trace Element Solution US^{Fe}	8.87 g L^{-1}	$FeSO_4$*7 H_2O
	4.12 g L^{-1}	$CaCl_2$*2 H_2O
	1.23 g L^{-1}	$MnCl_2$*2 H_2O
	1.87 g L^{-1}	$ZnSO_4$*7 H_2O
	0.30 g L^{-1}	H_3BO_3
	0.25 g L^{-1}	Na_2MoO_4*2 H_2O
	0.15 g L^{-1}	$CuCl_2$*2 H_2O
	0.84 g L^{-1}	Disodium EDTA*2 H_2O
1.000 x Thiamine stock	1 mg mL^{-1}	Thiamine*HCl
20.000 x Biotin stock	0.1 mg mL^{-1}	Biotin
1.000 x Kanamycin stock	40 mg mL^{-1}	Kanamycin
Resting cell buffer (RCB)	1% (w/v)	D(+)-Glucose
	2 mM	$MgSO_4$
	50 mM	Potassium Phosphate, KPi (K_2HPO_4, KH_2PO_4)
	pH 7	
50x TAE buffer	242 g L^{-1}	Tris
	14.6 g L^{-1}	EDTA
	57.1 mL L^{-1}	Acetic acid

2.3 Strains, plasmids and gene variants

As a cloning host, *E. coli* TOP10 (F^-*mcr*A Δ(*mrr-hsd*RMS-*mcr*BC) φ80*lac*ZΔM15 Δ*lac*X74 *rec*A1 *ara*D139 Δ(*ara-leu*)7697 *gal*U *gal*K λ–*rps*L(Str^R) *end*A1 *nup*G) was used for transformation and amplification of modified plasmid constructs. The plasmids isolated therefrom were afterwards transformed into *E. coli* BL21 (DE3) (*fhuA2 [lon] ompT gal (λ DE3) [dcm]* Δ*hsdS λ DE3 = λ sBamHIo* Δ*EcoRI-B int::(lacI::PlacUV5::T7 gene1) i21* Δ*nin5*), serving as an expression host of the selected genes of the alkane degradation pathway. These included the genes *alkBFG(L)_ST* derived from the natural *alk*-operon from *P. putida* GPo1 (Accession number NCBI GenBank: AJ245436.1, and Table 9 in Appendix). The plasmids used for cloning and expression were based on the backbone of the broad host range vectors pCom10[93] encoding the regulatory gene *alkS* and *alkB* under control of their natural promoters P_{alkS}[94] and P_{alkB}[30]*;* or pCom10_AlkL[95], which additionally encodes *alkL* for the outer membrane transporter. The final expression vectors encoding *alkBFG_ST or alkBFGL_ST* were referred to as pBT10[13] and pBTL10. For expression of the homologous monooxygenase, the same plasmid was used, but the open reading frame of *alkB* was replaced by the one of *Msp alkB* (Accession number NCBI protein data bank: MAB50652.1, and Table 9 in Appendix). The genes encoding the accessory proteins of *P. putida* were not changed.

For each monooxygenase variant (wild type and mutant variants), two strains were prepared with one carrying pBT10 and the other one pBTL10. Additionally, for both *Pp* GPo1 AlkB and *Msp* AlkB one inactive variant was used, serving as negative control. These were created by inserting an alanine in place of one of the essential histidine residues in the active site (H273A in AlkB and H278A in *Msp* AlkB), as published previously.[40,96] Lastly, based on the *Msp* AlkB wild type sequence, six single-point

mutants and one double-mutant were created. All the different gene combinations and enzyme variants tested in biotransformations are listed in Table 2.

Table 2 – List of plasmids used, containing either Pp GPo1 AlkB wild type or Msp AlkB wild type as well as single- and double-point mutants thereof. In all variants, alkF, alkG, alkL, alkS and alkT were co-expressed.

Plasmids and gene combination	Enzyme variant encoded	Source
pCom10_*Pp.* GPo1 *alkBFG_ST*	*Pp.* GPo1 AlkB	Available in house
pCom10_*Pp.* GPo1 *alkB* (H273A) *alkFG_ST*	*Pp.* GPo1 AlkB (H273A)	Available in house
pCom10_*Pp.* GPo1 *alkBFGL_ST*	*Pp.* GPo1 AlkB	Available in house
pCom10_*Msp alkB_alkFG_ST*	*Msp* AlkB	Available in house
pCom10_ *Msp alkB_alkFGL_ST*	*Msp* AlkB	Available in house
pCom10 _*Msp alkB* (H278A) *alkFGL_ST*	*Msp* AlkB (H278A*)*	Constructed during master thesis
pCom10_*Msp alkB* (W60S) *alkFGL_ST*	*Msp* AlkB (W60S)	Constructed during master thesis
pCom10_*Msp alkB* (F169L) *alkFGL_ST*	*Msp* AlkB (F169L)	Available in house
pCom10_*Msp alkB* (I238V) *alkFGL_ST*	*Msp* AlkB (I238V)	Available in house
pCom10_*Msp alkB* (F169V) *alkFGL_ST*	*Msp* AlkB (F169V)	Available in house
pCom10_*Msp alkB* (F169I) *alkFGL_ST*	*Msp* AlkB (F169I)	Available in house
pCom10_*Msp alkB* (T141A) *alkFGL_ST*	*Msp* AlkB (T141A)	Available in house
pCom10_*Msp alkB* (F169L_I238V) *alkFGL_ST*	*Msp* AlkB (F169L_I238V)	Available in house

2.4 Creation of new mutants and strains

2.4.1 Single site mutations

New enzyme variants with single amino acid exchanges were created through single site mutagenesis (SSM). The plasmid encoding the wild type DNA sequence of the *Msp* monooxygenase served as a template DNA and was amplified with mutagenic primers containing respective codon exchanges. As listed in Table 3, most of the variants had been created in advance and were available in-house. For the present work, two additional single mutants of *Msp* MO, H278A and W60S, were created, and five more for future experiments. These include I204L, G136M, G136V, I238A, I238F.

The choice of mutants was based on different sources. In literature several mutants of *Pp GPo1* AlkB were already described such as I233V leading to increased activity[8], W55S allowing to accept long chain substrates[14], T141A for improved substrate interaction.[67] The position H273 is known to be one of the essential histidine residues coordinating the iron atoms in the active site, required for catalysis.[45] An exchange to an alanine renders the enzyme inactive. Furthermore, docking experiments had been done (by Veronica Delsoglio) with isoprenyl acetate in *Pp* GPo1 AlkB, suggesting a mutation of the active site residue F164 to the more stable substituents leucine, isoleucine or valine. The mutations known from *Pp GPo1* AlkB were introduced into *Msp* AlkB in the corresponding positions I238V, W60S, H278A, F169L, F169I and F169V. A double mutant including F169L and I238V was created, too (by Andrea Nigl).

In the docking studies of *Msp* AlkB with octane, G136M, G136V and I204L were identified as possible mutations for more stable protein-substrate interaction. Also, 3DM analyses were conducted to identify alternative amino acid substituents, such as the exchange of I238 to an alanine.

Two different plasmids served as template for the reactions: pCom10_*Msp* AlkB and pCom10_*Msp* AlkB_AlkL only differing in the presence or absence of the gene *alkL*. For the amplification, each plasmid was combined with the primer pair carrying either the W60S mutation or the H278A, respectively (primer sequences see Appendix, Table 10). The reaction mixes were prepared according to the recommended standard protocol for PCR reactions. The negative controls only contained one aliquot of master mix, but no template DNA. The composition of the complete reaction mix is shown in Table 3.

Table 3 – Composition of the master mix used for the SSM reactions

Volume [µl]	Final concentration / amount	Component
31	-	ddH_2O
10	1 x	Q5 Buffer (5x)
2.5	0.5 µM	Primer forward (10 µM)
2.5	0.5 µM	Primer reverse (10 µM)
1.5	3 %	DMSO (100%)
1	0.2 mM	dNTPs (10 mM)
0.5	0.02 U	Q5 Polymerase (2 U/µl)
1	10 ng	Template DNA (10 ng/µl)
50		**Total**

The mixes were incubated in a thermocycler (Bio-Gener) with gradient from. For the annealing step, a temperature gradient from 70 to 72 °C was chosen, so that one of three identical replicates was incubated at either 70, 71.3 or 72 °C. Depending on the size of the template plasmids, the extension time was 06:00 min for pCOM10_*Msp* AlkB (11.6 kbp) and 06:15 min for pCOM10_*Msp* AlkB_AlkL (12.3 kbp). The whole temperature cycling program is shown in Table 4.

Table 4 – Temperature program for the SSM reaction.

Step	Temperature [°C]	Time (mm:ss)	Cycle number
Initial denaturation	98	00:30	1 x
Denaturation	98	00:30	25 x
Annealing	70 / 71.3 / 72	00:15	
Extension	72	06:00 / 06:15	
Final extension	72	08:00	1 x
Storage	4	∞	1 x

After SSM reaction, the success of PCR product formation was determined by agarose gel electrophoresis. A 5 µl aliquot of the PCR reaction mix was combined with 1 µl of TriTrack loading dye (6X) from ThermoFisher (10 mM Tris-HCl (pH 7.6), 0.03 % bromophenol blue, 0.03 % xylene

cyanol FF, 0.15 % orange G, 60 % glycerol, 60 mM EDTA) and loaded onto an agarose gel (1 %) in a running chamber with TAE buffer (1X). The GeneRuler 1 kb ladder from Thermo Fisher was used for the comparison. The electrophoresis was run for 30 min at 120 V and 400 Amp. Those samples, from which a single clear band of the desired size (above 10 kb) was obtained, were further subjected to DpnI digest, to remove any template DNA. In case additional bands appeared indicating byproduct formation, the remaining volume of the SSM reactions were loaded onto a preparative gel first. Only the bands of the expected size were excised and isolated from the gel using the Promega Wizard Gel and PCR purification kit, followed by DpnI digest.

One µl of DpnI (Thermo Fisher, 10 U/µl), was added to the remaining volume of each QC reaction mix. To the plasmid DNA isolated from the preparative gel, also 5 µl of Fast Digest buffer was added. The mixtures were then incubated at 37 °C for two hours and then for enzyme inactivation incubated at 80 °C for 20 minutes. After that, all replicates per plasmid variant were pooled.

2.4.2 Heat shock transformation

Following the SSM reaction and *Dpn*I digest of all positive replicates, the newly amplified plasmids were transformed into *E. coli* TOP10 using heat shock transformation. 50 µl of chemo-competent cells were first thawed on ice for 10 minutes and then 5 µl of the respective plasmid variant were added. Then the cells were incubated on ice for additional 30 minutes and mixed regularly. Afterwards, the cells were heat shocked in a thermoblock at 42 °C for 30 seconds, and then incubated on ice for 5 minutes. 950 µl of SOC medium were then added to the cells for the regeneration, which were subsequently incubated in a thermoblock for one hour, at 37 °C and 350 rpm. Finally, 100 µl aliquots of the cell suspensions were streaked out on LB agar plates supplemented with Kanamycin 40 µg mL^{-1} as well as the concentrated rest after centrifugation (8000 rpm, room temperature, 2 min). The plates were incubated at 37 °C overnight.

Of all transformants grown, four single colonies were picked per plasmid variant, streaked onto one fresh master plate with LB agar and used to inoculate ONCs of 4 mL LB medium (both with Kanamycin 40 µg mL^{-1}). The plasmid DNA from those *E. coli* TOP10 transformants, was harvested and the respective mutations were verified by sequencing (described in next section). Having confirmed the correct codon exchange, chemo-competent *E. coli* BL21 (DE3) were transformed with the modified plasmids by heat shock transformation, using the same procedure as before.

2.4.3 Plasmid isolation and sequencing

The transformants grown in liquid ONCs were harvested. Then, the plasmid DNA was isolated using the Wizard Plus SV Miniprep DNA purification kit from Promega, following the procedure described in the enclosed protocol. In the last step, however, the DNA was eluted from the spin column by transferring 50 µl nuclease-free water (preheated to 60°C) onto the column and incubating for five

minutes, with repeating the elution step twice. Finally, the plasmid DNA concentration was measured by NanoDrop spectrophotometry.

To verify the desired codon exchange, one replicate was selected for Sanger sequencing from each plasmid variant harvested. 12 µl of each plasmid isolated (80–100 ng/µl) were combined with 3 µl of one selected primer [10 µM] (primers p17 for pBT and p109 for pBTL). The mix was sent for sequencing analysis, carried out by MicroSynth Sequencing service. Using the Benchling online sequence alignment tool, the sequencing results obtained were analysed. Single positive transformants, in which the expected codon exchange was verified, were picked from the master plate and used to inoculate three identical ONCs. The plasmid DNA was isolated by Miniprep as described before and the three replicates from the same clone were pooled after isolation. To ensure that the plasmid also does not carry undesired mutations in other parts of the DNA sequence, the whole plasmids were sequenced using a set of eleven primers (p17, p35, p36, p44, p47, p67, p68, p73, p74, p90, p109; all primer sequences in Table 11 in the Appendix), before transforming into *E. coli* BL21 (DE3).

2.4.4 Glycerol stocks

For storage of the newly created strains, glycerol stocks were prepared from both *E. coli* TOP10 and *E. coli* BL21 (DE3) carrying the new plasmid variants. ONCs were prepared of each strain and on the following day, 1 mL of ONC was combined with 1 mL of sterile glycerol (60%), gently inverted, and afterwards stored at -80 °C.

2.5 Cultivation and cell harvest

E. coli BL21 (DE3) strains bearing the plasmid encoding the respective enzyme variant were streaked out on LB agar plates and single colonies were picked to inoculate ONCs. Precultures were prepared by transferring 200 µl of the ONC to 20 mL of $M9^{N2x}$ medium (Kanamycin 40 µg mL^{-1}) in 100 mL shake flasks (no baffles), which were incubated overnight at 30 °C and 120 rpm. For the main cultures, aliquots of the precultures and fresh $M9^{N2x}$ medium (Kanamycin 40 µg mL^{-1}) were combined in 1 L shake flasks (with baffles) for a total volume of 200 mL and an initial OD_{600} of 0.15. The main cultures were incubated under identical conditions as the precultures. About 2.5 hours after inoculation, when the OD_{600} reached values between 0.40-0.55, the protein expression was induced by adding 100 µl dicyclopropyl ketone (DCPK) to the main cultures (0.05 % (v/v)). Following induction, the incubation was continued for four hours under the same conditions as before. Four hours after induction, the cell cultures were harvested by centrifugation (15 min, 4000 rpm, 4 °C).

2.6 Biotransformation

For biotransformation, substrate stocks were always freshly prepared. The respective compounds were dissolved in DMSO for a final concentration of 80 mM. All substrates used in biotransformation experiments, and their abbreviations are summarized in Table 5 and Table 6. **2** and **4**–**6** were used in

biotransformations for quantification of the activities of different mutants towards the substrates provided.

Table 5 – Substrates used in biotransformation experiments. FAMEs and AAs with an alkyl chain length of C_5, C_9 or C_{12}.

Substrate type	Substrates		
FAMEs	**(1)** Methyl pentanoate 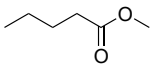	**(2)** Methyl nonanoate 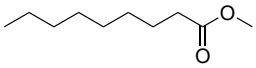	**(3)** Methyl laurate 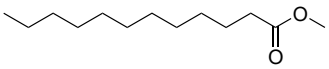
AAs	**(4)** Pentyl acetate 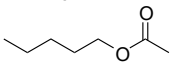	**(5)** Nonyl acetate 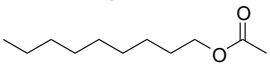	**(6)** Dodecyl acetate 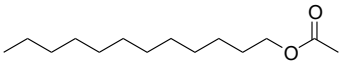

*Table 6 – The possible oxidation products of the substrates **1-6**, ranging from the terminal alcohol (**a**) to the over-oxidised terminal aldehyde (**b**) and -acid (**c**).*

Terminal alcohol	Terminal aldehyde	Over-oxidised product
(1a) Methyl 5-hydroxy pentanoate 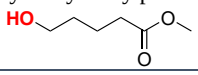	**(1b)** Methyl 5-oxopentanoate 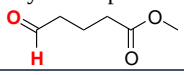	**(1c)** Pentanedioic acid monomethyl ester 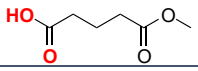
(2a) Methyl 9-hydroxy nonanoate 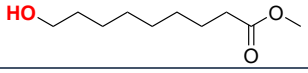	**(2b)** Methyl 9-oxononanoate 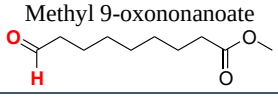	**(2c)** Nonanedioic acid monomethyl ester 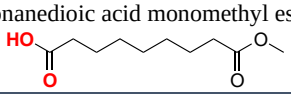
(3a) Methyl 12-hydroxy laurate 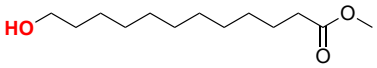	**(3b)** Methyl 12-oxododecanoate 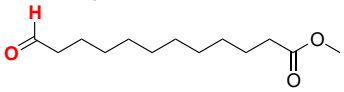	**(3c)** Dodecanedioic acid monomethyl ester 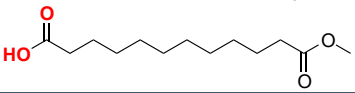
(4a) 1,5-Pentanediol monoacetate 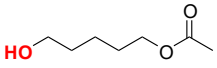	**(4b)** 5-Acetoxy pentanal 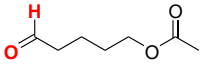	**(4c)** 5-Acetoxy pentanoic acid 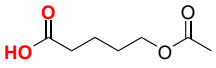
(5a) 1,9-Nonanediol monoacetate 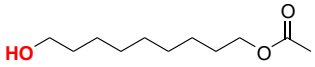	**(5b)** 9-Acetoxy nonanal 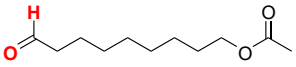	**(5c)** 9-Acetoxy nonanoic acid 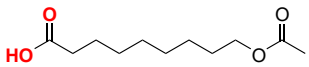
(6a) 1,12-Dodecanediol monoacetate 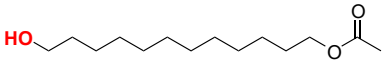	**(6)** 12-Acetoxy dodecanal 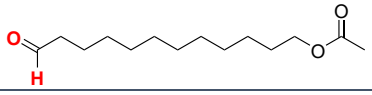	**(6c)** 12-Acetoxy dodecanoic acid 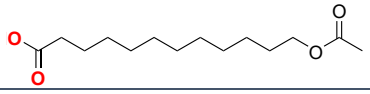

In the initial experiments, varying reaction conditions were tested, including cell densities of 0.08, 1.0, 2.2 and 3.1 g_{CDW} L^{-1}, reaction temperatures of 25 or 30 °C, incubation in orbital or bench-top shakers, substrate concentrations of 2 or 5 mM and substrate stocks prepared in ethanol or DMSO. The set-up used for the activity determination of the whole-cell reactions is described in the following.

After cell harvest, the supernatant was removed, and the pelleted cells were resuspended in ~10 mL resting cell buffer (RCB) and the OD_{600} was measured. In 15 mL falcon tubes, kept on ice, RCB was combined with the resuspended cells for a cell density of 1.0 g_{CDW} L^{-1} (with **2**, **4** and **5**) or 3.1 g_{CDW} L^{-1} (with **6**) in the final reaction mix. At last, the respective substrate was added to the mix for a final concentration of 2 mM and 2.5 % solvent (v/v). After substrate addition, the reaction mix was mixed by pipetting and vortexing. Immediately, a t_0 sample was taken and 300 µL aliquots of the reaction mixes were distributed into fresh GC-vials with a volume of 1.5 mL. The vials were incubated by shaking (180 rpm) at 25 °C in an orbital shaker. In initial experiments, the reaction was sampled 0, 1 and 24 hours after the start of the reaction, while for the activity determination, samples were taken at 0 and after, 15, 30, and 45 min, 1, 2 and 4 hours. For stopping the reactions, 250 µl aliquots were transferred to fresh 1.5 mL Eppendorf tubes on ice with the addition of 25 µL of 2M HCl. The samples were stored at -20 °C. Within one to two weeks after sampling, they were extracted and analysed by GC, as described later.

Additionally, two types of negative controls of the biotransformation reaction were made. In one, *E. coli* BL21 (DE3) cells expressing the inactive mutant of the respective monooxygenases, H273A or H278A, were used. The second one only comprised RCB and substrate solution, but no cells. Negative controls were set up the same way as biotransformations with cells expressing active variants. The samples were taken at 0, 1 and 4 hours after reaction start, stored, and analysed the same way as described above.

2.7 Sample preparation and GC analysis

For the analysis, frozen samples were thawn at room temperature and extracted. To each sample, 250 µl ethyl acetate containing methyl benzoate as internal standard (ISTD) [1 mM] were added. The mixture was shaken vigorously for 30 sec, vortexed for another 30 sec and centrifuged for the phase separation (5 minutes, 13,000 rpm, 4 °C). Subsequently, 200 µl of the upper organic phase were transferred into a fresh tube with a spatula tip of anhydrous $MgSO_4$ inside to bind any excess of aqueous phase. Again, the mixture was shaken and vortexed for 30 sec, respectively, and centrifuged. Finally, the dried organic phase was transferred to GC-vials and subjected to GC analysis (method and device details in Table 13-Table 14, Appendix).

Biotransformation samples were analysed via GC-MS (GCMS-QP2010 SE, Shimadzu, Japan) and via GC-FID (GC-2030 Nexis, Shimadzu, Japan). GC-MS analysis was used to determine the substrate conversion of each monooxygenase and identify products formed during whole-cell biocatalysis. Putative products and side-products were identified through analysis of the mass spectra and, if available, also verified by comparison to the standards of the respective compounds. The retention times of specific compounds seen in the GC-MS chromatograms were relatable to those of the peaks obtained from GC-FID analysis. The latter was used to quantify the substrate consumption and products formation.

The concentrations of the substrates and products were quantified via GC-FID analysis. The peak areas were integrated for the ISTD, the substrate and the products. A normalization factor was calculated for each sample, by dividing the mean of ISTD peak areas in one batch of samples analysed by the ISTD peak area of the respective sample (Equation 1). The factors obtained were multiplied with the peak areas in the respective a sample, giving the normalized peak area (Equation 2). The normalized peak areas were converted to concentrations in millimolar (Equation 3) by using the slope "k" of the calibration trendline (Table 12, Appendix).

Equation 1

$$\frac{\text{averaged standard peak area}}{\text{standard peak areas}} = \text{normalisation factor}$$

Equation 2

$$\text{Peak area} * \text{norm. factor} = \text{normalized peak area}$$

Equation 3

$$\frac{\text{normalized substrate peak area}}{k} = \text{substrate [mM]}$$

The changes in concentration between reaction start and a given time point up to 24 hours of reaction served to calculate the substrate depletion, conversion, and activity. The depletion of substrate [S] within 1, 4 or 24 hours of reactions with negative controls was determined according to Equation 4.

Equation 4

$$[\text{S}]\text{t0} - [\text{S}]\text{t1} = [\Delta S]\text{t1 [mM]} = \text{substrate depletion [mM]}$$

The percentage of conversion of substrate to the hydroxy-, carboxy- or hydrolysis products [P] within 2 hours of biotransformation was calculated as in Equation 5.

Equation 5

$$\left(\frac{[\text{P}]\text{t2 [mM]}}{[\text{S}]\text{t0 [mM]}}\right) * 100 = \text{conversion [\%]}$$

For the calculation of the activity, the concentration of hydroxy- or carboxy product was plotted against time. Depending on the linear range, a regression trendline was aligned to the data points of the first 30 to 60 min. The trendline can be described by the general formula $y = k * x + d$ and the slope k corresponds to the increase of product concentration over time in mM min^{-1}. By inserting k into Equation 6, the volumetric activity was obtained. The volumetric activity was then normalized by the average cell dry weight of e.g. 1.0 or 3.1 g_{CDW} L^{-1} (calibration for g_{CDW} determination obtained from Andrea Nigl, Figure 34) according to Equation 7, resulting in the specific activity.

Equation 6

$$\left(\text{slope}\left[\frac{\Delta \text{P}}{\text{min}}\right]\right) * 1000 = \text{Units [µmol/L/min]}$$

Equation 7

$$\frac{\text{Units [µmol/L/min]}}{\text{1 gCDW/L}} = \text{specific activity [µmol/min/gCDW]}$$

The parameters substrate depletion, conversion and specific activity were calculated from three replicates of an enzyme variant and finally the average was determined.

2.8 Calibration curves

Calibration curves were established with the substrates **2** and **4-6**, used in activity measurements, but also for those hydroxy-, acid- or hydrolysis products, for which standards were commercially available, i.e., **2a**, **2b** and nonanoic acid. The concentration of hydroxy products of the acetate esters, however, were estimated by using the calibration curve of the corresponding substrate.

Stock solutions with a concentration of 400 mM were prepared by solubilizing the respective compounds in DMSO. For **6**, stocks of 160 mM were made. From each stock, ten dilutions with increasing concentration were made by mixing aliquots from the stock with DMSO in the corresponding ratios. From each individual dilution, 6.25 µl were mixed with 243.75 µl RCB resulting in samples of 250 µl volume and with 2.5 % solvent inside. Additionally, 25 µl of 2 M HCl were added, as in the biotransformation samples. These mixtures were extracted for GC-FID analysis as described in the next section, except that the calibration samples were extracted directly without freezing.

Per compound, two calibration curves were prepared. The average signal intensities measured in two replicates of the same concentration were plotted against the respective concentration. A trendline was added to the data points (forced intercept through the origin) yielding the final calibration curve (Table 12, Appendix). The equation describing the linear regression trendline in the form of $y = k * x$ served to calculate the concentration of the compounds in the biotransformation samples, as described in the following section.

2.8.1 Standard synthesis

Since no standard compounds were available for the terminally hydroxylated acetate esters, product standards were synthesized in-house (by Jelena Spasic and Lenny Yap) via enzymatic reaction catalysed by the lipase from *Pseudomonas cepacia*, (38.6 U/mg, from Sigma-Aldrich). 50 mg of 1,5-pentane diol, 1,9-nonane diol or 1,12-dodecane diol, respectively, were solubilized in MTB, combined with the acetate donor vinyl acetate in a 1:1 molar ratio and the lipase (312 U/mmol substrate) based on protocols from Grisenti et. al.[97] and Ferraboschi et. al..[98] The reaction mixes with a total volume of 1 mL were incubated over-night in round bottom flasks rotating in a water bath at 30 °C.

After incubation, solid particles and precipitates in the 1 mL reaction mix were separated from the liquid by centrifugation (max. speed, 4 °C, 15 min). The liquid supernatant was transferred to a fresh tube and stored at -20 °C. For GC analysis, a 1:10 dilution of the synthesis mix was prepared by mixing an aliquot

with ethyl acetate containing an ISTD [1 mM]. The dilution was shaken, centrifuged, dried over $MgSO_4$ and centrifuged again, following the same sample preparation procedure as described before.

.

3 Results

3.1 Standard synthesis

To obtain standards for the expected reaction products, three standards were synthesised for the terminal hydroxy products of acetate esters **4-6**. In a lipase catalysed reaction, the respective C_5, C_9, C_{12} diols were acetylated with vinyl acetate as donor. The GC-MS results had shown that the synthesis of each standard yielded the desired hydroxy esters. Additionally, on GC-MS unreacted diol, di-acetates, and acrylates were observed. Through analysis of the mass spectra the desired product was identified and by overlapping with chromatograms from biotransformation samples, the biocatalytic hydroxylation of the acetate esters could be verified. The results from the GC-MS analysis of the synthesis reactions are shown in (Figure 35-Figure 37, Appendix)

3.2 Site-directed mutagenesis of *Msp* AlkB and transformation

It was shown by agarose gel electrophoresis that the plasmid DNA amplification with the mutagenic primers in the SSM reactions was largely successful (Figure 12). For most reactions one clear band at 11.6 kbp and 12.3 kbp corresponding to the plasmid size can be seen for the pCOM10 *Msp* AlkB AlkFG_ST pCOM10 *Msp* AlkB AlkFGL_ST, respectively. In those reactions with the primers bearing the mutations H278A (Figure 12, A) or I204L (Figure 12, B), an additional band of around 500 bp or 800 bp was observed, which indicates by-product formation due to unspecific binding of the primers to off-target sequences within the template DNA.

The mutated plasmids were transformed into *E. coli* TOP10, and the desired codon exchange was confirmed by sequencing. Finally that the mutated plasmids were successfully transformed into *E. coli* BL21 (DE3).

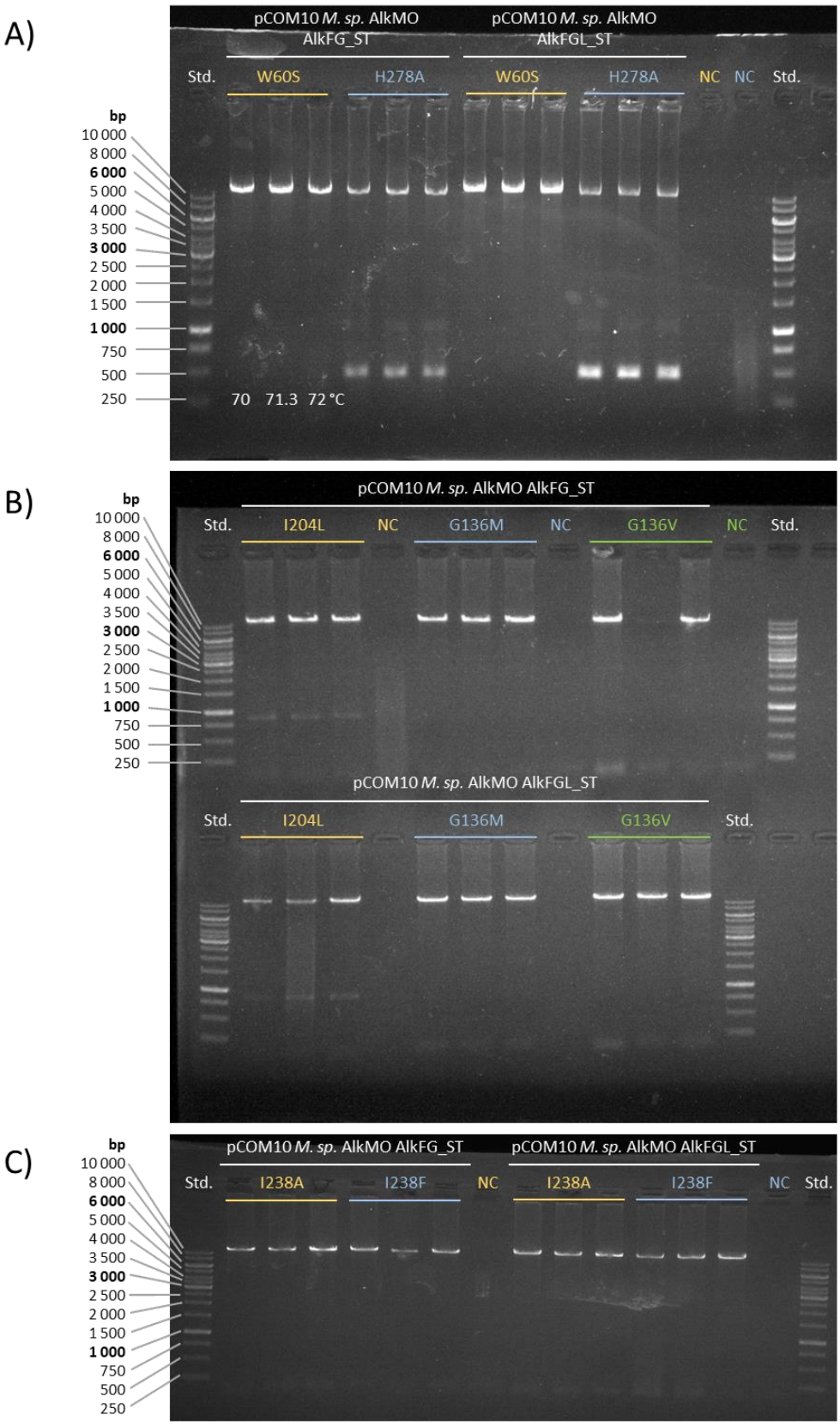

Figure 12 – Control agarose gel. The results of the SSM reactions are shown for both plasmid variants (pCom10 Msp AlkB AlkFG_ST and pCom10 Msp AlkB AlkFGL_ST). The desired amino acid mutation to be introduced by the mutagenic primer pairs used are indicated in colours. (A) W60S and H278A, (B) I204L, G136M and G136V, (C) I238A and I238F. The negative control (NC)containing the same primers, but no template DNA is shown in the same colour. The temperature indicates the annealing temperature for each replicate, that was used for all SSM reactions.

3.3 Substrate acceptance of the wildtypes of *Pp* AlkB and *Msp* AlkB

In preliminary tests, the substrate acceptance of *Pp* GPo1 AlkB- and *Msp* AlkB wild type towards the esters **1-6** (Table 7) and the influence of AlkL co-expression were evaluated by GC-MS. By analysing the samples taken after zero, one and 24 hours, it was determined if the compounds were converted and, if yes, which oxidation products were formed. The peak assignment based on the GC-MS results further helped to identify the peaks obtained in the GC-FID analysis.

In general, all substrates seemed to be oxidised in biotransformations with both *Pp* AlkB and *Msp* AlkB, respectively. However, the amount of hydroxylated product formed varied drastically between the substrates (Table 7). Clearly visible peaks of the hydroxy products **1a**, **2a, 4a** and **5a** were detected in samples from one and 24 hours of reaction. The hydroxy products **3a** and **6a** were hardly detectable in those reactions without AlkL co-expression. In those biotransformations with AlkL co-expressed, the product peaks **3a** and **6a** were detected in samples taken after one hour of reaction, but still the signal from these products was quite low.

Table 7 – Terminal hydroxylation by Pp GPo1 AlkB and Msp AlkB of linear fatty acid methyl esters and alkyl acetates..The product formations estimated from the peak sizes are categorised into highest (++), high (+) and small amounts (~) or not detected (-).

Substrate		**Terminal hydroxylation by *Pp* GPo1 AlkB**	**Terminal hydroxylation by *Msp* AlkB**
Methyl pentanoate	(**1**)	+	-
Methyl nonanoate	(**2**)	++	++
Methyl laurate	(**3**)	~	~
Pentyl acetate	(**4**)	++	++
Nonyl acetate	(**5**)	++	++
Dodecyl acetate S6	(**6**)	~	~

Overall, similar patterns of product formation were observed, and apart from **1**, all six substrates were functionalized to the respective terminal alcohols by both AlkB enzymes. Substrate **1**, however, seemed to be converted to two different products, since *Pp* AlkB formed a product that eluted earlier (6.4 min) than the one produced by *Msp* AlkB (6.8 min). Mass spectrum analysis of both products suggested that *Pp* AlkB had formed the putative hydroxy product **1a** and *Msp* AlkB the over-oxidised **1c** (Figure 38).

The formation of **2a** was confirmed by comparison with the commercially available standard, which showed an overlap at a retention time of around 8.5 min (Figure 13). Using the standards synthesized in-house, also the conversion of the acetate esters to the terminal alcohols **4a**, **5a** and **6a** were verified (Figure 40-Figure 42, Appendix). In biotransformations with *Msp* AlkB the overoxidation products **2c** and, putatively, **4c** (Figure 40) and **5c** (Figure 41) were detected as well, but only in samples taken after 24 hours of reaction. In samples from biotransformations with *Pp* GPo1 AlkB these overoxidation products were not detected.

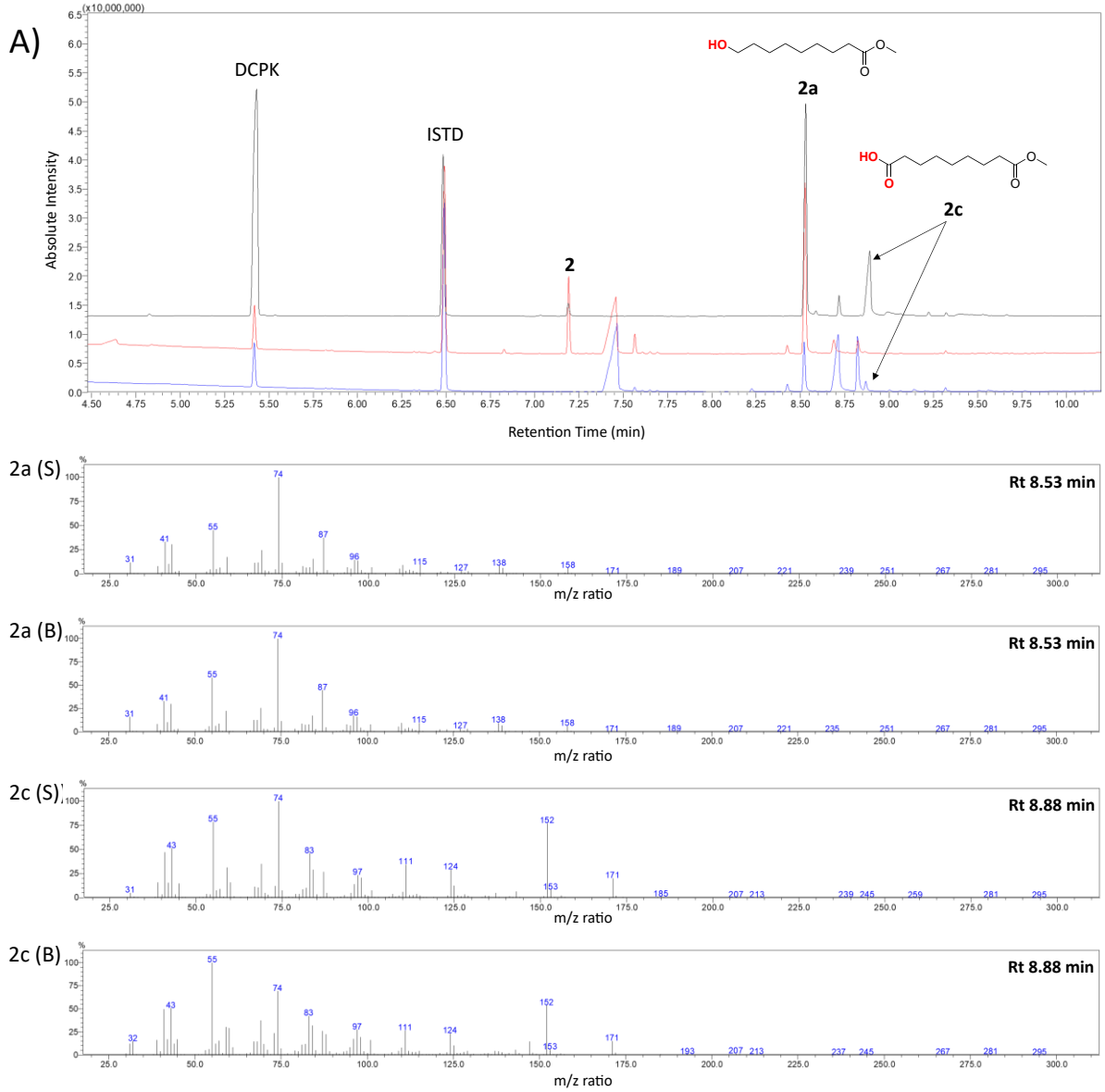

Figure 13 – (A) Comparison between GC-MS *chromatograms of the standards for **2a** and **2c** (black), with samples from biotransformations of **2** with Msp AlkB wild type (+ AlkL), taken 1h (red) and 24 h (blue) after reaction start. Mass spectra are shown for the **2a** standard (S) and the biotransformation product (B), and **2c** standard (S) and biotransformation product (B).*

The putative oxidation products **1a**, **1c**, **3a** (Figure 39), **4c** and **5c** were identified by analysis of the respective mass spectra but were not confirmed by other means. Even though the overoxidation of the terminal hydroxy group involves the oxidation to the intermediate aldehyde (**b**) first, before it is further over-oxidised to the carboxylic acid group (**c**), no products peaks were identified as aldehyde. The chromatograms of all initial biotransformations with *Pp* AlkB and *Msp* AlkB are shown in the Appendix (Figure 43-Figure 54).

3.4 Substrate acceptance of *Msp* alkane-1-monooxygenase variants

The substrate acceptance of the enzyme variants W60S, F169L, I238V, F169I, F169V, T141A and F169L/I238V towards substrates **2** and **4-6** were evaluated and compared to the wild type enzyme. All seven mutants showed a similar pattern of products formed from **2**, mainly differing in the ratio of

hydroxylated to overoxidized products formed. Especially the mutants in position F169 showed the most prominent peaks of **2b** (Figure 14).

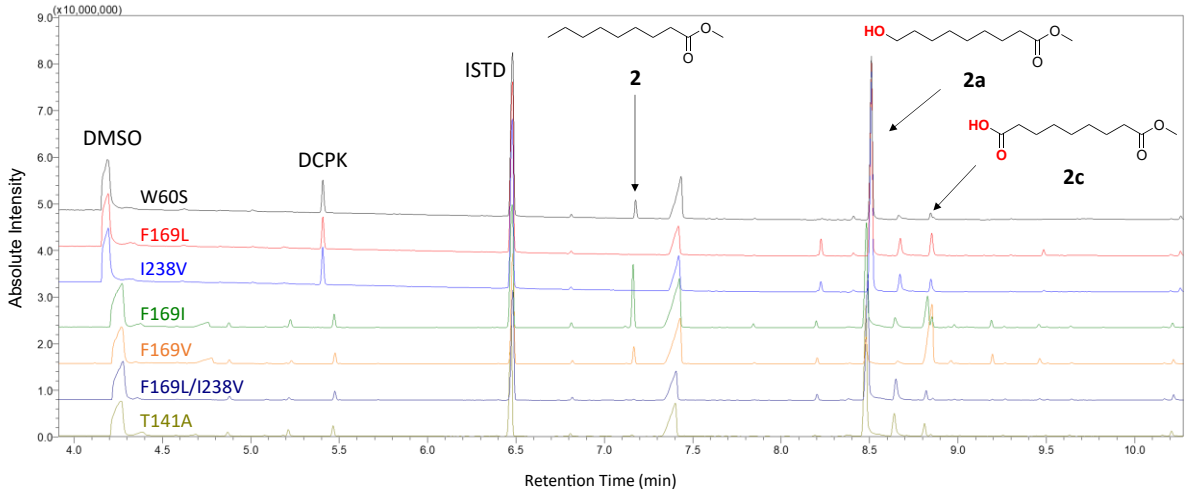

*Figure 14 – GCMS chromatograms. Samples from biotransformations of **2** with Msp AlkB (+AlkL) mutants, taken 1 or 4 hours after reaction start: W60S t1, F164L t1, I238V t1, F169I t4, F169V t4, F169L_I238V t4 and T141A t4. For the reaction, a cell density of 3.1 g_{CDW} L^{-1} (W60S – I238V) or 1.0 g_{CDW} L^{-1} (F169I – T141A), an initial substrate concentration of 2 mM and a reaction temperature of 25 °C were used.*

Substrate **4** was converted to **4a** by the three variants W60S, F169L and I238V, of which mainly the latter two formed the putative **4c** (Figure 15). Interestingly though, F169L and I238V had formed another peak eluting shortly after the internal standard. Upon analysis of its mass spectrum, it was tentatively identified as the terminal aldehyde **4b** (Figure 55). In biotransformations with *Pp* AlkB or *Msp* AlkB this peak was not seen.

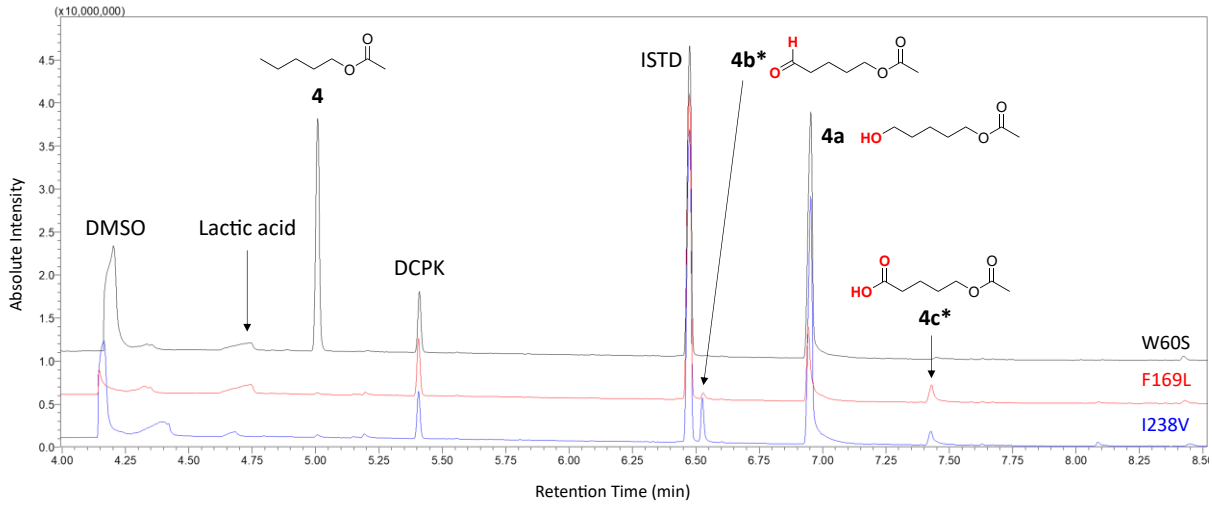

*Figure 15 – GCMS chromatograms. Samples from biotransformations of **4** with Msp AlkB (+AlkL) mutants, taken 1 hour after reaction start: W60S t1, F169L t1, I238V t1. For the reaction, a cell density of 3.1 g_{CDW} L^{-1}, an initial substrate concentration of 2 mM and a reaction temperature of 25 °C were used.*

Substrate **5** was hydroxylated to **5a** by the three mutant variants and all of them seemed to form a potential overoxidation product **5c** (Figure 16).

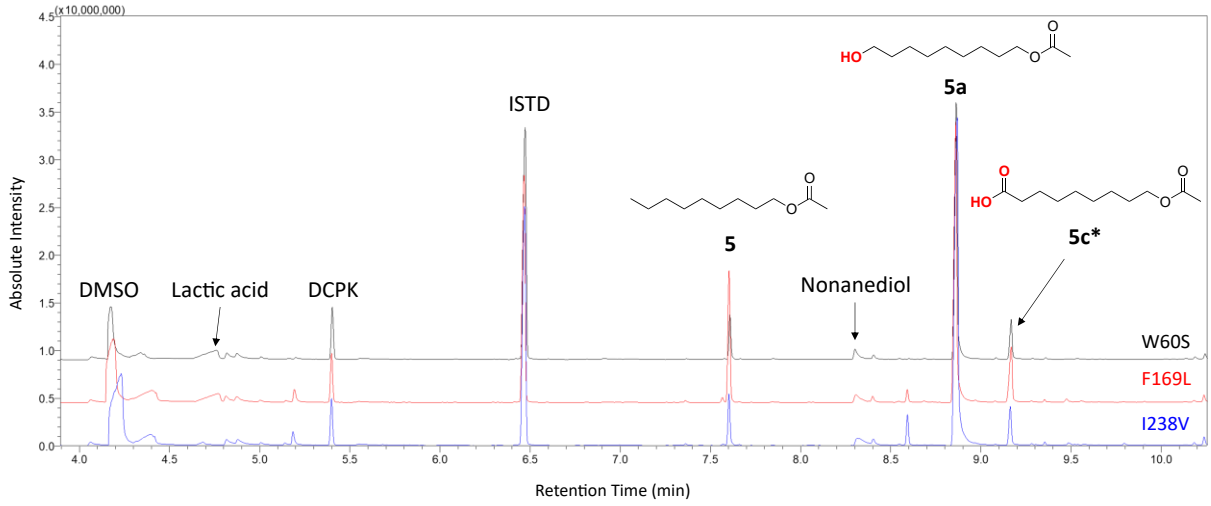

*Figure 16 – GCMS chromatograms. Samples from biotransformations of **5** with Msp AlkB (+AlkL) mutants, taken 1 hour after reaction start: W60S t1, F169L t1, I238V t1. For the reaction, a cell density of 3.1 g_{CDW} L^{-1}, an initial substrate concentration of 2 mM and a reaction temperature of 25 °C were used.*

Substrate **6** was only converted to **6a** by the W60S variant, and the signal obtained from that product was clearly stronger than seen previously in samples of biotransformations with *Msp* AlkB wild type (Figure 17). The other two mutants did not show any signal for the formation of **6a**. However, in the chromatograms of the samples from all three mutants another prominent peak was seen (Rt = 10.2 min), shortly after **6a** (Rt = 9.9 min). Based on mass spectrum analysis, it was hypothesised that it might represent an overoxidation or hydrolysis product. Since the peak was seen in all reactions irrespective of the presence of **6a**, it seems more likely to be a hydrolysis product. Also, the same peak can be seen in the GC-MS results from the preliminary test reactions with *Pp* AlkB and *Msp* AlkB (Figure 53Figure 54) as well as in negative controls (Figure 57 and Figure 59), even if not that prominently. Through comparison with available standards for probable hydrolysed and oxidised products, it could however be excluded that the peak represents dodecanol, dodecanediol, dodecanoic acid and 12-hydroxy dodecanoic acid, which elute at different time points (Data not shown). Thus, further analysis is required to determine the identity of this compound.

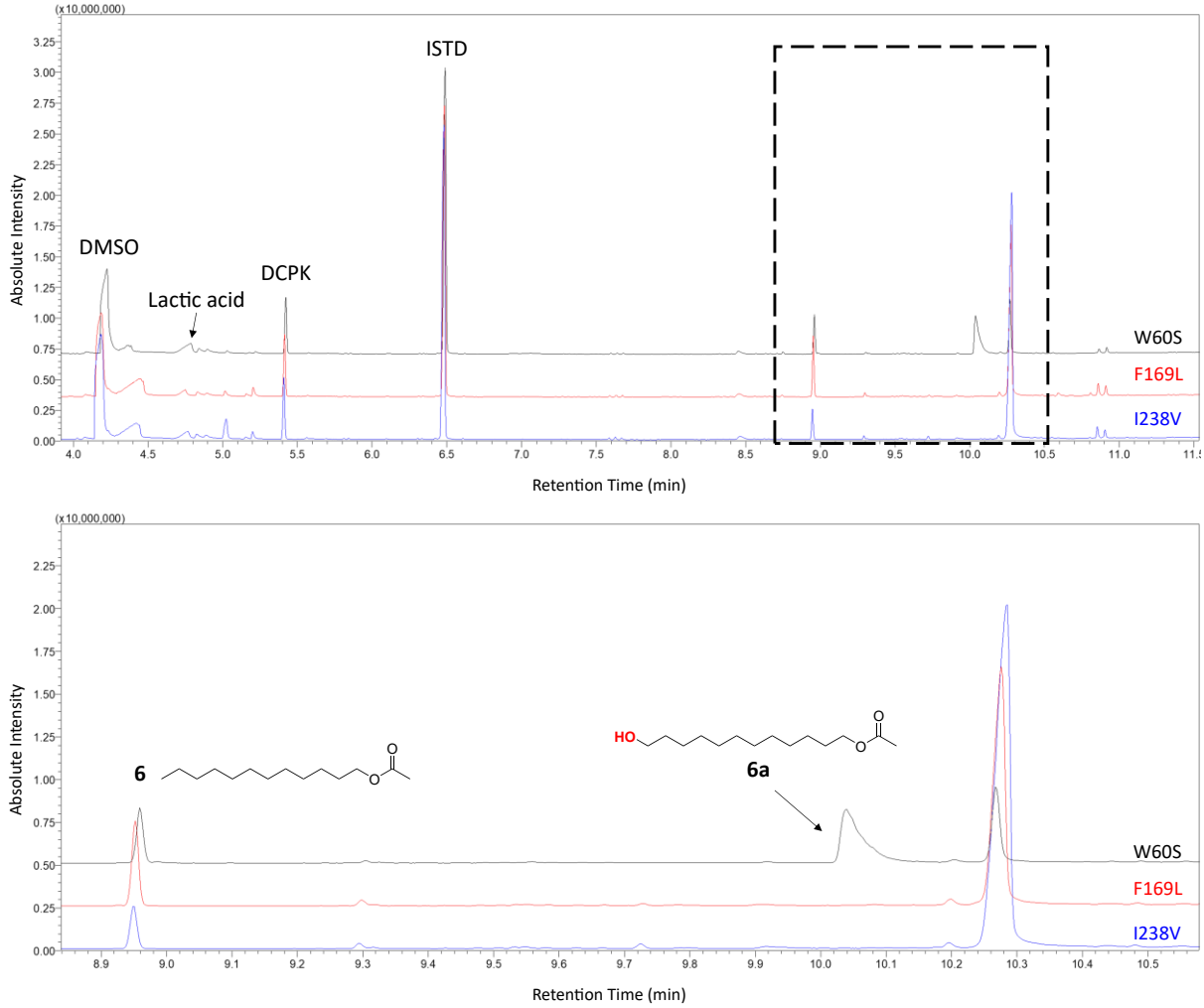

*Figure 17 – GCMS chromatograms. Samples from biotransformations of **6** with Msp AlkB (+AlkL) mutants, taken 1 hour after reaction start: W60S t1, F169L t1, I238V t1. For the reaction, a cell density of 3.1 g_{CDW} L^{-1}, an initial substrate concentration of 2 mM and a reaction temperature of 25 °C were used.*

3.5 Optimization of reaction conditions

In the initial experiments, also hydrolysed and trans-esterified side-products of the substrates were observed. These were most prominent in reactions with methyl ester substrates (**1-3**), of which particularly free nonanoic and dodecanoic acid were formed as well as ethyl esters thereof. From the acetate esters also the respective nonanol and dodecanol were detected in trace amounts. The formation of trans-esters could be avoided by preparing substrate stocks in DMSO instead of ethanol (Figure 56 and Figure 58, Appendix). Additionally, lactic acid accumulated over time, which indicates a fermentative metabolism of *E. coli* due to oxygen limitations within the closed reaction system. This effect was reduced by lowering the reaction volume from 1 mL to 300 µl, however, it could not be avoided completely. After the initial screening for substrate acceptance by both AlkB wild type enzymes with **1-6**, only **2** and **4-6** were used in further tests for activity determination with *Msp* AlkB wild type and mutants.

Initial biotransformation tests with varying cell densities (1.0, 2.2, and 3.1 g_{CDW} L^{-1}) in the reaction suspension gave mixed results. The activities of *Msp* AlkB wild type towards **2** ranged between

4.4-5.8 U g_{CDW}^{-1} and the activity of the mutant I238V between 7.9-9.7 U g_{CDW}^{-1} (Figure 18, A), indicating that the specific activities were not drastically affected by the cell density. In contrast, with substrate **4** increased cell density seems to lead to higher conversion rates. At 3.1 g_{CDW} L^{-1}, *Msp* AlkB wild type and I238V reached around 3.6 and 7.8 U g_{CDW}^{-1}, respectively, while the specific activities of both variants were about 2-fold lower when tested at 1.0 and 2.2 g_{CDW} L^{-1} (Figure 18, B). It should be noted though, that the data shown for 1.0 g_{CDW} L^{-1} were derived from three replicates, whereas only one replicate each was tested at 2.2 and 3.1 g_{CDW} L^{-1}.

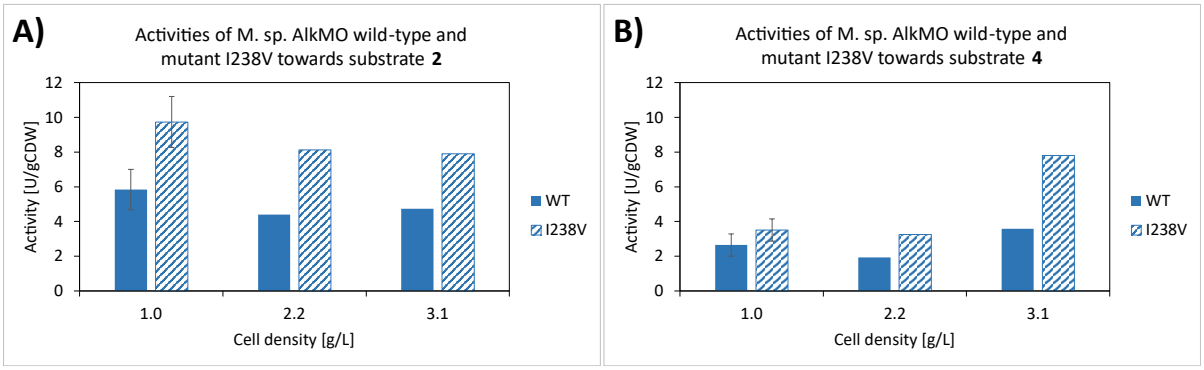

*Figure 18 – Comparison between the specific activities of Msp AlkB wild type and the mutant I238V towards (A) **2** and (B) **4** in dependence of the cell density. Three replicates were tested at 1 g_{CDW} L^{-1}, while only single replicates were tested at 2.2 and 3.1 g_{CDW} L^{-1}, respectively. For the reaction an initial substrate concentration of 2 mM and a reaction temperature of 25 °C were used.*

Comparing of the millimoles of hydroxy product formed within two hours, indicated a similar trend (Figure 19). At a cell density of only 1 g_{CDW} L^{-1}, *Msp* AlkB wild type and I238V led to the formation of around 0.6 and 0.9 mM of **2a.** For the wild type the product concentrations reached comparable levels at higher densities. For the mutant I238V, however, the final product concentrations obtained seemed to drop with increasing cell density.

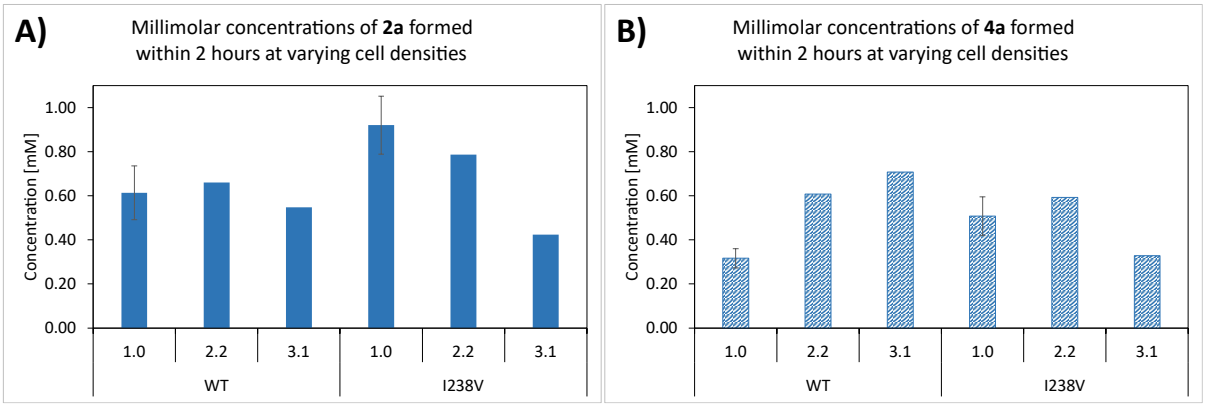

*Figure 19 – Conversion of (A) **2** and (B) **4** to the hydroxylated product within two hours in dependence of the cell densities 1.0, 2.,2 and 3.1 g_{CDW} L^{-1}. The data shown for 2.2 and 3.1 g_{CDW} L^{-1} were obtained from single replicates and those for 1.0 g_{CDW} L^{-1} from triplicates (error bars shown). For the reaction, an initial substrate concentration of 2 mM and a reaction temperature of 25 °C were used.*

The results from reactions with **4**, however, rather showed inverse dependencies. In reactions with the wild type, it appeared that the highest product concentration of around 0.7 mM was reached at the highest density of 3.1 g_{CDW} L^{-1}, less product was formed at the lower cell densities. With I238V the highest

product concentration of roughly 0.6 was reached at 2.2 g_{CDW} L^{-1}, similar to the result at lower density, but higher than at 3.1 g_{CDW} L^{-1}.

As will be discussed later, it was observed that substrate depletion in the very beginning of the reactions is one major issue that could be a limiting factor causing low activities. In an attempt to determine initial reaction rates before substantial amounts of substrate is depleted, another experiment was conducted with different reaction conditions and earlier sampling times. Following the procedure reported by Schrewe et al.[13], cell densities of 0.08 and 1 g_{CDW} L^{-1}, an initial substrate concentration of 2 mM, reaction temperatures of 25 and 30°C were used, and samples were taken within 7.5 minutes after reaction start. However, the absolute amount of product formed in this time span was below the detection limit of the GC-FID device used for quantification and, therefore, no activities could be calculated.

In addition to different cell densities, also varying substrate concentrations were tested. The activities towards **2** obtained with initial substrate concentration of 2 and 5 mM were highly similar with 5.8-6.0 U g_{CDW}^{-1} for *Msp* AlkB wildtype and 9.3-9.7 U g_{CDW}^{-1} for the mutant I238V (Figure 20, A). Comparison of the substrate depletion within four hours of reaction showed that independently of the initial amount of substrate added, the substrate concentration drops to around 0.4 mM after only 15 minutes in both cases, which corresponds to a drop by 80 and 92 %, respectively. Afterwards the concentration stays roughly constant or drops to zero after 4 hours. (Figure 20, B). The amount of substrate depleted within the first 15 minutes, is however not reflected in the amount of product formed. After that time, both the hydroxylated product **2a** and the hydrolysis product nonanoic acid were only below 0.1 mM each. Even though the concentrations of both products rise with time, and after four hours also the over-oxidised **2c** is detected, the final concentration of each product is still below 1 mM and the sum of all products together do not match the amount of substrate depleted. This shows that the mass balance is not closed. The vast depletion of the substrate can partially be explained by the hydrolysis of the substrate to nonanoic acid, however most of the substrate seems to get lost due to other factors.

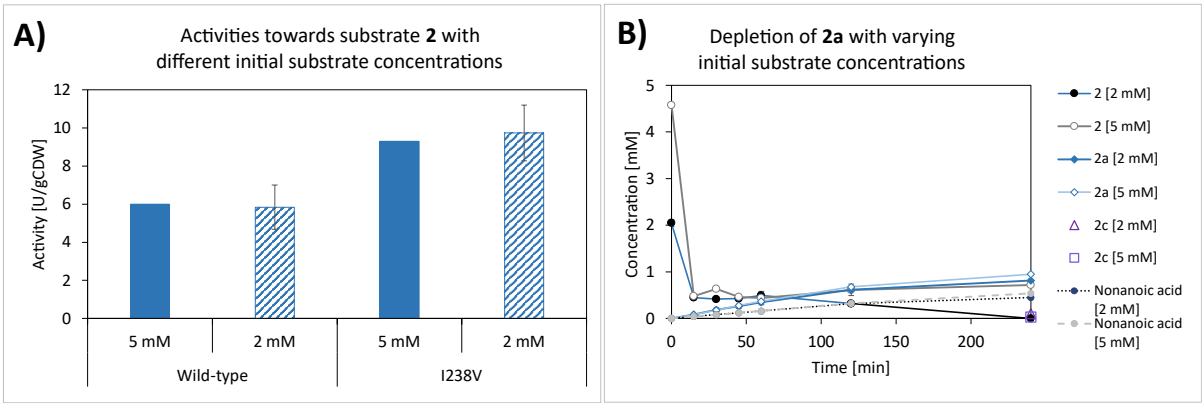

*Figure 20 – (A) Specific enzyme activities of Msp AlkB wild type and the mutant I238V towards **2** with initial substrate concentrations of 2 and 5 mM, respectively. The activities determined at 5 mM were tested in singlets and the activities at 2 mM in triplicates (error bars shown). (B) Depletion of the substrate **2** within four hours and the formation of the oxidation products **2a** and **2c**, as well as the hydrolysis product nonanoic acid, shown for both initial substrate concentrations. The cell density used was 1 g_{CDW} L^{-1} and a reaction temperature of 25 °C.*

A similar phenomenon was observed in reactions with the other substrates (Figure 22). Not only with **2**, but also with **5-6**, a drastic drop in substrate concentration to around 0.5 mM or even less was observed within the first 15 minutes of biotransformation. Only **4** showed a roughly linear substrate depletion. With substrate **6** it seemed that after around 45 minutes the decrease in substrate concentration was followed by a slight rise again. The substrate increase closely correlates with the formation of **6a,** which was around 0.05 mM, the product concentration seemed to stagnate up to 45-60 minutes. Only afterwards the concentration rose to 0.29 after two hours. indicative for issues with proper mixing in the practical workflow during preparation of the reaction.

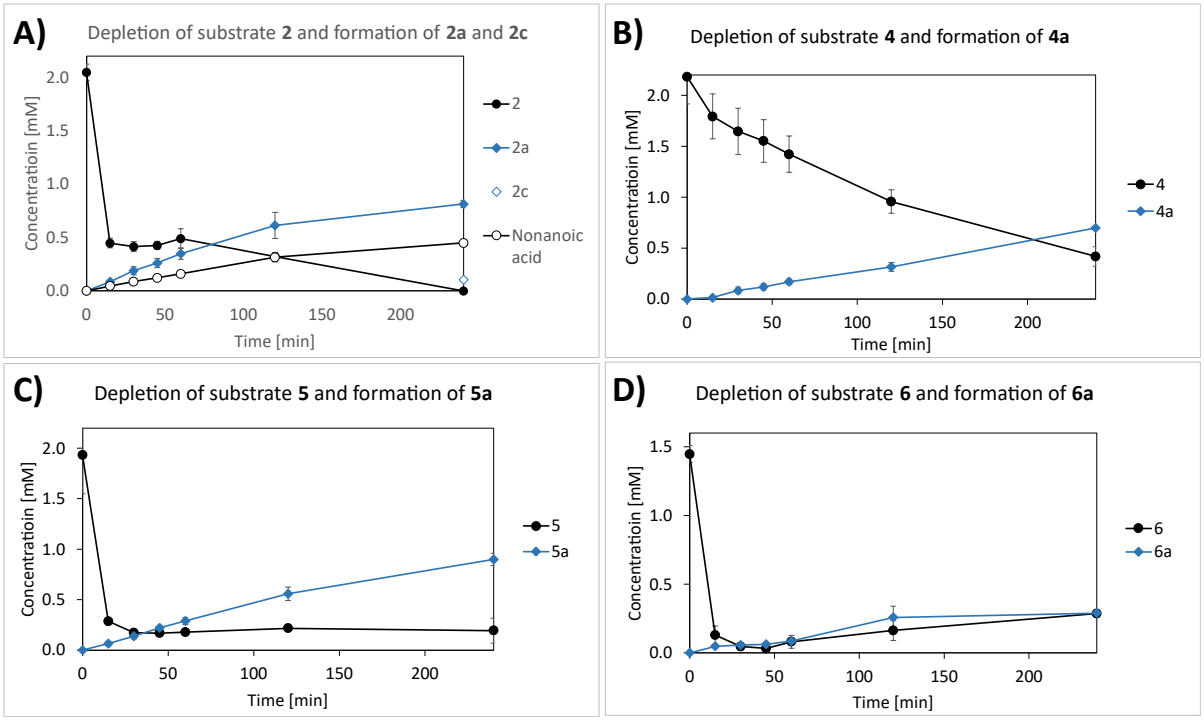

*Figure 21 – Depletion of substrates (A) **2**, (B) **4**, (C) **5** and (D) **6** and the product formation therefrom within four hours. Data shown in (A)-(C) were obtained from biotransformations with Msp AlkB wild type at 1 g_{CDW} L^{-1}. Data in (D) were obtained from biotransformations with the mutant W60S, at 3.2 g_{CDW} L^{-1}. An initial substrate concentration of 2 mM and a reaction temperature of 25 °C were used.*

In most reactions the product formation follows a linear curve almost up to two hours after reaction start, but with a way lower rate than the substrate depletion. Solely the formation of **6a** did not follow a linear curve, but rather shows a plateau within 15-60 minutes, and rises again between 1-2 hours, which could be due to irregular initial substrate concentrations as mentioned before. In the case of **2**, the substrate was not only converted to **2a** but at the same time also hydrolysed to nonanoic acid. The overoxidation product **2c** was only detected after four hours. In reactions with **4** and **5** overoxidized products were detected as well, however, mostly at very low concentrations after 4-24 hours and only in some replicates. Nevertheless, with those products identified and quantified, the mass balance of these reactions could not be closed. After four hours of biotransformation, the concentrations of **2a**, **4a** or **5a** ranged between 0.50-1.0 mM, and **6a** only around 0.25 mM.

All four substrates, **2** and **4**-**6**, showed comparable substrate depletion curves in the control reactions with the inactive mutant *Msp* AlkB H278A and only RCB without any cells (Figure 22). The concentration of **4** decreased only slightly and stayed at levels between 1.5-2.0 mM after 24 or 4 hours. With the other three substrates, the same drop in concentration as in the reactions with active enzyme variants to less than 0.25 mM within the first hour was observed. In tests with the inactive variant the substrate loss after one hour was on average 99 % (**2**), 11 % (**4**), 86 % (**5**) and 80 % (**6**). 28 % of **2** was hydrolysed to nonanoic acid. Without cells the substrate concentration decreased by 81 % (**2**), 14 % (**4**), 94 % (**5**) and 94 % (**6**) within one hour. The decrease in substrate concentration even without cells could be attributed to loss due to the high volatility or the poor miscibility and solubility of the compounds in the aqueous phase.

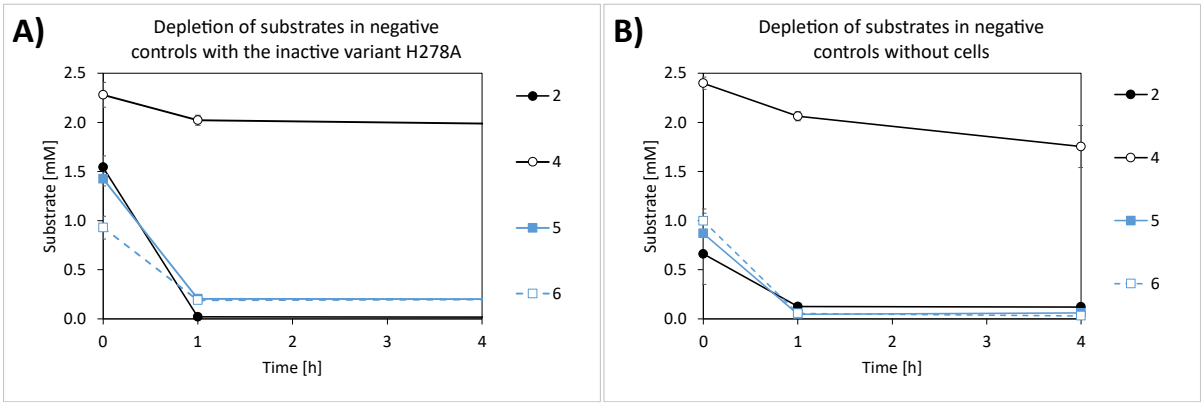

Figure 22 – Comparison between negative controls. (A) Substrate depletion within 24 hours of incubation with cells expressing the inactive variant H278A or (B) within 4 hours of incubation in resting cell buffer without cells. For the negative controls, a cell density of 1.0 g_{CDW} L^{-1}, an initial substrate concentration of 2 mM and an incubation temperature of 25 °C were used.

Moreover, an obvious difference between the initial substrate concentrations was seen. For substrate **4** an initial concentration between 2.0-2.5 mM was measured, while the initial concentrations for the other three substrates ranged between 1.0-1.5 mM both in the experiment with inactive variants or 0.5-1.0 mM without cells. In biotransformations with cells expressing active variants, the initial substrate concentrations were usually between 1.5 and 2.0 mM, in some cases however, also only 1 mM or less. Similar to the mixing issues with **6**, this might be caused by the volatility and limited miscibility of the substrates in aqueous solution.

3.6 Activities of *Msp* AlkB wild type and mutant variants

At first, the specific activities of the *Msp* AlkB wild type and the three mutants W60S, F169L and I238V were tested at a cell density of 3.1 g_{CDW} L^{-1} (Figure 23, A). The results were obtained from a single replicate but showed a clear trend. The I238V consistently outperformed the other enzyme variants with activities of between 7.8-8.7 U g_{CDW}^{-1} towards **2**, **4** and **5**. That represents a 1.8-fold increase compared to the wild type activities of 4.7-5.1 U g_{CDW}^{-1} towards **2** and **5**, and 3.6 U g_{CDW}^{-1} towards **4**. F169L also showed higher conversion rates than the wild type, especially towards **2** with 6.3 U g_{CDW}^{-1}, but also towards **4** and **5** with 4.2-5.2 U g_{CDW}^{-1}. With the wild type, **2** and **5** were converted at a rate between 4.7 and 5.1 U g_{CDW}^{-1}, and **4** with 3.6 U g_{CDW}^{-1}. The mutant W60S was 25 and 33 % less active towards **2** and

5 compared to the wild type, while **4** was converted with a 1.2-fold higher activity. Only one variant, however, was able to convert **6** to the terminal alcohol in detectable amounts with a rate of 0.6 U g_{CDW}^{-1}, The other enzyme variants showed a substrate preference for **2** and **5**, followed by **4**.

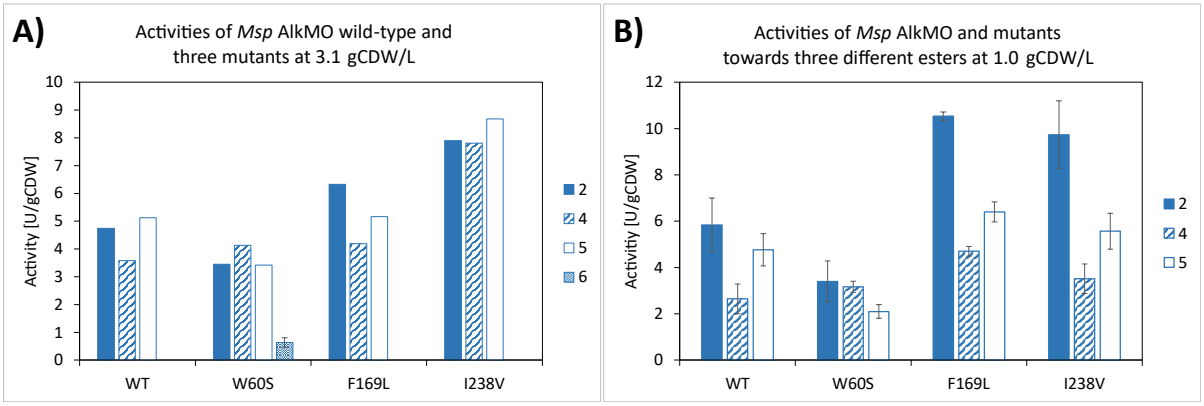

*Figure 23 – Comparison of specific activities between Msp AlkB wild type and the mutants W60S, F169L and I238V. (A) Activities determined at cell densities of 3.1, tested in single replicates. Only the activity of the mutant W60S towards **6** was derived from triplicates (error bar shown). (B) Activities determined at cell densities of 1.0 g_{CDW} L^{-1}, tested in triplicates (error bars shown). For the reaction an initial substrate concentration of 2 mM and a reaction temperature of 25 °C were used.*

The activities of the same four variants were also quantified at a lower cell density of 1.0 g_{CDW} L^{-1} and tested in triplicates (Figure 23, *B*). Overall, the rates follow the same trend as for 3.1 g_{CDW} L^{-1} except for the variant F169L. Surprisingly at lower cell densities, this variant surpasses the activities the I238V for all three substrates, in contrary to the experiment at higher cell density. However, in comparison to the wild type which converted **2** with a rate of 5.8 U g_{CDW}^{-1}, both mutants F169L and I238V showed around a 1.8- or 1.7-fold enhanced activity with 10.5 and 9.7 U g_{CDW}^{-1}, respectively. The specific rate of 10.5 U $gCDW^{-1}$, was the highest measured across all tests with these mutants and substrates. In general, the substrate preference for **2** appears to be much more significant for all four variants at lower cell densities. Substrates **4** and **5** were converted by the wild type with 2.6 U g_{CDW}^{-1} and 4.8 U g_{CDW}^{-1}, respectively. The single-mutants F169L and I238 exceeded the wild type activity towards **4** by a factor of 1.8 and 1.3, and towards **5** by 1.3- and 1.2-fold. Nevertheless, the rates towards those two acetates were lower than in the previous experiments with higher cell densities. The mutant W60S showed lowest conversion rates towards **2** and **5** with only 40 and 55 % of the activity obtained with the wild type. For **4** a 1.2-fold increase to the wild type, was observed, same as in biotransformations with higher cell densities. Activity toward **6** at a cell density of 1.0 g_{CDW} L^{-1} is not shown since no product formation could be detected under these conditions.

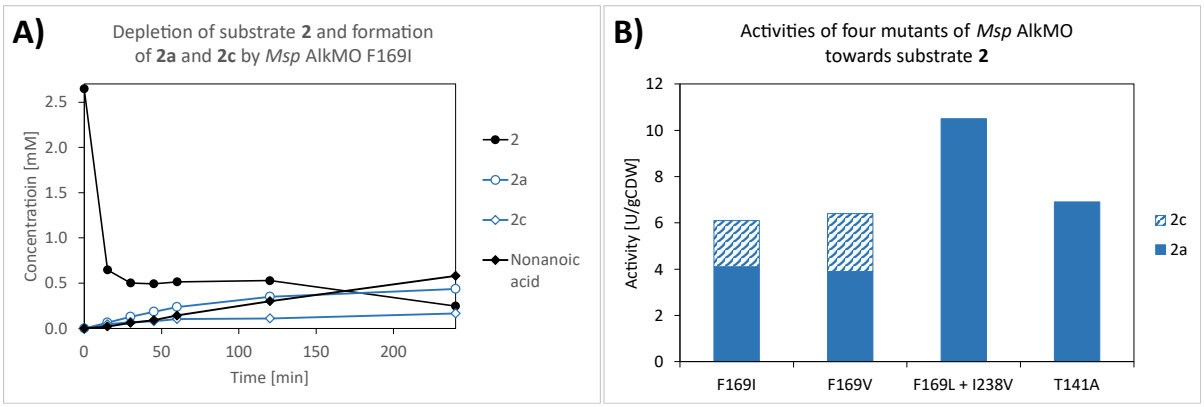

*Figure 24 – (A) Depletion of substrate **2** within four hours and the formation of **2a**, **2c** as well as the hydrolysis product nonanoic acid by the mutant F169I. (B) Comparison of the specific activities towards **2** among the Msp* AlkB *mutants F169I, F169V, T141A and the double mutant* F169L/I238V. *For the reaction a cell density of 1 g_{CDW} L^{-1}, an initial substrate concentration of 2 mM and a reaction temperature of 25 °C were used.*

Four additional enzyme variants, F169I, F169V, T141A and the double mutant F169L/I238V, were tested as a single replicate and characterized regarding their activities towards **2**. The conversion rates to **2a**, ranged from 3.9-4.1 U g_{CDW}^{-1} in the F169 mutants, to 10.5 U g_{CDW}^{-1} in the double mutant and 6.9 U g_{CDW}^{-1} in the T141A variant. While the double mutant performed best, followed by the T141A variant, the F169 mutants exhibited even lower hydroxylation rates than that found for the wild type with 5.8 U g_{CDW}^{-1}. Remarkably though, those two variants showed significant overoxidation to **2c** which could already be detected after 15 minutes. As represented in the diagram (Figure 24, A), the formation of overoxidized product occurred simultaneously to the hydroxylation reaction, indicating overoxidation by the monooxygenase itself rather than the cell background. The formation rate of both compounds followed a linear curve up to 45 minutes and allowed calculations of separate conversion rates towards the **2a** and **2c**. The overall activities are represented by the sum of hydroxylation - and overoxidation rate, which made up 6.1 U g_{CDW}^{-1} and 6.4 U g_{CDW}^{-1} for F169I and F169V, respectively (Figure 24, B). In comparison to the wild type this represents 1.1-fold increase in activity. In contrast, with the wild type enzyme and other variants, the formation of **2c** was either not observed at all or only after 4 hours (Figure 20, B and Figure 21, A).

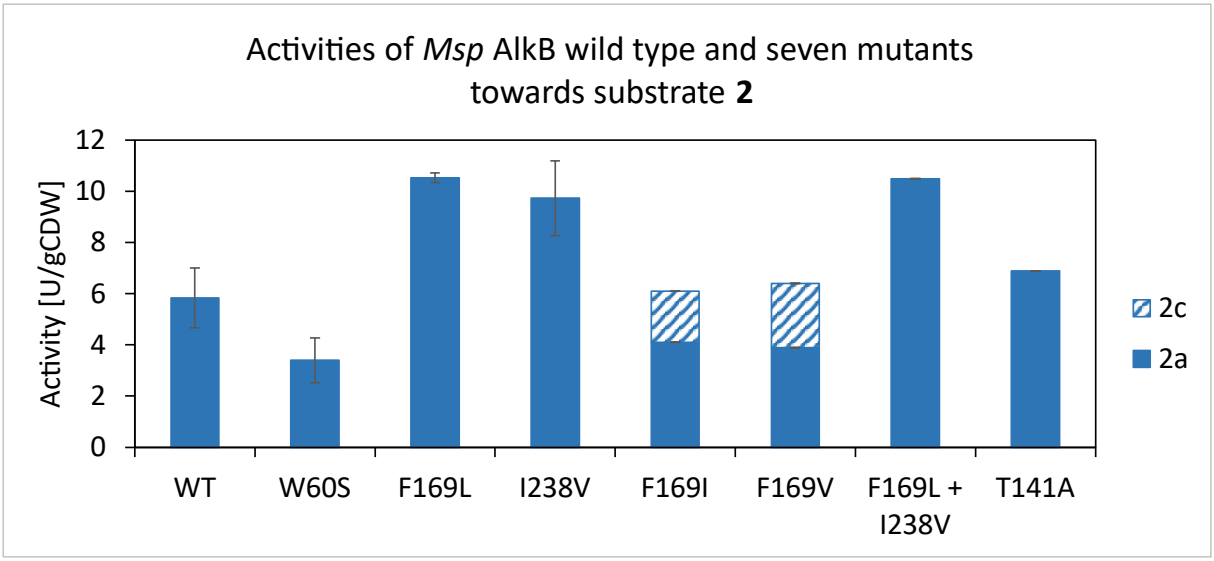

*Figure 25 – Comparison of the specific activities towards **2** of Msp AlkB wild type and seven other mutants. The first four variants (wild type – I238V) were tested in triplicate. The last four variants (F169I – T141A) were tested in singlets and show preliminary results. For the reaction a cell density of 1 g_{CDW} L^{-1}, an initial substrate concentration of 2 mM and a reaction temperature of 25 °C were used.*

Comparison of all variants tested with **2** and the same conditions, showed that almost all mutants outperformed the wild type variant of *Msp* AlkB, except for the W60S mutant (Figure 25). Both single mutants F169L and I238V, as well as the double mutant harbouring both mutations, showed around 1.8-fold improved hydroxylation rate. The T141A variant exhibited a 1.2-fold increase. Even though the cumulative activity of the single mutants F169I and F169V were found to be only by 10 and 5% higher than wild type, respectively, they showed enhanced potential to catalyse overoxidations to the terminal acid.

4 Discussion

4.1 Substrate acceptance

The wild type variants of *Pp* AlkB and *Msp* AlkB showed an overall very similar pattern of substrate preferences. While the short and medium chain esters **1**-**2** and **4**-**5** were well accepted, **3** and **6** were hardly oxidised as only trace amounts of the hydroxylated product were detected by GC-MS and were not detectable by GC-FID at all. Interestingly, only substrate **1** seemed to be converted to the terminal alcohol by *Pp* AlkB and to the terminal acid by *Msp* AlkB (Figure 38), although the identity of these products still needs to be confirmed. Even though putative overoxidation products from the other substrates were detected as well, it was not observed that any of both enzymes exclusively formed either the terminal alcohol or the acid. The other substrates were primarily converted to the alcohol and, if overoxidation occurred, a lower signal from the terminal acid was detected. In the case of substrate **6** it remains to be clarified which compound is represented by the second peak eluting after **6a**, since the hypothesized hydrolysis products did not match with this peak in GC-MS analysis. (Figure 17 and Figure 42). It cannot be excluded, that host intrinsic aldehyde- and alcohol dehydrogenases catalyse the hydrolysis and oxidation of the substrate. In negative controls with substrate **6** and the inactive variant H278A, a low signal peak was observed at the same retention time, which indicates that host intrinsic might play a role in the background. However, more experimental evidence is needed to draw a clear conclusion.

Initially, the co-expression of AlkL showed a beneficial effect for the long esters **3** and **6**. As far as could be assessed from GC-MS analysis without quantification, the hydroxylated products were hardly detectable in biotransformation samples with the *alkBFGST* system, whereas a more distinct peak of the hydroxy product was detected in reactions with *alkBFGLST*. Thus, AlkL seemed beneficial for making the esters with a C_{12} alkyl chain better available for the hydroxylation system. This confirms that the long substrates are accepted by *Msp* AlkB and that outer membrane transporter is especially important for longer substrates with $\geq C_{12}$, as reported for linear alkanes and long chain esters [34], and that it also supports the import of esterified linear compounds consistent with previous findings.[13,51,95,99] Although the hydroxy-product peaks of the C_5 and C_9 esters consistently appeared lower with AlkL, their successful functionalization was clearly confirmed, both from reactions with and without AlkL. Therefore, only strains co-expressing AlkL were used in the follow-up experiments for the activity determination. Nevertheless, it could be interesting to quantify the effect of AlkL on the small and medium chain length esters, with regard to the optimization of the whole cell activity for larger scale applications. Even though AlkL was reported in several publications to allow for improved availability and conversion of longer substrates, the expression of *alkBFGLST* was also found to cause slower cell growth compared to *alkBFGST*. The authors suggest that inappropriate ratios of expression of individual alkane hydroxylase pathway genes could have a detrimental effect on the cell and showed that a more

finely modulated expression of AlkL from a separate plasmid improved the toxic effect and increased the product yield.[34]

Comparing the conversion rates of *Msp* AlkB wild type for the substrates **2** and **4**-**5**, revealed that **2** was the preferred substrate which was converted with 5.8 U g_{CDW}^{-1}, followed by **5** and **4** with 4.8 and 2.6 U g_{CDW}^{-1}. Since substrates **2** and **5** were converted faster than **4**, there is an indication that esters with a C_9 alkyl chain are preferred over those with C_5 or C_{12}. Since the whole molecules including the ester and methyl group are longer, it might be that a minimal length of hydrophobic tail is required for efficient binding in the hydrophobic pocket without repulsion of the polar ester group, while esters with a C_{12} alkyl chain simply cannot be accommodated well. The preference for **2** is consistent with previous findings for *Pp* AlkB[13,51], but the reported activities of around 105 and 128 U g_{CDW}^{-1} (with AlkL co-expressed)[51,95], could not be reproduced despite several attempts. The main difference is that the reported activities represent initial activities that were measured within the first five minutes of reaction whereas the activities in this work were determined within the time frame of linear product formation rates, which was between 30-60 minutes. When sampling within only 5-7 minutes, the absolute amount of hydroxylated product formed was below the limit of detection of the GC-FID device used, making it impossible to determine any rates.

4.2 Optimisation of the experimental procedure

4.2.1 Substrate depletion

The initial experiments with both *Pp* and *Msp* AlkB revealed that methyl esters were hydrolysed and trans-esterified to ethyl esters to a significant extent, as the substrate stock was prepared in ethanol. The exchange of substrate solvent from ethanol to DMSO helped to obtain clearer chromatograms without any ethyl esters, but the substrate hydrolysis could not be avoided. In a negative control with cells expressing inactive variant *Msp* AlkB (H278A) about 28% of **2** was hydrolysed to the free fatty acid in one hour. Although, it must be pointed out that in biotransformations with e.g. *Msp* AlkB wild type the hydrolysis of **2** only yielded 0.17 mM of nonanoic acid from around 2 mM, which indicates that alkane monooxygenases compete with host intrinsic hydrolases and thus counteract to some extent substrate degradation. Altough the hydrolysis of methyl esters **1** and **3** were not quantified, the respective free fatty acids were clearly detected by GC-MS. This probably leads to metabolization of the free fatty acids along the β-oxidation pathway, decreasing the amount of substrate available for the biotransformations. In contrast, from the acetate esters **4**, **5** and **6** only low or no signals of hydrolysis products were detected GC-MS, but in such low quantities so that they could not be quantified via GC-FID. In some cases, hydrolysis of oxidised products was observed, but the respective hydroxy acids and diols were found at even lower levels and could not be quantified., Ester hydrolysis was mentioned in previous publications, but mostly reporting product hydrolysis, while substrate hydrolysis was not observed or only to a limited extent.[13,73,100,101] Previously, substrate **3** was terminally oxidised by the AlkBGT system in *E. coli*, and the undesired hydrolysis of the oxidised products thereof was reported to be effectively reduced through

a knock-out of the *bioH* gene. The BioH enzyme was found to be one of the host-intrinsic enzymes responsible for hydrolysis of medium chain length FAMEs. Even though the opposite was observed in this work (the primary hydrolysis of the substrate and less of the oxidised products), it could be interesting to test the *BioH* deletion mutant for future work.[101]

In addition, evaporation seemed to be the main cause of substrate depletion. In biotransformations with substrates **2** and **5**-**6**, the initial concentration of 2 mM dropped by 75 % or more within only the first 15 minutes of reaction which was by far not reflected in the less than 0.1 mM of oxidation products formed in that time (Figure 21). The depletion of substrate **4** and the conversion to the hydroxy product followed rather a linear trend, even though the mass balances were not closed here either. In negative controls without any cells the substrates **2** and **4**-**6** only **4** showed a rather linear decrease and dropped by 14 % in one hour, while the other three substrates showed a drastic drop by 81-94 %. Except for **2**, to other substrates were not hydrolysed as extensively, so that these side products could not be quantified by GC-FID. Regarding the volatility of the esters, the drastic depletion is therefore mainly attributed to evaporation. In controls with resting cells expressing the inactive *Msp* AlkB (H278A) **2**, **5** and **6** were depleted by 80-99 %, while **4** declined by 11 % within one hour. Only for substrate **2** the depletion was highest in controls with living cells as almost one third of the initial 2 mM were hydrolysed to nonanoic acid in one hour. However, this also means that less was lost exclusively due to evaporation, comparing to the controls without cells. In the presence of cells, the substrates generally seemed to disappear to a lower extent, indicating that they are taken up by the cells.

It was reported that in similar experiments negative controls with ethyl nonanoate and cells harbouring an empty plasmid showed a substrate depletion of about 48 % within one hour.[73] In the work of Schrewe et al.[13] substrate **2** was tested as well, with initial concentrations of 2.5 and 5 mM. It was shown that the substrate depletion closely matched the product formation. In that case the mass balances were almost closed. This could not be reproduced, and the reason for this discrepancy in substrate stability remains to be clarified. There is room for optimisation in the experimental procedure when working with volatile compounds. Several publications working with similar esters did not mention if or how the samples were stored frozen, or if they were extracted directly.[5,13,51] Freezing and thawing of samples may contribute to the loss of analytes, which was also discussed in our group, but since the initial substrate concentration in most cases matched the expected concentration quite well, there are probably other factors that cause this loss during reactions. As in some cases even the initial substrate concentration was lower than expected, it is assumed that volatility plays the major role that leads to loss of the substrate already during substrate addition and reaction setup and during sample extraction afterwards.

4.2.2 Cell density

From the three different cell densities tested (1.0, 2.2 and 3.1 $g_{CDW}\,L^{-1}$) different results were obtained depending on the substrate. In biotransformations of **2** with *Msp* AlkB wild type or I238V, all three cell

densities showed similar activities, but at the lowest density 1.0 $g_{CDW}\,L^{-1}$ the activities of *Msp* wild type and I238V were highest with close to 6 and 10 U g_{CDW}^{-1}, respectively. Analysing the conversions, a similar pattern showed that **2** was converted most at lower cell densities. With **4** quite the opposite was observed, with activities of 4 and 8 U g_{CDW}^{-1} for *Msp* wild type and I238V, at the highest cell density, while the activities at lower densities only reached half. The conversions however indicated 2.2 $g_{CDW}\,L^{-1}$ as optimal cell density, which seemed contradictory. In the case of **4**, the frozen samples from experiments with the lower cell densities had been stored at -20 °C for two weeks which might have led to loss of analytes due to evaporation and in following experiments samples were always analysed within one week. This again points out the importance of proper handling of samples with volatile compounds. As a consequence, the results with **2** were taken as basis for further experiment, therefore the activity determination at a cell density of 1.0 $g_{CDW}\,L^{-1}$ was used. Moreover, this decision was led by previous publications reporting high activity levels of the AlkBGT system, when 1 $g_{CDW}\,L^{-1}$ was applied.[13,51] Additional reasoning was regarding oxygen availability, where we expect that lower cell densities might be advantageous compared to higher ones.

4.2.3 Substrate concentration

In the initial experiments, a substrate concentration of 2 mM was used, but as discussed above, large amounts of it were lost through evaporation and to a small extent through hydrolysis. Aiming for improved substrate availability, substrates **2** and **4** were tested with starting concentrations of 2 and 5 mM. The resulting activities of *Msp* AlkB wild type and I238V and the time course of the substrate and product formation were compared. Against expectation, the substrate concentration had dropped to roughly 0.4 mM, irrespective of the starting concentration and the product formation curves looked almost alike (Figure 20). Consequently, no differences were seen when comparing the product formation rates, which were around 6 and 10 U g_{CDW}^{-1} for *Msp* AlkB wild type and I238V, respectively.

This finding contrasted what was expected based on publications from comparable experiments. Schrewe et al. demonstrated that a starting concentration of 5.1 mM led to the highest conversion with 95 % of the terminal alcohol and 4 % aldehyde. In that case a closed mass balance was obtained, whereas at lower substrate concentrations of 1.0 and 2.5 mM, the difference between substrates consumed and products formed left an unclosed mass balance. Even though the authors attributed the gap to product degradation[13], a higher amount of substrate was expected to make a higher amount available for the cells. Putatively, the amount of substrate that is lost within the first 15 min is due to evaporation from the reaction buffer and only a small fraction of the substrate added is retained by the cells. As the same cell density was used, it could explain why the concentration after 15 minutes was almost identical regardless of the amount added. Maybe the substrate uptake by the cells is too slow compared to their volatility which, counterintuitively, might be connected to the AlkL co-expression and the toxicity mentioned before.

4.3 Activities in comparison

The activities of the *Msp* AlkB wild type and especially the three mutants W60S, F169L and I238V towards the substrates **2** and **4-6** were initially determined at 3.1 g_{CDW} L^{-1} and then at the optimised cell density of 1.0 g_{CDW} L^{-1}. The methyl esters **1** and **3**, however, were excluded from activity determination experiments due to their instability towards hydrolysis.

At higher cell density, the variant I238V had shown the highest activities towards the three substrates **2** and **4-5** with hydroxylation rates of rounded 8 U g_{CDW}^{-1}, surpassing the wild type activity by 1.8-fold (Figure 23). The mutant F169L had also shown improved activity towards **2** and **5** with around 6 and 5 U g_{CDW}^{-1}, respectively. The variant W60S had shown slower activity overall but was the only variant that had formed detectable amounts of **6a** and for which a conversion rate of 0.6 U g_{CDW}^{-1} could be calculated. In principle, lower activities towards longer substrates is in accordance with findings by van Nuland et al. who reported decreasing activity of *Pp* AlkB towards esters with a longer aliphatic chain of C_8.[51] On the other hand with AlkL co-expression, *Pp* AlkB wild type was also shown to convert **6** with 53 U g_{CDW}^{-1}.[95] However, that is probably also due substrate limitations due to evaporation as discussed before. In all three replicates the hydroxylation rate of **6** did not follow a clear linear curve, and the substrate concentration seemed to increase after two hours. Supposedly, this is due to a technical issue during reaction set-up that led to uneven initial substrate concentrations in the individual vials. Limited amounts of hydroxy product of **6** formed by the wild type were observed in GC-MS as well, but were too low for quantification with by GC-FID. This showed that the exchange of the bulky residue W60 to a smaller one in *Msp* AlkB is also a key to enable conversions of longer substrates, in accordance with findings on the corresponding position in *Pp* AlkB (W55S).[14,8,41]

Interestingly, at 1.0 g_{CDW} L^{-1} the mutant F169L surpassed the activity of I238V, regardless of the substrate. The highest activity reached towards **2** were 10.5 U g_{CDW}^{-1} by F169L and 9.7 U g_{CDW}^{-1} by I238V, which represented a 1.8- and 1.7 increased activity compared to the wild type. Since the variant F169L outperformed I238V at lower cell densities, the observation hints at a correlation between cell density and the beneficial effect of exchanging Phe to a Leu residue in position 169, which could be connected to oxygen availability. Since position 169 faces the active site, it seems plausible that the exchange of a Phe to a Leu might offer more space for rapid entry or more stable coordination of O_2 during catalysis. At higher cell densities this effect could be decreased due to oxygen limitation. In general, with decreased cell density the activities towards **2** seemed to have risen across the four variants. The conversion rates of the other substates **4**-**5** were lower, though, when compared to the higher cell density. Why only for the conversion of substrate **2** was beneficial the lower cell densityis still an open question. One reasons could be that the acetate esters are taken up less efficiently by AlkL than the methyl esters, so that a higher cell density is required to convert the same amount of substrate which, however, also decreases the specific activity in turn.

Finally, three more single mutants (F169I, F169V, T141A) and the double mutant F169L_I238V of *Msp* AlkB were tested with substrate **2**. Even though they were only tested in single replicates, the results indicated interesting tendencies. Both variants F169I and F169V had shown a total activity only around 6.1 and 6.4 U g_{CDW}-1 but two thirds of the product formed represented the hydroxylated product and one third for the over oxidised one (Figure 24). These were the first mutant variants for which a simultaneous formation of hydroxylation and overoxidation products was observed in the time course of the reaction that was followed. Usually, overoxidation of **2** was observed earliest 2 hours after reaction start. As hypothesised by van Nuland et al.[5] this is probably due to a competition between the alcohols formed and the un-oxidised substrate, which is the preferred substrate at first, and at limiting substrate concentrations the alcohol is being increasingly accepted and over-oxidised. Therefore, it is interesting that these two mutants seemed to catalyse hydroxylation and over-oxidation in parallel. In combination with the finding that the highest activities were obtained with the variant F169L, the results suggest, that an exchange of the aromatic and comparably bulky Phe in this position to a smaller hydrophobic residue improves oxidation efficiency. There are two hypotheses that could explain this tendency. If hydroxylation and over-oxidation is catalysed consecutively without the newly formed product leaving the enzyme, the residues 169I and 169V might lead to increased oxygenation efficiency that exceeds the rate of hydroxylated product leaving the active site. On the other hand, it is also possible that the entrance of an already hydroxylated product is facilitated due to more space in the active site and the substrate preference for hydrophobic methyl termini is reduced. Interestingly though, despite the replacement of Phe169 in F169L, this mutant did not show simultaneous hydroxylation and over- oxidation, while the exchange to the smaller Val and the larger Ile both led to higher over-oxidation. The reason for this effect is not completely understood, thus it could be interesting to test mutants with even smaller amino acids in this position. Nevertheless, it shows that the mutation of a single amino acid can shift the tendency towards overoxidation which might be especially interesting for the production of di-acids.

In contrast T141A and F169L_I238V had shown the exclusive formation of terminally hydroxylated product, at least in the time that the reaction was followed. T141A showed similar hydroxylation rates compared to the total activity of the mutants F169I and F169V. The double mutant F169L_I238V however had the highest activity of 10.5 U g_{CDW}^{-1} in accordance with the mean activities found for both single mutants F169L and I238V tested individually. This finding showed that the individual mutations F169L and I238V do not lead to additive or multiplicative effects when combined. The reason for this might be their spatial distance and diverse roles for enhancing the activity compared to the wild type and it is consistent with other findings from our lab as published before.[66]

Methyl ester **2** served as standard substrate for comparison with values stated in literature, as it was reported to be oxidized at rates between 84-104 U g_{CDW}^{-1} by the *alkBGT* system, and with the co-expression of AlkL the activity was even elevated 1.25-fold to 105 U g_{CDW}^{-1}.[13,51] With neither of the conditions and mutants tested, these high activities could be reproduced. It should be noted though, that the reported activities refer to initial rates. The significant drop in substrate concentration, however,

precluded the determination of initial conversion rates in this work, so that the full catalytic potential of the enzyme variants tested is probably higher than the specific rates presented here suggest.

5 Conclusion and outlook

This thesis reports the characterisation of an alkane-1-monooxygenase from an unspecified *Marinobacter* species, which was analysed for its substrate scope and employed for targeted oxyfunctionalization of linear esters for the first time. Regiospecific oxyfunctionalization employing alkane monooxygenases offers sustainable pathways toward interesting products such as diols, hydroxy esters and diacids. While AlkB from *Pseudomonas putida* is well-studied converting a range of different substrate types, its rather narrow range of substrate sizes accepted still represents a limitation for its versatile applications. For the rational enzyme engineering it is therefore essential to learn further about these membrane-bound monooxygenases by comparing with related and mutated enzymes. This will facilitate identifying features that determine a given substrate preference and activity.

Overall, the substrate acceptance of *Pp* and *Msp* AlkB was very similar. All six substrates **1-6** were accepted by both enzymes and converted to the terminal hydroxylated products. For the long C_{12} esters the AlkL co-expression increased the amount of hydroxylated product to amounts detectable by GC-MS, but these levels were still not quantifiable by GC-FID. However, it was shown that the *Msp* AlkB wild type has the potential to catalyse their conversion. Interestingly substrate **1** was converted to two distinct products by the two homologs, putatively to the **1a** by *Pp* AlkB and overoxidized to **1c** by *Msp* AlkB, although these findings were not confirmed yet. It is not known what could cause this discrepancy, since the pattern of products formed from the other substrates was highly similar.

Among the different mutants interesting candidates were identified. Almost all mutants tested with substrate **2** outperformed the wild type, with the best performing mutants F169L, I238V and the double mutant F169L_I238V, reaching up to a 1.8-fold improvement. Also, F169I and F169V were identified as interesting candidates due to their ability to hydroxylate and over-oxidise the hydroxy product in parallel, even though their cumulative activity in preliminary results was only a 1.1-fold improvement compared to the wild type. Besides, the AAs **4** and **5** were converted by the mutants W60S, F169L and I238V as well, with preference for the medium chain length ester **5**, although the activities towards those were 2- and 3- fold lower, respectively compared to **2**. Lastly, variant W60S was the only mutant that was capable of hydroxylating **6** in detectable quantities so that specific rates could be determined. This shows that, despite the seemingly more spacious substrate binding site in *Msp* AlkB, the position W60 plays a decisive role in the acceptance of long chain substrates.

Overall, both the *Msp* AlkB wild type and mutant variants showed about 10-fold lower activities than published for **2** and **6** before.[13,95] On the one hand, the reported rates indicate initial rates which could not be reproduced here due to the detection limit of the GD-FID device used. Moreover, the substrate limitation caused by evaporation and substrate hydrolysis depending on the substrate caused substrate limitation and precluded the determination of the full potential of the biocatalytic system in *E. coli* BL21 (DE3). If *Msp* AlkB is superior to *Pp* AlkB for the oxyfunctionalization of the esters **1-6**, cannot be concluded as the results obtained here are not comparable with values reported in literature. It is unclear,

why other groups using the same expression host and a similar experimental procedure mainly reported product degradation but not substrate hydrolysis as a practical issue and how the volatility of such substrates could be avoided. Hence, additional experiments could be approached in which an *E. coli* strain containing the *BioH* knockout could be tested to see if this can reduce substrate hydrolysis. Also, head-space analysis can be done to determine if the largest proportion of the substrates are indeed lost through evaporation. Additionally, the direct extraction of samples without freezing should be tested to avoid potential substrate loss, as well as the establishment of calibration curves with cells expressing an inactive AlkB variant or freezing the calibration samples as well.

The data presented here nevertheless showed that AlkB from *Marinobacter* exhibits high regioselectivity for the oxidation the terminal methyl groups, comparable to *Pp* AlkB. Therefore, it can be applied for the terminal oxidation of FAMEs and alcohol acetates with alkyl chains of C_5-C_{12} in length. Enzyme variants catalysing exclusive terminal hydroxylation could be especially interesting for the synthesis of hydroxy fatty acids and diols. Since product mixes are generally undesired in large scale processes, the two variants F169I and F169V might represent two interesting candidates for further tuning towards even higher over-oxidation of their substrates for the synthesis of di-acids. In accordance with the observations reported in literature, substrate **2** was functionalised most efficiently under all condition tested, and at 3.1 g_{CDW} L^{-1} substrate **5** also showed comparable conversions. Thus, both C_9 esters can be regarded as suitable substrates for biotransformations with *Msp* AlkB. Regarding the practical experiment design there are still some obstacles to overcome to improve substrate stability and availability. This would help to reveal the true potential of the enzyme variants tested herein, as well as improving the efficiency of AlkB towards a high-performance biocatalyst. Nevertheless, this work provides a basis for further investigation of a so far uncharacterised homolog of AlkB, which can streamline further optimisation of members of this class of monooxygenases for their application in more environmentally friendly industrial processes.

6 References

1. Wu, Y., Paul, C. E. & Hollmann, F. Mirror, mirror on the wall, which is the greenest of them all? A critical comparison of chemo- and biocatalytic oxyfunctionalisation reactions. *Green Carbon* **1**, 227–241 (2023).

2. Torres Pazmiño, D. E., Winkler, M., Glieder, A. & Fraaije, M. W. Monooxygenases as biocatalysts: Classification, mechanistic aspects and biotechnological applications. *J. Biotechnol.* **146**, 9–24 (2010).

3. Xu, F. Applications of oxidoreductases: Recent progress. *Ind. Biotechnol.* **1**, 38–50 (2005).

4. Urlacher, V. B., Lutz-Wahl, S. & Schmid, R. D. Microbial P450 enzymes in biotechnology. *Appl. Microbiol. Biotechnol.* **64**, 317–325 (2004).

5. van Nuland, Y. M., de Vogel, F. A., Scott, E. L., Eggink, G. & Weusthuis, R. A. Biocatalytic, one-pot diterminal oxidation and esterification of n-alkanes for production of α,ω-diol and α,ω-dicarboxylic acid esters. *Metab. Eng.* **44**, 134–142 (2017).

6. van Beilen, J. B. & Funhoff, E. G. Expanding the alkane oxygenase toolbox: new enzymes and applications. *Curr. Opin. Biotechnol.* **16**, 308–314 (2005).

7. Scheps, D. *et al.* Synthesis of ω-hydroxy dodecanoic acid based on an engineered CYP153A fusion construct. *Microb. Biotechnol.* **6**, 694–707 (2013).

8. J, K. D. & H, A. F. Regioselective alkane hydroxylation with a mutant AlkB enzyme. (2012).

9. Peters, M. W., Meinhold, P., Glieder, A. & Arnold, F. H. Regio- and Enantioselective Alkane Hydroxylation with Engineered Cytochromes P450 BM-3. *J. Am. Chem. Soc.* **125**, 13442–13450 (2003).

10. Fu, H., Newcomb, M. & Wong, C. H. Pseudomonas oleovorans monooxygenase-catalyzed asymmetric epoxidation of allyl alcohol derivatives and hydroxylation of a hypersensitive radical probe with the radical ring-opening rate exceeding the oxygen-rebound rate. *J. Am. Chem. Soc.* **113**, 5878–5880 (1991).

11. Eggink, G., Lageveen, R. G., Altenburg, B. & Witholt, B. Controlled and functional expression of the Pseudomonas oleovorans alkane utilizing system in Pseudomonas putida and Escherichia coli. *J. Biol. Chem.* **262**, 17712–17718 (1987).

12. van Beilen, J. B., Kingma, J. & Witholt, B. Substrate specificity of the alkane hydroxylase system of Pseudomonas oleovorans GPo1. *Enzyme Microb. Technol.* **16**, 904–911 (1994).

13. Schrewe, M., Magnusson, A. O., Willrodt, C., Bühler, B. & Schmid, A. Kinetic Analysis of Terminal and Unactivated C□H Bond Oxyfunctionalization in Fatty Acid Methyl Esters by Monooxygenase-Based Whole-Cell Biocatalysis. *Adv. Synth. Catal.* **353**, 3485–3495 (2011).

14. van Beilen, J. B. *et al.* Identification of an amino acid position that determines the substrate range of integral membrane alkane hydroxylases. *J. Bacteriol.* **187**, 85–91 (2005).

15. Schaffer, S. & Haas, T. Biocatalytic and Fermentative Production of α,ω-Bifunctional Polymer Precursors. *Org. Process Res. Dev.* **18**, 752–766 (2014).

16. Bińczak, J., Dziuba, K. & Chrobok, A. Recent Developments in Lactone Monomers and Polymer Synthesis and Application. *Mater. (Basel, Switzerland)* **14**, (2021).

17. Mathys, R. G., Schmid, A. & Witholt, B. Integrated two-liquid phase bioconversion and product-

recovery processes for the oxidation of alkanes: Process design and economic evaluation. *Biotechnol. Bioeng.* **64**, 459–477 (1999).

18. Hoschek, A., Bühler, B. & Schmid, A. Stabilization and scale-up of photosynthesis-driven ω-hydroxylation of nonanoic acid methyl ester by two-liquid phase whole-cell biocatalysis. *Biotechnol. Bioeng.* **116**, 1887–1900 (2019).

19. Favre-Bulle, O., Schouten, T., Kingma, J. & Witholt, B. Bioconversion of n-octane to octanoic acid by a recombinant Escherichia coli cultured in a two-liquid phase bioreactor. *Biotechnology. (N. Y).* **9**, 367–371 (1991).

20. Groves, J. T., Feng, L. & Austin, R. N. Structure and Function of Alkane Monooxygenase (AlkB). *Acc. Chem. Res.* **56**, 3665–3675 (2023).

21. Lee, M. & Chandler, A. C. A Study of the Nature, Growth and Control of Bacteria in Cutting Compounds. *J. Bacteriol.* **41**, 373–386 (1941).

22. van Beilen, J. B. *et al.* Analysis of Pseudomonas putida alkane-degradation gene clusters and flanking insertion sequences: evolution and regulation of the alk genes. *Microbiology* **147**, 1621–1630 (2001).

23. Peterson, J. A., Kusunose, M., Kusunose, E. & Coon, M. J. Enzymatic ω-Oxidation: II. Function of rubredoxin as the electron carrier in ω-hydroxylation. *J. Biol. Chem.* **242**, 4334–4340 (1967).

24. Chakrabarty, A. M., Chou, G. & Gunsalus, I. C. Genetic regulation of octane dissimilation plasmid in Pseudomonas. *Proc. Natl. Acad. Sci. U. S. A.* **70**, 1137–1140 (1973).

25. Eggink, G. *et al.* Structure of the Pseudomonas putida alkBAC operon. Identification of transcription and translation products. *J. Biol. Chem.* **262**, 6400–6406 (1987).

26. Kok, M. *et al.* The Pseudomonas oleovorans alkBAC operon encodes two structurally related rubredoxins and an aldehyde dehydrogenase. *J. Biol. Chem.* **264**, 5442–5451 (1989).

27. van Beilen, J. B., Eggink, G., Enequist, H., Bos, R. & Witholt, B. DNA sequence determination and functional characterization of the OCT-plasmid-encoded alkJKL genes of Pseudomonas oleovorans. *Mol. Microbiol.* **6**, 3121–3136 (1992).

28. Eggink, G. *et al.* Alkane utilization in Pseudomonas oleovorans. Structure and function of the regulatory locus alkR. *J. Biol. Chem.* **263**, 13400–13405 (1988).

29. Grund, A. *et al.* Regulation of alkane oxidation in Pseudomonas putida. *J. Bacteriol.* **123**, 546–556 (1975).

30. Kok, M. *et al.* The Pseudomonas oleovorans alkane hydroxylase gene. Sequence and expression. *J. Biol. Chem.* **264**, 5435–5441 (1989).

31. Peterson, J. A., Basu, D. & Coon, M. J. Enzymatic ω-Oxidation: I. Electron carriers in fatty acid and hydrocarbon hydroxylation. *J. Biol. Chem.* **241**, 5162–5164 (1966).

32. Peterson, J. A. & Coon, M. J. Enzymatic ω-Oxidation: III. Purification and properties of rubredoxin, a component of the ω-hydroxylation system of pseudomonas oleovorans. *J. Biol. Chem.* **243**, 329–334 (1968).

33. Kirmair, L. & Skerra, A. Biochemical analysis of recombinant AlkJ from Pseudomonas putida reveals a membrane-associated, flavin adenine dinucleotide-dependent dehydrogenase suitable for the biosynthetic production of aliphatic aldehydes. *Appl. Environ. Microbiol.* **80**, 2468–2477 (2014).

34. Grant, C. *et al.* Identification and use of an alkane transporter plug-in for applications in biocatalysis and whole-cell biosensing of alkanes. *Sci. Rep.* **4**, 5844 (2014).

35. Williams, S. C. & Austin, R. N. An Overview of the Electron-Transfer Proteins That Activate Alkane Monooxygenase (AlkB) . *Frontiers in Microbiology* vol. 13 (2022).

36. Benson, S., Fennewald, M., Shapiro, J. & Huettner, C. Fractionation of inducible alkane hydroxylase activity in Pseudomonas putida and characterization of hydroxylase-negative plasmid mutations. *J. Bacteriol.* **132**, 614–621 (1977).

37. Benson, S. & Shapiro, J. Plasmid-determined alcohol dehydrogenase activity in alkane-utilizing strains of Pseudomonas putida. *J. Bacteriol.* **126**, 794–798 (1976).

38. van Beilen, J. B., Penninga, D. & Witholt, B. Topology of the membrane-bound alkane hydroxylase of Pseudomonas oleovorans. *J. Biol. Chem.* **267**, 9194–9201 (1992).

39. Shanklin, J., Achim, C., Schmidt, H., Fox, B. G. & Münck, E. Mössbauer studies of alkane omega-hydroxylase: evidence for a diiron cluster in an integral-membrane enzyme. *Proc. Natl. Acad. Sci. U. S. A.* **94**, 2981–2986 (1997).

40. Shanklin, J., Whittle, E. & Fox, B. G. Eight histidine residues are catalytically essential in a membrane-associated iron enzyme, stearoyl-CoA desaturase, and are conserved in alkane hydroxylase and xylene monooxygenase. *Biochemistry* **33**, 12787–12794 (1994).

41. Guo, X. *et al.* Structure and mechanism of the alkane-oxidizing enzyme AlkB. *Nat. Commun.* **14**, 2180 (2023).

42. Smits, T. H. M., Röthlisberger, M., Witholt, B. & Van Beilen, J. B. Molecular screening for alkane hydroxylase genes in Gram-negative and Gram-positive strains. *Environ. Microbiol.* **1**, 307–317 (1999).

43. Chai, J., Guo, G., McSweeney, S. M., Shanklin, J. & Liu, Q. Structural basis for enzymatic terminal C–H bond functionalization of alkanes. *Nat. Struct. Mol. Biol.* **30**, 521–526 (2023).

44. Alonso, H. & Roujeinikova, A. Characterization and two-dimensional crystallization of membrane component AlkB of the medium-chain alkane hydroxylase system from Pseudomonas putida GPo1. *Appl. Environ. Microbiol.* **78**, 7946–7953 (2012).

45. Alonso, H. *et al.* Structural and mechanistic insight into alkane hydroxylation by Pseudomonas putida AlkB. *Biochem. J.* **460**, 283–293 (2014).

46. McKenna, E. J. & Coon, M. J. Enzymatic omega-oxidation. IV. Purification and properties of the omega-hydroxylase of Pseudomonas oleovorans. *J. Biol. Chem.* **245**, 3882–3889 (1970).

47. Bertrand, E. *et al.* Reaction mechanisms of non-heme diiron hydroxylases characterized in whole cells. *J. Inorg. Biochem.* **99**, 1998–2006 (2005).

48. Lipscomb, J. D. Biochemistry of the soluble methane monooxygenase. *Annu. Rev. Microbiol.* **48**, 371–399 (1994).

49. van Beilen, J. & Funhoff, R. van Beilen JB, Funhoff EG.. Alkane hydroxylases involved in microbial alkane degradation. Appl Microbiol Biotec 74: 13-21. *Appl. Microbiol. Biotechnol.* **74**, 13–21 (2007).

50. Schwartz, R. D. & McCoy, C. J. Pseudomonas oleovorans hydroxylation-epoxidation system: additional strain improvements. *Appl. Microbiol.* **26**, 217–218 (1973).

51. van Nuland, Y. M., Eggink, G. & Weusthuis, R. A. Application of AlkBGT and AlkL from Pseudomonas putida GPo1 for Selective Alkyl Ester ω-Oxyfunctionalization in Escherichia coli. *Appl. Environ. Microbiol.* **82**, 3801–3807 (2016).

52. Favre-Bulle, O. & Witholt, B. Biooxidation of n-octane by a recombinant Escherichia coli in a two-liquid-phase system: Effect of medium components on cell growth and alkane oxidation

activity. *Enzyme Microb. Technol.* **14**, 931–937 (1992).

53. Lyu, L. *et al.* Degradation potential of alkanes by diverse oil-degrading bacteria from deep-sea sediments of Haima cold seep areas, South China Sea. *Front. Microbiol.* **13**, (2022).

54. Venkateswaran, K. *et al.* Distribution and biodegradation potential of oil-degrading bacteria in North Eastern Japanese coastal waters. *FEMS Microbiol. Lett.* **86**, 113–121 (1991).

55. Sorkhoh, N. A., Ghannoum, M. A., Ibrahim, A. S., Stretton, R. J. & Radwan, S. S. Crude oil and hydrocarbon-degrading strains of Rhodococcus rhodochrous isolated from soil and marine environments in Kuwait. *Environ. Pollut.* **65**, 1–17 (1990).

56. Yergeau, E., Sanschagrin, S., Beaumier, D. & Greer, C. W. Metagenomic Analysis of the Bioremediation of Diesel-Contaminated Canadian High Arctic Soils. *PLoS One* **7**, e30058 (2012).

57. Margesin, R., Labbé, D., Schinner, F., Greer, C. W. & Whyte, L. G. Characterization of hydrocarbon-degrading microbial populations in contaminated and pristine Alpine soils. *Appl. Environ. Microbiol.* **69**, 3085–3092 (2003).

58. Gutierrez, T. *et al.* Hydrocarbon-degrading bacteria enriched by the Deepwater Horizon oil spill identified by cultivation and DNA-SIP. *ISME J.* **7**, 2091–2104 (2013).

59. Gauthier, M. J. *et al.* Marinobacter hydrocarbonoclasticus gen. nov., sp. nov., a new, extremely halotolerant, hydrocarbon-degrading marine bacterium. *Int. J. Syst. Bacteriol.* **42**, 568–576 (1992).

60. Klein, B., Grossi, V., Bouriat, P., Goulas, P. & Grimaud, R. Cytoplasmic wax ester accumulation during biofilm-driven substrate assimilation at the alkane–water interface by Marinobacter hydrocarbonoclasticus SP17. *Res. Microbiol.* **159**, 137–144 (2008).

61. Smith, C. B., Tolar, B. B., Hollibaugh, J. T. & King, G. M. Alkane hydroxylase gene (alkB) phylotype composition and diversity in northern Gulf of Mexico bacterioplankton. *Front. Microbiol.* **4**, (2013).

62. Rughöft, S., Jehmlich, N., Gutierrez, T. & Kleindienst, S. Comparative Proteomics of Marinobacter sp. TT1 Reveals Corexit Impacts on Hydrocarbon Metabolism, Chemotactic Motility, and Biofilm Formation. *Microorganisms* **9**, (2020).

63. Smits, T. H. M., Balada, S. B., Witholt, B. & van Beilen, J. B. Functional analysis of alkane hydroxylases from gram-negative and gram-positive bacteria. *J. Bacteriol.* **184**, 1733–1742 (2002).

64. Gunasekera, T. S., Bowen, L. L., Radwan, O., Striebich, R. C. & Ruiz, O. N. Genomic and transcriptomic characterization revealed key adaptive mechanisms of Marinobacter hydrocarbonoclasticus NI9 for proliferation and degradation of jet fuel. *Int. Biodeterior. Biodegradation* **175**, 105502 (2022).

65. Nie, Y. *et al.* Diverse alkane hydroxylase genes in microorganisms and environments. *Sci. Rep.* **4**, 4968 (2014).

66. Nigl, A. *et al.* Engineering of Transmembrane Alkane Monooxygenases to Improve a Key Reaction Step in the Synthesis of Polymer Precursor Tulipalin A. *bioRxiv* 2024.07.04.601532 (2024) doi:10.1101/2024.07.04.601532.

67. Skerra, A. *et al.* Mutant alkb gene. (2017).

68. Kuipers, R. K. *et al.* 3DM: Systematic analysis of heterogeneous superfamily data to discover protein functionalities. *Proteins Struct. Funct. Bioinforma.* **78**, 2101–2113 (2010).

69. Choi, Y. J. & Lee, S. Y. Microbial production of short-chain alkanes. *Nature* **502**, 571–574 (2013).

70. Agler, M. T., Wrenn, B. A., Zinder, S. H. & Angenent, L. T. Waste to bioproduct conversion with undefined mixed cultures: the carboxylate platform. *Trends Biotechnol.* **29**, 70–78 (2011).

71. Tomás-Pejó, E. *et al.* Production of short-chain fatty acids (SCFAs) as chemicals or substrates for microbes to obtain biochemicals. *Biotechnol. Biofuels Bioprod.* **16**, 96 (2023).

72. Stadler, B. M., Wulf, C., Werner, T., Tin, S. & de Vries, J. G. Catalytic Approaches to Monomers for Polymers Based on Renewables. *ACS Catal.* **9**, 8012–8067 (2019).

73. van Nuland, Y. M., de Vogel, F. A., Eggink, G. & Weusthuis, R. A. Expansion of the ω-oxidation system AlkBGTL of Pseudomonas putida GPo1 with AlkJ and AlkH results in exclusive mono-esterified dicarboxylic acid production in E. coli. *Microb. Biotechnol.* **10**, 594–603 (2017).

74. Sarel, S., Tsai, L. & Newman, M. S. Rates of Alkaline Hydrolysis of a Series of Primary and Secondary Alkyl Acetates. *J. Am. Chem. Soc.* **78**, 5420–5423 (1956).

75. Kocieński, P. J. 6.3 Methyl Esters and Derivatives (I). *Protecting Groups* (2005) doi:10.1055/b-0035-108281.

76. Engel, J., Cordellier, A., Huang, L. & Kara, S. Enzymatic Ring-Opening Polymerization of Lactones: Traditional Approaches and Alternative Strategies. *ChemCatChem* **11**, 4983–4997 (2019).

77. Zhao, H. Enzymatic Ring-Opening Polymerization (ROP) of Polylactones: Roles of Non-Aqueous Solvents. *J. Chem. Technol. Biotechnol.* **93**, 9–19 (2018).

78. Hollingsworth. Rawle L. & Haslett. Process for the preparation of 3,4-dihydroxybutanoic acid and salts thereof. (1992).

79. Fortunati, T., D'Acunto, M., Caruso, T. & Spinella, A. Chemoenzymatic preparation of musky macrolactones. *Tetrahedron* **71**, 2357–2362 (2015).

80. Antczak, U., Góra, J., Antczak, T. & Galas, E. Enzymatic lactonization of 15-hydroxypentadecanoic and 16-hydroxyhexadecanoic acids to macrocyclic lactones. *Enzyme Microb. Technol.* **13**, 589–593 (1991).

81. Tan, X. *et al.* Lactonization of Diols Over Highly Efficient Metal-Based Catalysts. *ChemSusChem* **n/a**, e202400909 (2024).

82. Tang, D. *et al.* Aerobic oxidative lactonization of diols at room temperature over defective titanium-based oxides in water. *J. Catal.* **418**, 237–246 (2023).

83. Zhang, X. *et al.* Biosynthesis of lactones from diols mediated by an artificial flavin. *Bioresour. Bioprocess.* **8**, 94 (2021).

84. Kumar, A., Kalra, B., Dekhterman, A. & Gross, R. A. Efficient Ring-Opening Polymerization and Copolymerization of ε-Caprolactone and ω-Pentadecalactone Catalyzed by Candida antartica Lipase B. *Macromolecules* **33**, 6303–6309 (2000).

85. Namekawa, S., Suda, S., Uyama, H. & Kobayashi, S. Lipase-catalyzed ring-opening polymerization of lactones to polyesters and its mechanistic aspects. *Int. J. Biol. Macromol.* **25**, 145–151 (1999).

86. Li, Z., Shen, Y. & Li, Z. Ring-Opening Polymerization of Lactones to Prepare Closed-Loop Recyclable Polyesters. *Macromolecules* **57**, 1919–1940 (2024).

87. Middleton, J. C. & Tipton, A. J. Synthetic biodegradable polymers as orthopedic devices. *Biomaterials* **21**, 2335–2346 (2000).

88. Malik, N. Thermally exfoliated graphene oxide reinforced polycaprolactone-based bactericidal nanocomposites for food packaging applications. *Mater. Technol.* **37**, 345–354 (2022).

89. Thakur, M., Majid, I., Hussain, S. & Nanda, V. Poly(ε-caprolactone): A potential polymer for biodegradable food packaging applications. *Packag. Technol. Sci.* **34**, 449–461 (2021).

90. Ebrahimifar, M. & Taherimehr, M. Evaluation of in-vitro drug release of polyvinylcyclohexane carbonate as a CO2-derived degradable polymer blended with PLA and PCL as drug carriers. *J. Drug Deliv. Sci. Technol.* **63**, 102491 (2021).

91. Woodruff, M. A. & Hutmacher, D. W. The return of a forgotten polymer—Polycaprolactone in the 21st century. *Prog. Polym. Sci.* **35**, 1217–1256 (2010).

92. Taghe, S., Mirzaeei, S., Pakdaman, N., Kazemi, A. & Nokhodchi, A. Macrolide-loaded nanofibrous inserts with polycaprolactone and cellulose acetate base for sustained ocular delivery: Pharmacokinetic study in Rabbit's eye. *Int. J. Pharm.* **665**, 124699 (2024).

93. Smits, T. H., Seeger, M. A., Witholt, B. & van Beilen, J. B. New alkane-responsive expression vectors for Escherichia coli and pseudomonas. *Plasmid* **46**, 16–24 (2001).

94. Canosa, I., Yuste, L. & Rojo, F. Role of the alternative sigma factor sigmaS in expression of the AlkS regulator of the Pseudomonas oleovorans alkane degradation pathway. *J. Bacteriol.* **181**, 1748–1754 (1999).

95. K., J. M. *et al.* Outer Membrane Protein AlkL Boosts Biocatalytic Oxyfunctionalization of Hydrophobic Substrates in Escherichia coli . *Appl. Environ. Microbiol.* **78**, 5724–5733 (2012).

96. Shanklin, J. & Whittle, E. Evidence linking the Pseudomonas oleovorans alkane omega-hydroxylase, an integral membrane diiron enzyme, and the fatty acid desaturase family. *FEBS Lett.* **545**, 188–192 (2003).

97. Grisenti, P., Ferraboschi, P., Casati, S. & Santaniello, E. Studies on the enantioselectivity of the transesterification of 2-methyl-1,4-butanediol and its derivatives catalyzed by Pseudomonas fluorescens lipase in organic solvents. *Tetrahedron: Asymmetry* **4**, 997–1006 (1993).

98. Ferraboschi, P., Grisenti, P., Manzocchi, A. & Santaniello, E. Regio- and enantioselectivity of Pseudomonas cepacia lipase in the transesterification of 2-substituted-1,4-butanediols. *Tetrahedron: Asymmetry* **5**, 691–698 (1994).

99. Schrewe, M. *et al.* Reaction and catalyst engineering to exploit kinetically controlled whole-cell multistep biocatalysis for terminal FAME oxyfunctionalization. *Biotechnol. Bioeng.* **111**, 1820–1830 (2014).

100. Schrewe, M., Ladkau, N., Bühler, B. & Schmid, A. Direct Terminal Alkylamino-Functionalization via Multistep Biocatalysis in One Recombinant Whole-Cell Catalyst. *Adv. Synth. Catal.* **355**, 1693–1697 (2013).

101. Kadisch, M., Schmid, A. & Bühler, B. Hydrolase BioH knockout in E. coli enables efficient fatty acid methyl ester bioprocessing. *J. Ind. Microbiol. Biotechnol.* **44**, 339–351 (2017).

7 Appendix

7.1 Materials

Table 8 – Compounds used for induction, biotransformation, product standards and standard synthesis for analysis.

Compound	CAS number	Purity	Manufacturer
Dicyclopropyl ketone (DCPK)	1121-37-5	>95.0 %	Tokyo Chemical Industries
Methyl pentanoate	624-24-8	99.0 %	Sigma Aldrich
Methyl nonanoate	1731-84-6	>96.0 %	Tokyo Chemical Industries
Methyl-9-hydroxynonanoate	34957-73-8	>95 %	AmBeed
Nonanedioic acid monomethyl ester	2104-19-0	85 %	Sigma Aldrich
Methyl laurate	L0015	99.5 %	Sigma Aldrich
Pentyl acetate	A0021	>98.5 %	Sigma Aldrich
Nonyl acetate	A0041	>99 %	Tokyo Chemical Industries
Dodecyl acetate	A0902	>95 %	Tokyo Chemical Industries
1-Pentanol	71-41-0	>99.0 %	Sigma Aldrich
1,5-Pentanediol	111-29-5	>97.0 %	Tokyo Chemical Industries
1-Nonanol	143-08-8	>99.0 %	Tokyo Chemical Industries
1,9-Nonanediol	3937-56-2	>98.0 %	Tokyo Chemical Industries
Nonanoic acid	112-05-0	>98.0 %	Tokyo Chemical Industries
9-Hydroxynonanoic acid	3788-56-5	95 %	BLD Pharmatech GmbH
1-Dodecanol	112-53-8	>99.0 %	Tokyo Chemical Industries
1,12-Dodecanediol	5675-51-4	>99.0 %	Tokyo Chemical Industries
Lauric acid	143-07-7	≥99.0 %	Merck
12-Hydroxy dodecanoic acid	505-95-3	97 %	BLD pharma
Azelaic acid	123-99-9	>98.0 %	Tokyo Chemical Industries
Methyl Benzoate	93-58-3	99 %	Merck

7.2 DNA Sequences

7.2.1 Plasmids

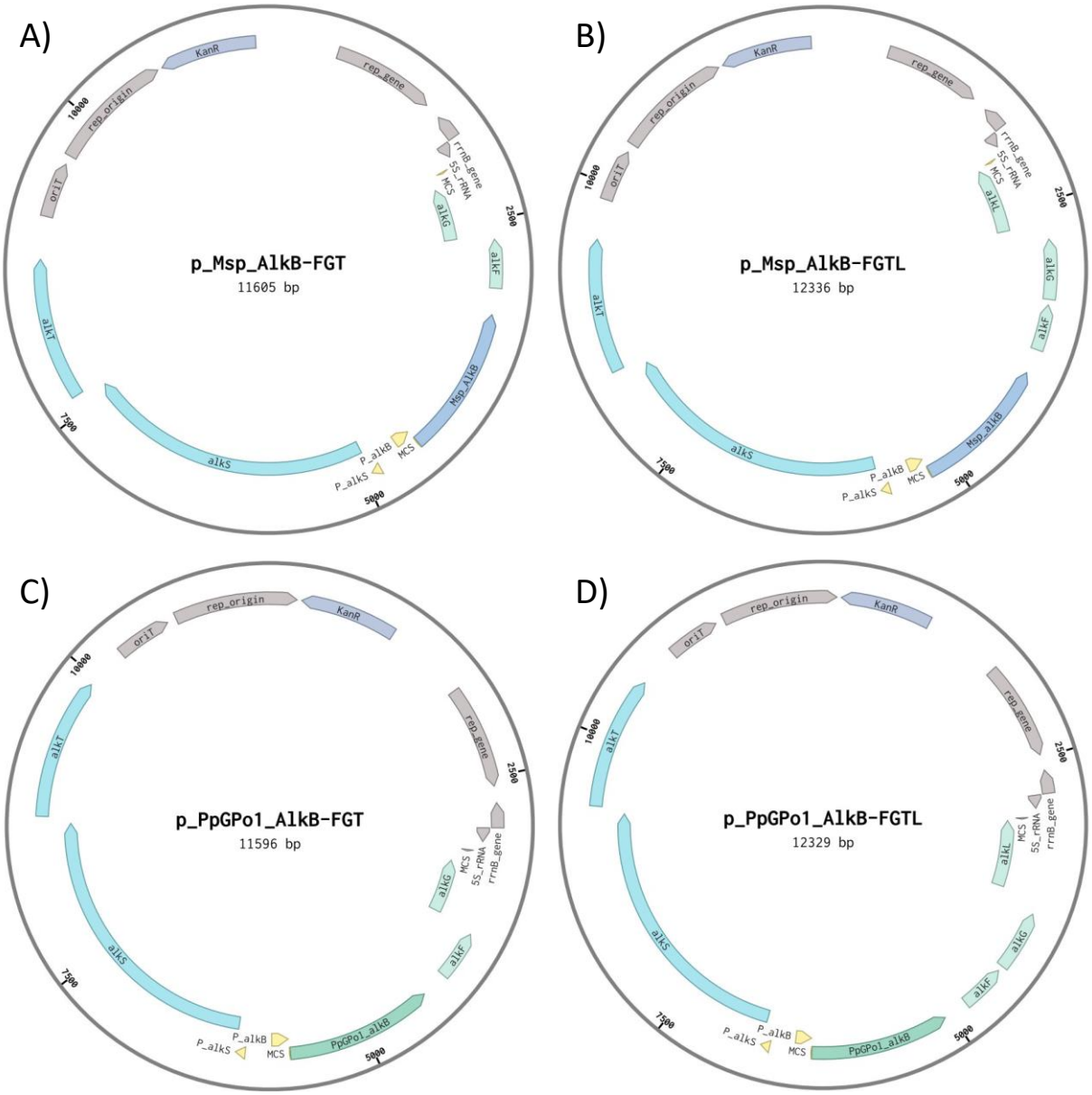

Figure 26 – Plasmid map of pBT10 carrying the genes alkB (Msp), alkF, alkG, alkS and alkT (created by Andrea Nigl). As in the natural OCT plasmid, one operon includes the genes alkS and alkT, and the second operon contains alkB, alkF and alkG.

Table 9 – DNA and amino acid sequences of AlkB from Pp GPo1 and Msp, respectively.

***Pp* GPo1 AlkB**	**Amino acid sequence** **MLEKHRVLDSAPEYVDKKKYLWILSTLWPATPMIGIWLANETGWGIFYGLVLLVWYGALPLLDAM FGEDFNNPPEEVVPKLEKERYYRVLTYLTVPMHYAALIVSAWWVGTQPMSWLEIGALALSLGIVNG LALNTGHELGHKKETFDRWMAKIVLAVVGYGHFFIEHNKGHHRDVATPMDPATSRMGESIYKFSIR EIPGAFIRAWGLEEQRLSRRGQSVWSFDNEILQPMIITVILYAVLLALFGPKMLVFLPIQMAFGWWQL TSANYIEHYGLLRQKMEDGRYEHQKPHHSWNSNHIVSNLVLFHLQRHSDHHAHPTRSYQSLRDFPG LPALPTGYPGAFLMAMIPQWFRSVMDPKVVDWAGGDLNKIQIDDSMRETYLKKFGTSSAGHSSSTSA VAS** **DNA sequence** atgcttgagaaacacagagttctggattccgctccagagtacgtagataaaaagaaatatctctggatactatcaactttgtggccggctactccgatgatcggaatctggct tgcaaatgaaactggttgggggatttttatgggctggtattgctcgtatggtacggcgcacttccattgcttgatgcgatgtttggtgaggactttaataatccgcctgaagaa gtggtgccgaaactagagaaggagcggtactatcgagttttgacatatctaacagttcctatgcattacgctgcattaattgtgtcagcatggtgggtcggaactcagccaat gtcttggcttgaaattggtgcgcttgccttgtcactgggtatcgtgaacggactagcgctcaatacaggacacgaactcggtcacaagaaggagacttttgatcgttggatg gccaaaattgtgttggctgtcgtagggtacggtcacttctttattgagcataataagggtcatcaccgtgatgtcgctacaccgatggatcctgcaacatcccggatgggag aaagcatttataagttttcaatccgtgagatcccaggagcatttattcgtgcttgggggcttgaggaacaacgcctttcgcgccgtggccaaagcgtttggagtttcgataatg aaatcctccaaccaatgatcatcacagttattctttacgccgttctccttgccttgtttggacctaagatgctggtgttcctgccgattcaaatggctttcggttggtggcagctga ccagtgcgaactatattgaacattacggcttgctccgtcaaaaaatggaggacggtcgatatgagcatcaaaagccgcaccattcttggaatagtaatcacatcgtctctaat ctagtgctgttccaccttcagcggcactcggatcaccacgcgcatccaacacgttcttatcagtcacttcgggattttcccggcctgccggctcttccgacgggttaccctgg tgcatttttgatggcgatgattcctcagtggtttagatcagttatggatcccaaggtagtagattgggctggtggtgaccttaataagatccaaattgatgattcgatgcgagaa acctatttgaaaaaatttggcactagtagtgctggtcatagttcgagtacctctgcggtagcatcgtag
***Msp* AlkB**	**Amino acid sequence** MSENVLTESLQRDPGAENYVDRKRHLWILSVLWPATPLIGLYLVAQTGWSIWYGLVLILWYGAVPLIDAM FGEDFSNPPESAVPRLEQDRYYRVLTYLTVPIHYAALIVSAWWVSTQPMSVFEFLALALSLGIVNGLALNTG HELGHKKETFDRWMAKLVLAVVGYGHFFIEHNKGHHRDVATPMDPATSRMGESIYSFSLREIPGAFKRAW DLEEQRLSRCGKSVWSLENEVLQPMILTAVLYAGLLAFFGPLMLIFLPIQMAFGWWQLTSANYIEHYGLLR EKMSDGRYERQQPHHSWNSNHIMSNLILFHLQRHSDHHAHPTRSYQSLRDFKDLPSLPSGYPGMFLAAMFP SWFRSIMDHRVLDWAKGDLDKIQIQPGKREFYVRKFGGTDSESVDTAASK** DNA sequence atgtcagaaaatgtactaacggaatccctgcaacgcgaccctggtgcggaaaattatgtggaccgaaaacgccacctgtggatcctgtctgttctgtggccagcaacacc gttgataggcctttatctggtcgcccagaccggatggagcatctggtacggcttggtgttgatcctttggtacggcgcagttccgctcattgatgccatgtttggtgaggatttt agcaacccgcctgagtcggcggtgcctcgcttagaacaggatcgttactatcgggtactgacctacctcacggttcctattcactatgccgccttgattgtcagtgcgtggtg ggtatcaacgcagccaatgagtgttttcgagtttctggcattggcgctgtccctggggatcgtgaatggcctggctctgaacacaggccatgaactgggccataaaaaaga aacgtttgaccgttggatggcgaaacttgttctcgccgtggtaggctatggtcatttcttcatcgaacacaataaggggcatcaccgcgatgtggccaccccgatggatccg gcgacttcccgcatgggcgaaagcatttacagcttctcactgcgtgaaattcccggtgctttcaagcgggcatgggatttagaggaacagcgcctcagtcgttgcggtaaa agtgtctggagcctggaaaatgaagttcttcagccgatgattttaaccgcggtgctttatgcgggattactggcgtttttggcccgttaatgctgatcttttgccgattcaaatg gcgtttggctggtggcagctgaccagcgccaactacattgagcattacggactactgcgcgagaagatgagcgatggtcgttatgaacgtcagcaaccgcaccacagct ggaactcaaaccatattatgtcgaacctgattctgtttcatttacagcgacatagcgaccatcacgcccatccgacccgctcctatcagtcgcttcgcgacttcaaagacctg ccgagcttaccatcgggctatccgggtatgttcctggccgcaatgtttccctcatggtttaggtcgattatggaccaccgcgtgctggattgggctaaaggagatctcgataa gattcagatccaacccggcaaacgtgaattctacgtgcgtaaattcggtgggactgattctgaaagcgtcgataccgcagcgtctaaataa

7.2.2 Primers

Table 10 – Primers used for SSM reactions and the respective sequences. The new, mutated codons are highlighted in bold.

Primer	Sequence (5' → 3')
W60S_forward	ATCCTTAGCT**ACG**GCGCAGTTCCGC ATCCTTAGCT**ACG**GCGCAGTTCCGC
W60S_reverse	GCCGTA**GCT**AAGGATCAACACCAAGCC
H278A_forward	TCCGTA**GGC**CTCAATGTAGTTGGCGCTG
H278A_reverse	ATTGAG**GCC**TACGGACTACTGCGCGAGAAGATG
I204L_forward	CGTGAA**CTG**CCCGGTGCTTTCAAGC
I204L_reverse	CCGGG**CAG**TTCACGCAGTGAGAAGC
G136M_forward	TGAAT**ATG**CTGGCTCTGAACACAGGCCATG
G136M_reverse	AGCCAG**CAT**ATTCACGATCCCCAGGG
G136V_forward	TGAAT**GTG**CTGGCTCTGAACACAGGCCATG
G136V_reverse	GAGCCAG**CAC**ATTCACGATCCCCAGG
I238A_forward	GATG**GCG**TTAACCGCGGTGCTTTATG
QC_I238A_reverse	GGTTAA**CGC**CATCGGCTGAAGAACTTCATTTTC
QC_I238F_forward	GATG**TTT**TTAACCGCGGTGCTTTATGCG
QC_I238F_reverse	CGGTTAA**AAA**CATCGGCTGAAGAACTTCATTTTCC

Table 11 – Primers for sequencing (provided by Andrea Nigl)

Primer	Sequence (5' → 3')
p17_pCom10_seq_prom	TACCCGTAGGTGTAGTTGGC
P35_pCom10_seqST_rv	TTCCAGACGAACGAAGAGC
p36_pCom10_seq_term	GTTTTATCAGACCGCTTCTGCG
P44_amp_alkT_rv	GAACGCTTACCGCCAACAC
P47_seq_pCom10AlkST_mid	CAAGCGATTGGGGCTTTTAG
P67_seq_alKH_rv	CCATACCAATTAGCCTAGCCAAG
P68_seq_AlkF_rv	AAAAATGAGGGCTGTGCG
P73_seq_alkBS_prom_fw	CTGAGAAAGTTAAGCCGCC
P74_seq_AlkSmid_rv	ATTCCATCATCTGCGCGC
P90_FC_lin_pBT10-AlkB_rv	TTATGTGAGCACGCAGAG
P109_seq_Alk_rv	TTGTGAGAGCTTTCAACGCC

7.3 Single site mutations

7.3.1 3DM Analysis

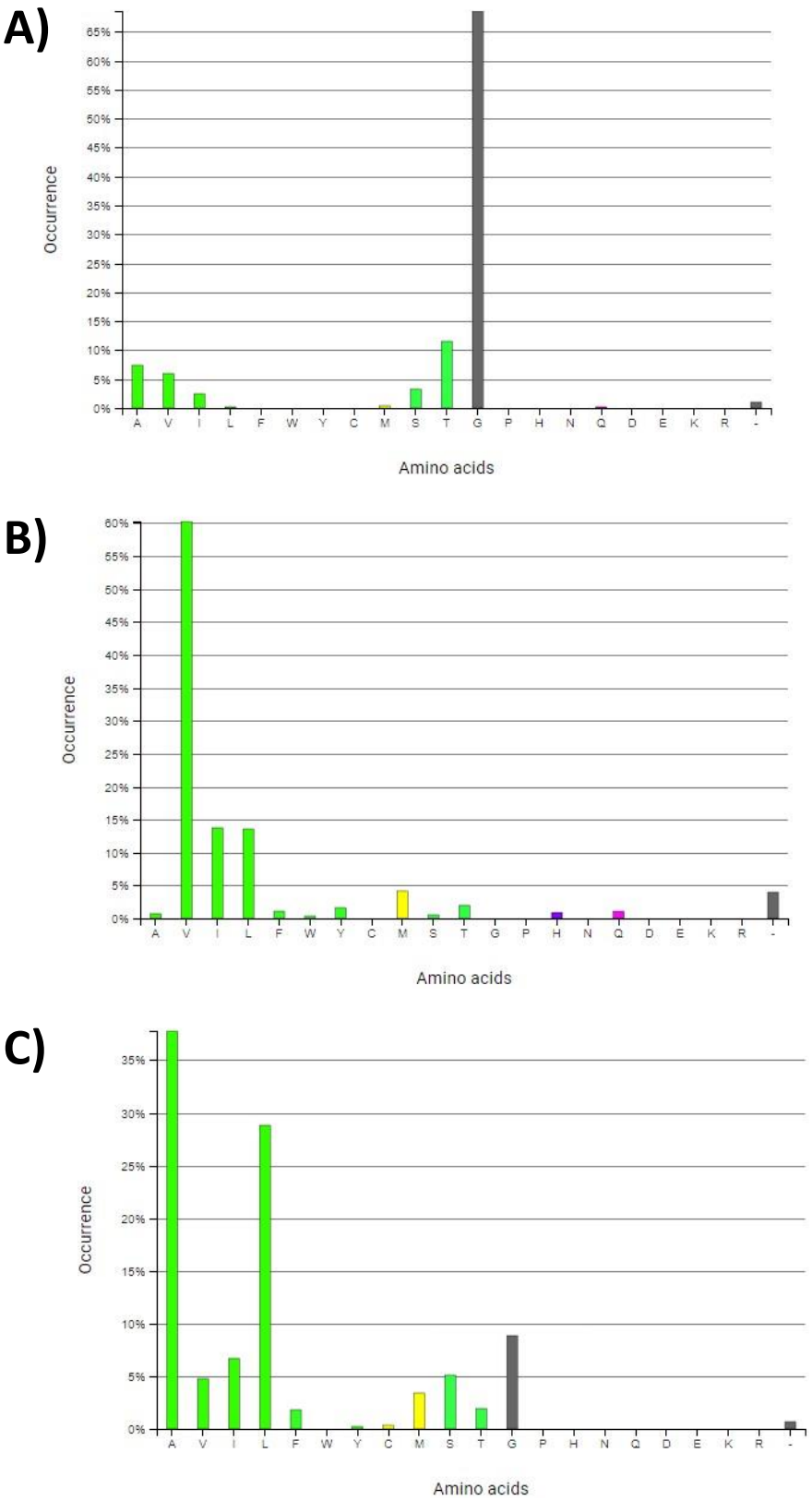

Figure 27 – Results of the 3DM analysis using the primary sequences of Pp and Msp AlkB as input data. The Bars indicate the frequency of the respective amino acids at positions (A) G136, (B) I204, (C) I238. The numbers refer to respective positions in the sequence of Msp AlkB.

7.3.2 Sequencing results

The sequencing results proved that the desired codons were successfully exchanged through the SSM reactions (Figure 28-Figure 33). In the second round of sequencing for quality check of the entire operon, no undisired variation in the DNA sequence was found (data not shown).The the mutation I204Lin the *Msp* AlkB gene in both plasmids (with and without *alkL*) as well as the I238A in the plasmid with *alkL* still needs to be confirmed.

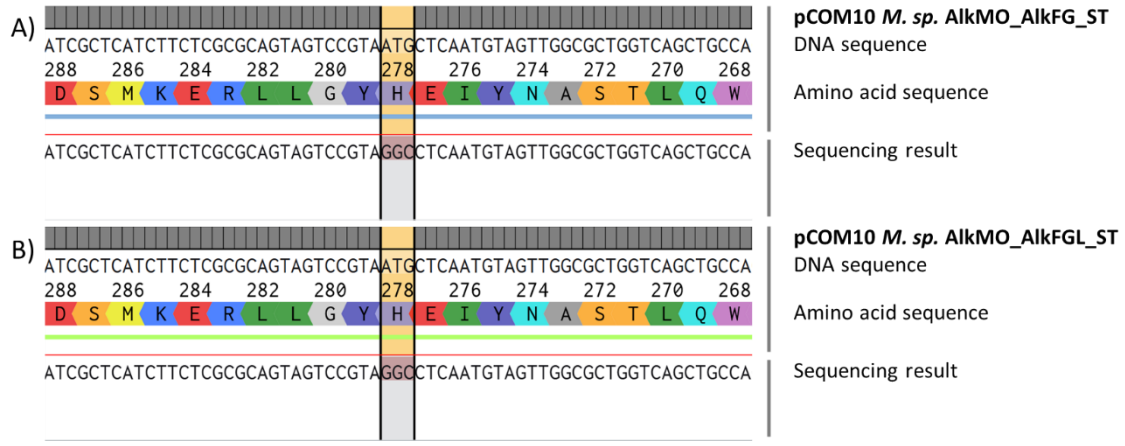

Figure 28 – Sequence alignment. Confirmation of the codon exchange for the H287A mutation in the plasmids (A) pCOM10 Msp AlkB_AlkFG_ST and (B) pCOM10 Msp AlkB_AlkFGL_ST.

Figure 29– Sequence alignment. Confirmation of the codon exchange for the W60S mutation in the plasmids (A) pCOM10 Msp AlkB_AlkFG_ST and (B) pCOM10 Msp AlkB_AlkFGL_ST.

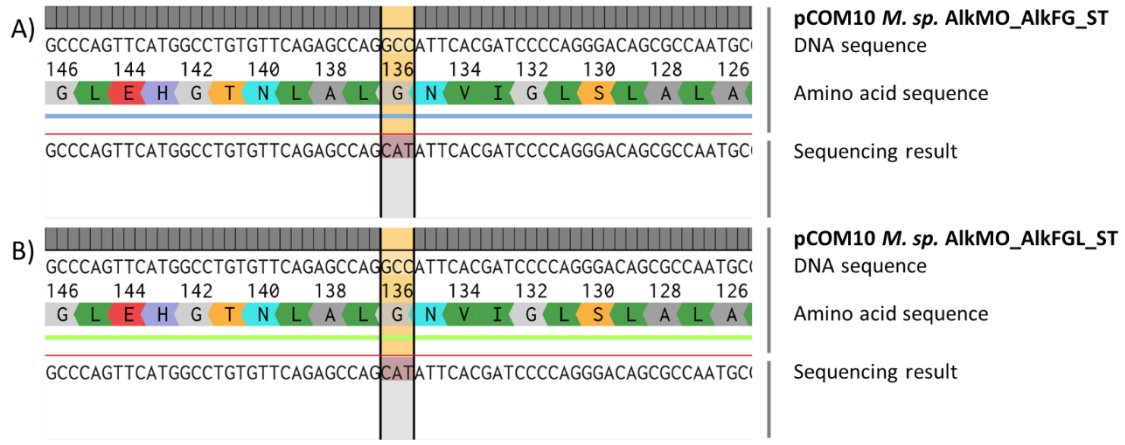

Figure 30 – Sequence alignment. Confirmation of the codon exchange for the G136M mutation in the plasmids (A) pCOM10 Msp AlkB_AlkFG_ST and (B) pCOM10 Msp AlkB_AlkFGL_ST.

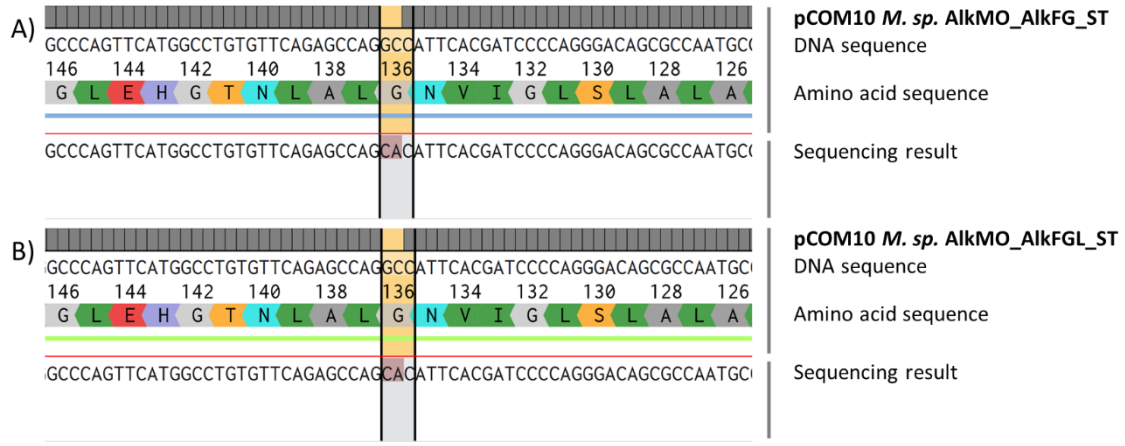

Figure 31 – Sequence alignment. Confirmation of the codon exchange for the G136V mutation in the plasmids (A) pCOM10 Msp AlkB_AlkFG_ST and (B) pCOM10 Msp AlkB_AlkFGL_ST.

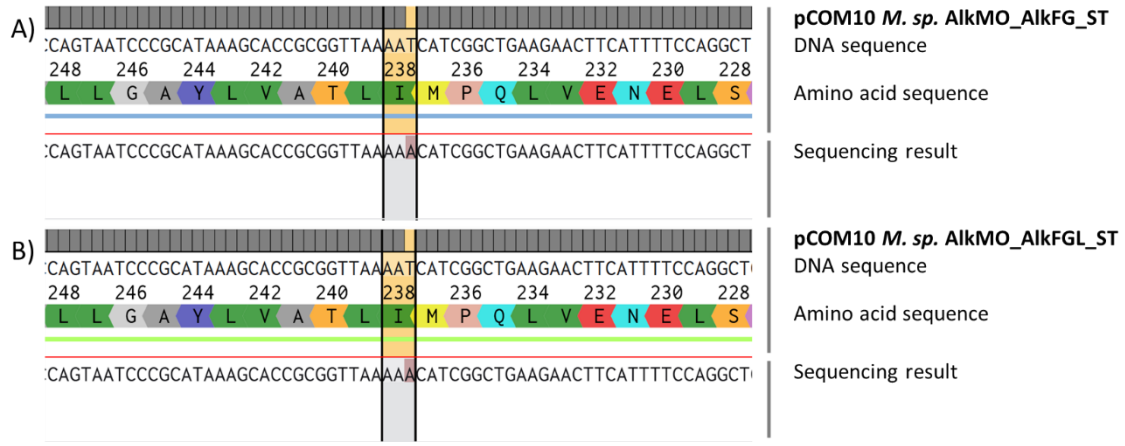

Figure 32 – Sequence alignment. Confirmation of the codon exchange for the I238F mutation in the plasmids (A) pCOM10 Msp AlkB_AlkFG_ST and (B) pCOM10 Msp AlkB_AlkFGL_ST.

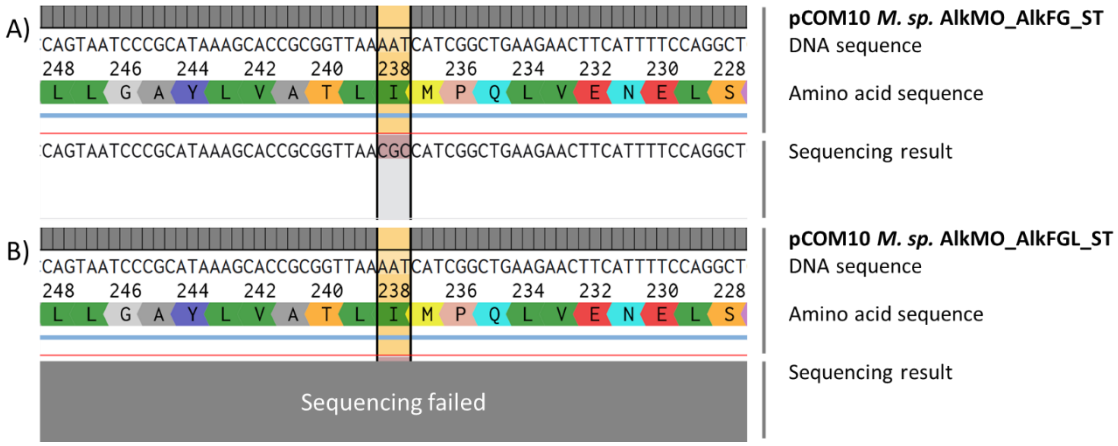

Figure 33– Sequence alignment. Confirmation of the codon exchange for the I238F mutation in the plasmid (A) pCOM10 Msp AlkB_AlkFG_ST. In (B) pCOM10 Msp AlkB_AlkFGL_ST the mutation could not be confirmed due to failed sequencing.

7.4 Cell dry weight determination

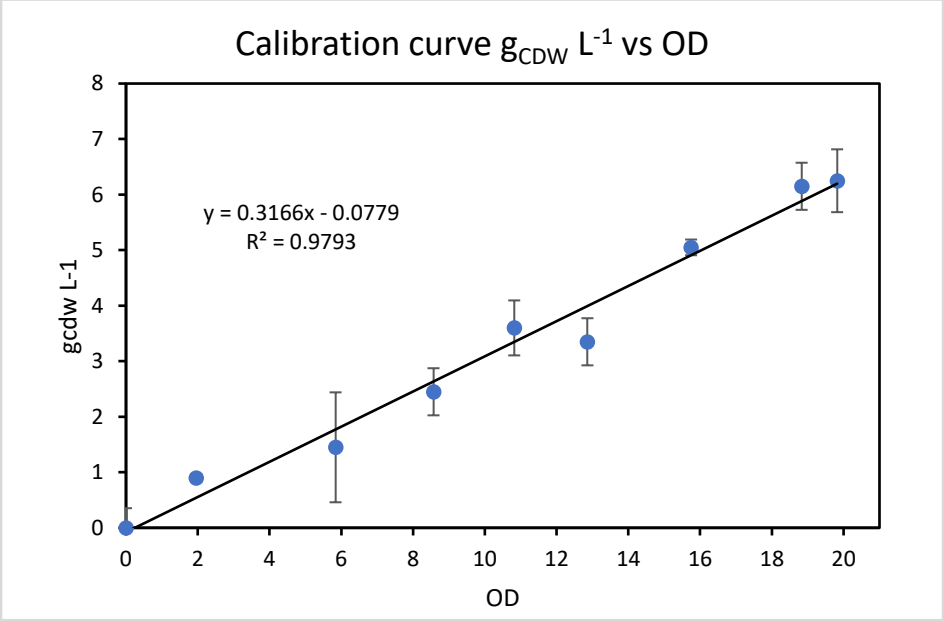

Figure 34 – Calibration curve correlating the cell density gCDW L^{-1} to the optical density (OD). Data kindly provided by Andrea Nigl.

Table 12 – Compounds used for calibration curve establishment and quantification in biotransformation samples.

Compound	Curve	Equation
Methyl nonanoate (**2**)	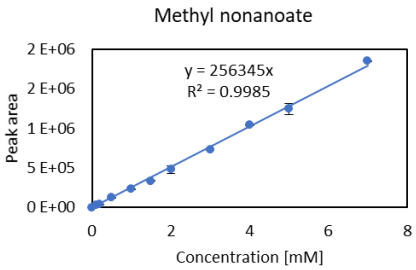	y = 256345x
Methyl 9-hydroxy nonanoate (**2a**)	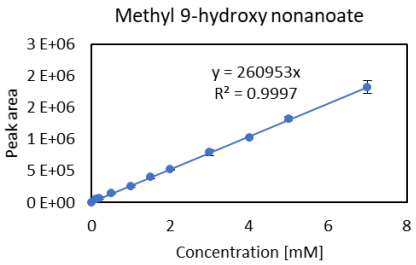	y = 260953x
Nonanedioic acid monomethyl ester (**2c**)	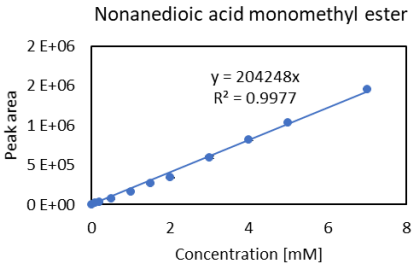	y = 204248x
Nonanoic acid	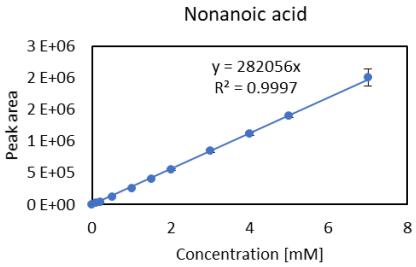	y = 282056x
Pentyl acetate (**4**)	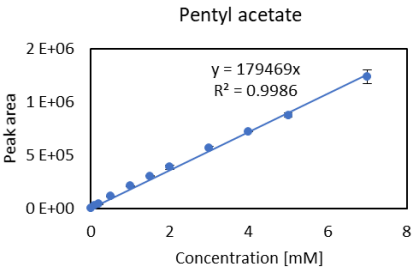	y = 179469x

Nonyl acetate (**5**)	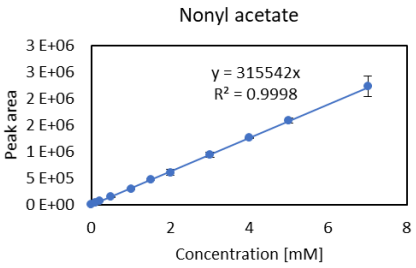	y = 315542x
Dodecyl acetate (**6**)	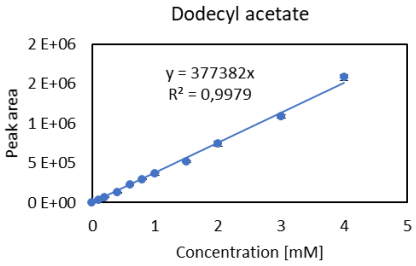	y = 377382x

7.5 GC-MS and GC-FID analysis

7.5.1 Methods

Table 13 – Specifications on the GC-MS device and settings used for analysis.

Component	Details	
Column	Name	ZB-5MS / ZB-5 plus
	Phase	5 % Phenyl, 95 % Dimethylpolysiloxane
	Dimensions	Length: 30.0 m Inner diameter: 0.25 mm Film thickness: 0.25 µm
	Temperature	Min.: -60 °C Max.: 360 °C
Temperature	Profile	Hold: 50 °C, 3 min Heating: to 300 °C, 30 °C min^{-1} Hold: 300 °C, 3 min
Injection port	Volume	1 µl
	Carrier Gas	He
	Temperature	250 °C
	Split Ratio	9.1
	Temperature	Ion source: 250 °C Interface: 250 °C
MS Detector	Total flow	15.0 mL/min
	Column flow	1.19 mL/min
	Pressure	67.2 kPa

Table 14 – Specifications on the GC-FID device and the settings used for analysis.

Component	Details	
Column	Name	Zebron ZB-5
	Phase	5% Penyl, 95 % Dimethylpolysiloxane
	Dimensions	Length: 30 m Inner diameter: 0.32 mm Film thickness: 0.25 µm
	Temperature	Min.: -60 °C Max.: 360 °C
Temperature	Profile	Hold: 50 °C, 1 min Heating: to 150 °C, 40 °C min^{-1}, Heating: to 250 °C, 20 °C min^{-1} Hold: 250 °C, 2 min
Injection port	Volume	1 µl
	Carrier Gas	N2
	Temperature	250 °C
	Split Ratio	10.0
FID Detector	Temperature	320 °C
	N2 flow rate	32.0 mL/min
	H2 flowrate	40.0 mL/min
	Air flow rate	400.0 mL/min

Table 15 – Table of compounds and their retention times determined by GC-MS and GC-FID with the methods described above. Those compounds that were identified as putative products, but not verified through comparison to standards, are marked by an asterisk (*). Some compounds were not determined via GC-FID, indicated by "n.d.".

Number/Abbreviation	Compound	RT (min) on GCMS	RT (min) on GCFID
DCPK	Dicyclo propyl ketone	5.5	4.9
DMSO	Dimethyl sulfoxide	4.2	4.2
ISTD	Methyl benzoate	6.5	5.6
1	Methyl pentanoate	4.1	4.1
1a*	Methyl 5-hydroxy pentanoate	6.4	n.d.
1c*	Pentanedioic acid monomethyl ester	6.8	n.d.
	Pentanoic acid	7.8	n.d.
2	Methyl nonanoate	7.1	6.2
2a	Methyl 9-hydroxy nonanoate	8.5	7.6
2c	Nonanedioic acid monomethyl ester	8.9	8.1
	Nonanoic acid	7.4	6.4
3	Methyl laurate	8.6	7.8
3a*	Methyl 12-hydroxy laurate	9.8	n.d.
3c*	Dodecanedioic acid monomethyl ester	8.8	n.d.
4	Pentyl acetate	5.0	4.6
4a	1,5-Pentanediol monoacetate	6.9	6.1
4b*	5-Acetoxy pentanal	6.6	n.d.
4c*	Acetoxy pentanoic acid	7.5	6.4
	Pentanediol	6.1	5.4
5	Nonyl acetate	7.6	6.6
5a	1,9-Nonanediol monoacetate	8.8	8.1
5c*	Acetoxy nonanoic acid	9.2	9.1
	Nonanol	6.8	9.0
	Nonanediol	8.3	7.4
6	Dodecyl acetate	8.9	8.2
6a	1,12-Dodecanediol monoacetate	9.9	9.9
6c*	Acetoxy dodecanoic acid	10.2	10.4
	Dodecanol	8.4	7.6
	Dodecanediol	9.6	9.3

7.5.2 Standard synthesis

Standards for the terminal hydroxy products of **4-6** were synthesized by lipase-catalysed acetylation of the diols and was confirmed by GC-MS analysis (Figure 35 -Figure 37). In all three reactions the corresponding monoacetylated diols (1,5-pentanediol-, 1,9-nonanediol-, and 1,12-dodecanediol monoacetate) and some side-products were found such as di-acetates, acrylates, and di-acrylates as well as some starting material.

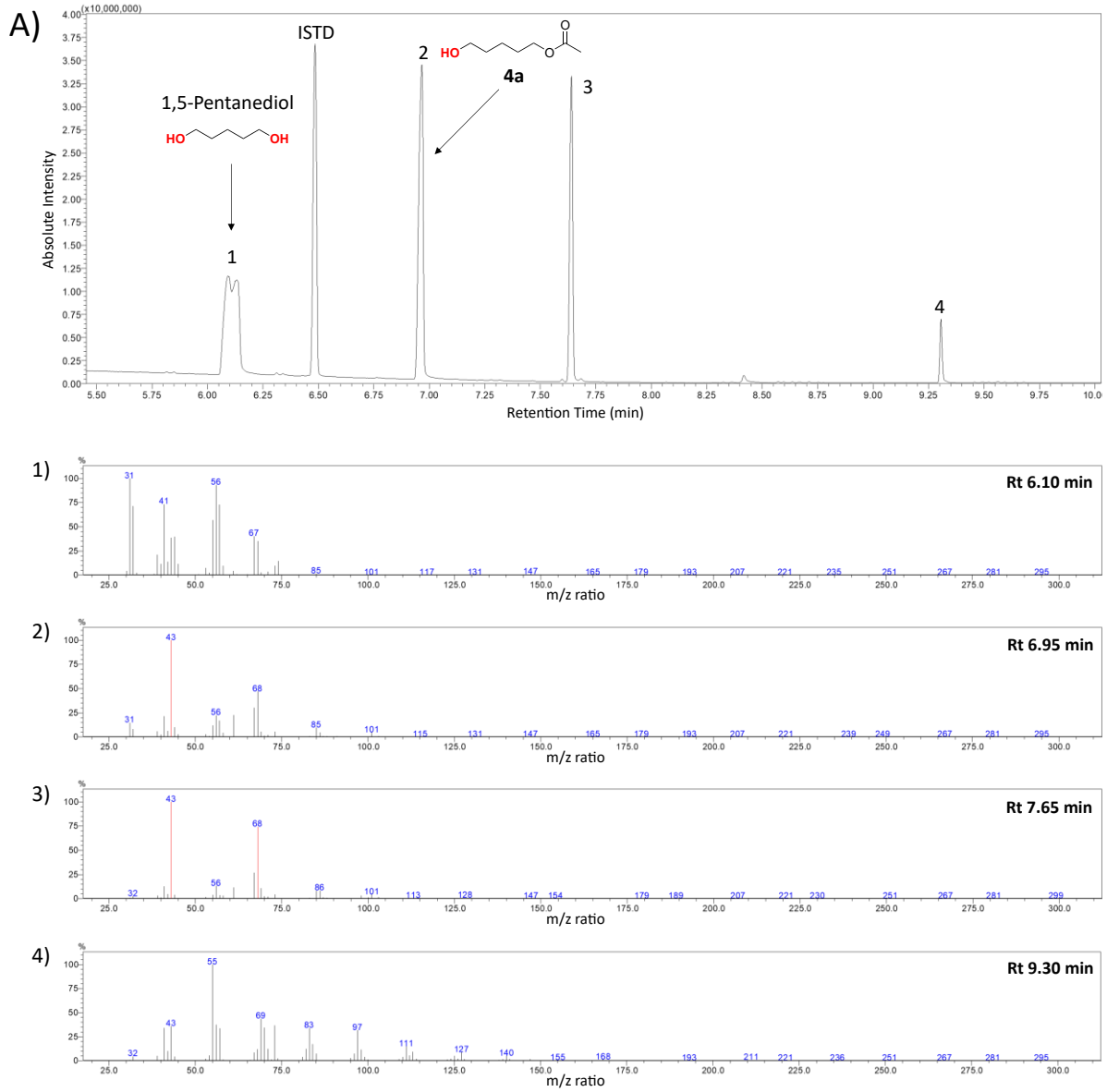

*Figure 35 – (A) GC-MS chromatogram of the synthesis reaction with 1,5-pentane diol and vinyl acetate, showing the substrate (1) and the products formed (2)-(4). Mass spectra of the respective compounds are shown for (1) pentane diol, (2) **4a**, (3) di-acetoxy pentane and (4) pentanoic acid diacrylate. The identity of the side products (3) and (4) was determined by mass spectrum analysis and assisted by digital library search but was not confirmed by other means.*

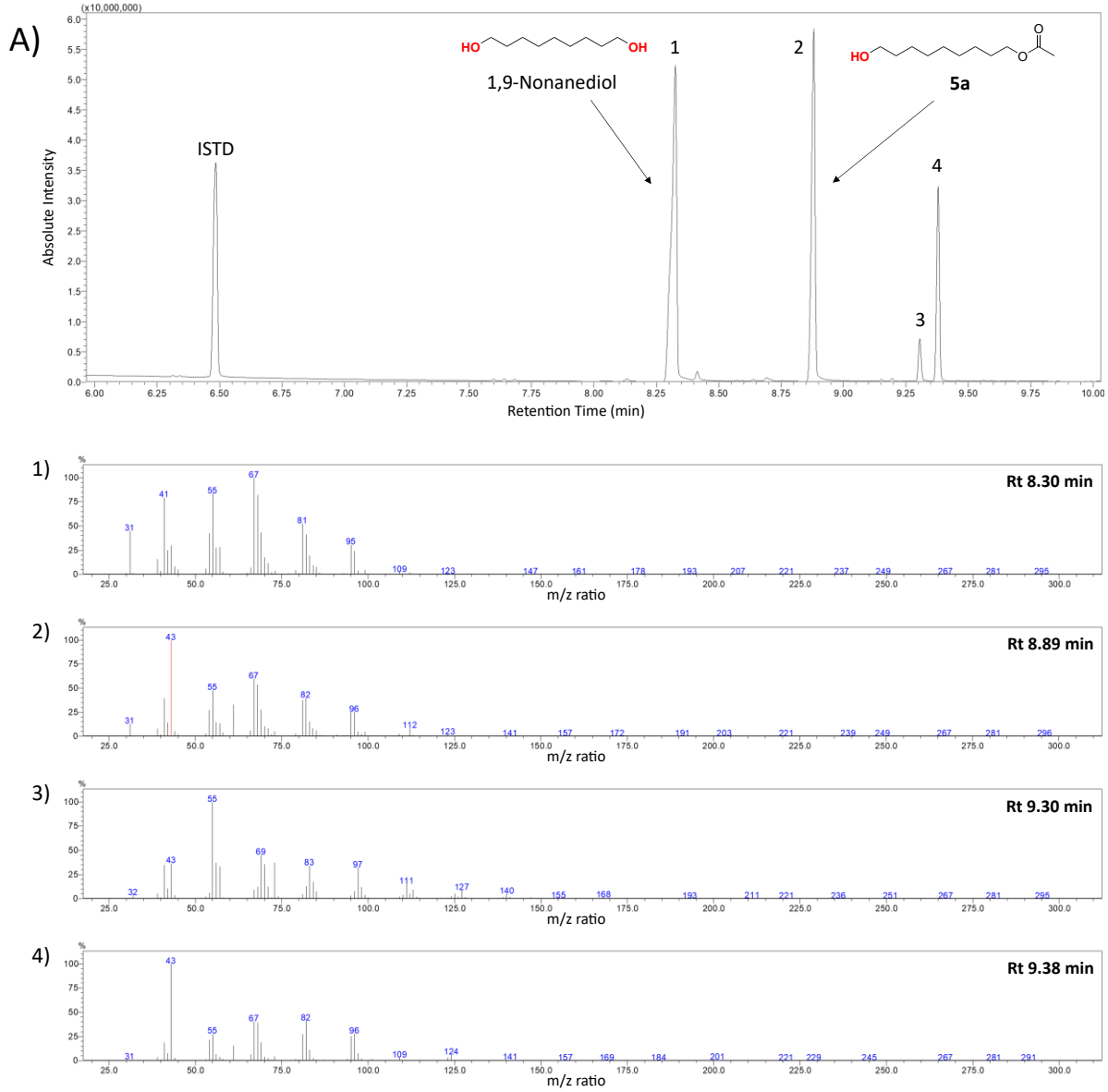

Figure 36 – (A) GC-MS *chromatogram of the synthesis reaction with 1,9-nonane diol and vinyl acetate, showing the substrate (1) and the products formed (2)-(4): Mass spectra of the respective compounds are shown for (1) Nonane diol, (2)* ***5a****, (3) Nonane-1-acrylate and (4) Nonane-1,9-diacrylate. The identity of the side products (3) and (4) was determined by mass spectrum analysis and assisted by digital library search but was not confirmed by other means.*

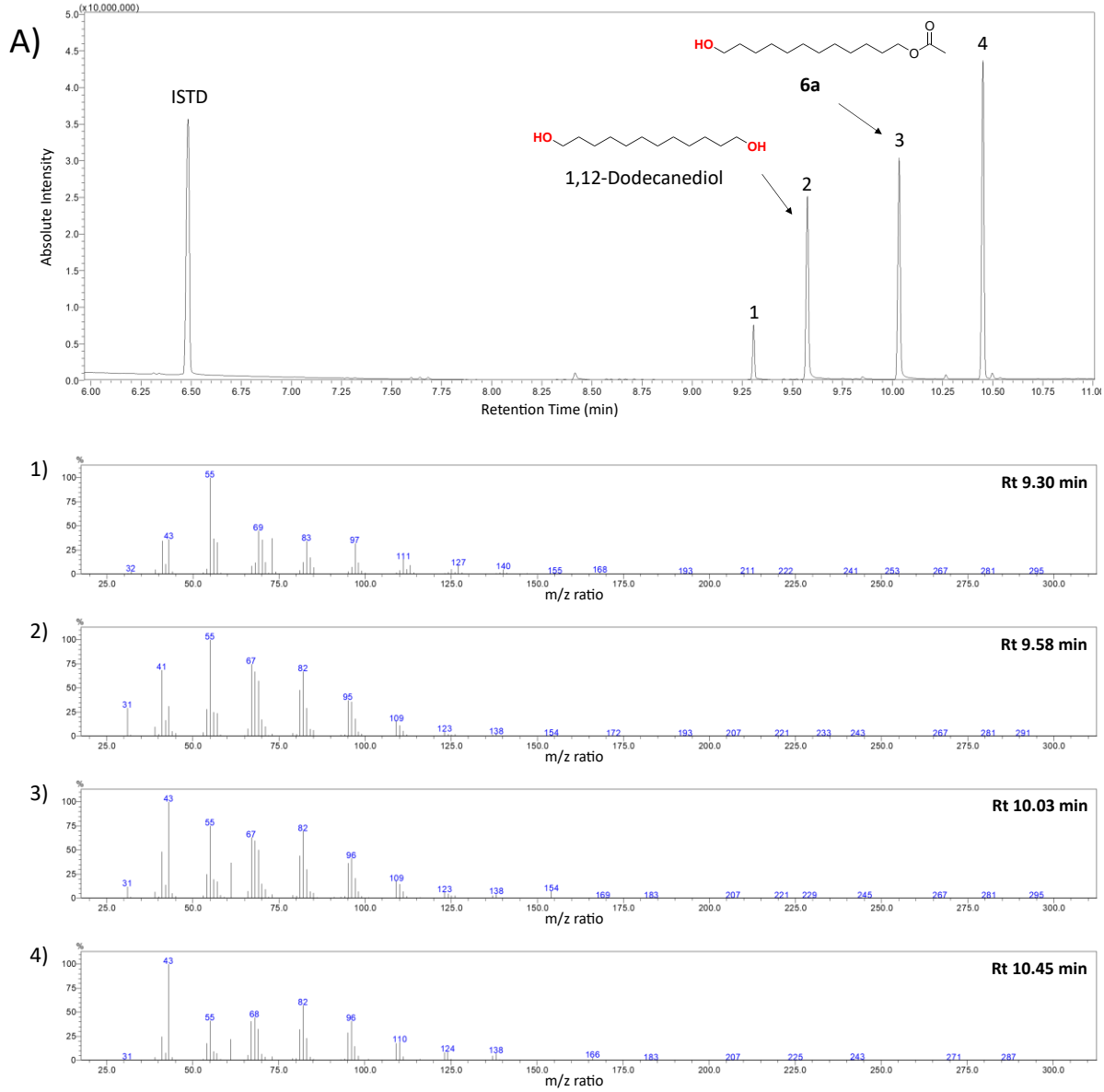

Figure 37 – (A) GC-MS *chromatogram of the synthesis reaction with 1,12-dodecane diol and vinyl acetate, showing the substrate (3) and the products formed. (1-2 and 4): Mass spectra of the respective products and side products formed. (1) Dodecane diol-1-acrylat, (2) Dodecane diol, (3)* ***6a*** *and (4) Dodecane diol-diacetate. The identity of the side products (1) and (4) was determined by mass spectrum analysis and assisted by digital library search but was not confirmed by other means.*

7.5.3 Peak identification

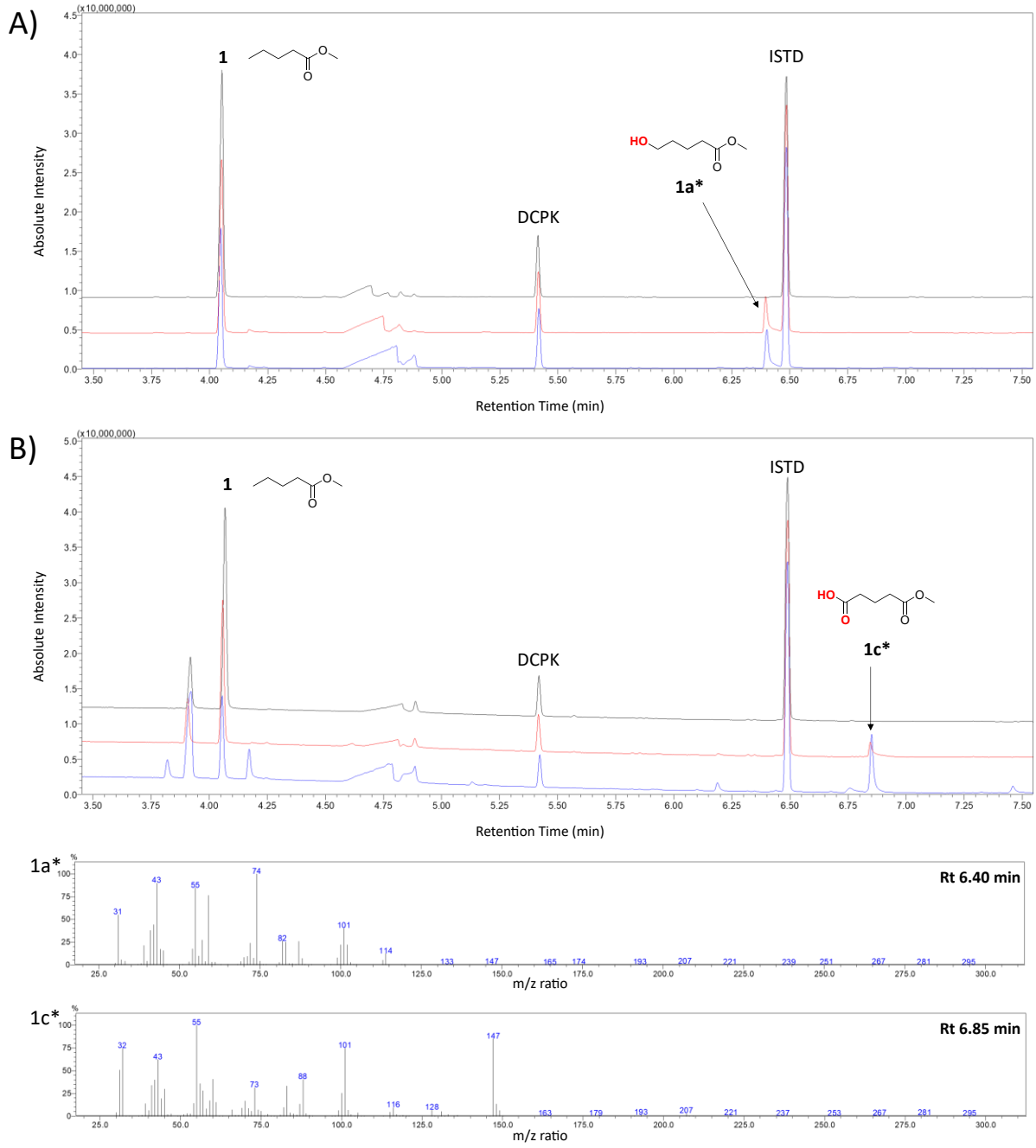

*Figure 38 – GCMS chromatograms of samples from biotransformation of **1** with GPo1 AlkB (A) and Msp AlkB (B), taken after 0 h (black), 1 h (red) and 24 h (blue). Mass spectra are shown for the putative products **1a*** and **1c***. Compounds marked by an asterisk (*) were preliminarily identified by mass spectrum analysis, but not confirmed by other means.*

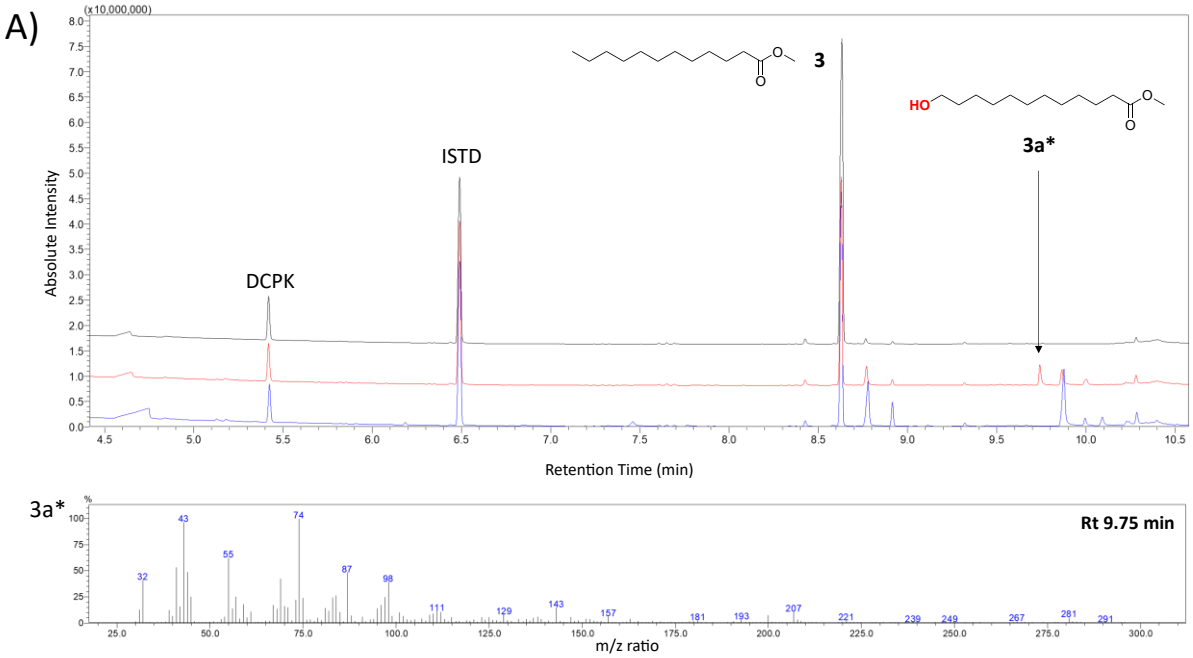

*Figure 39 – (A) GCMS chromatogram of a sample from biotransformation of **3** with Msp AlkB (+ AlkL), taken after 0 h (black), 1 h (red) and 24 h (blue). Mass spectrum is shown for the putative biotransformation product **3a*.** Compounds marked by an asterisk (*) were preliminarily identified by mass spectrum analysis, but not confirmed by other means.*

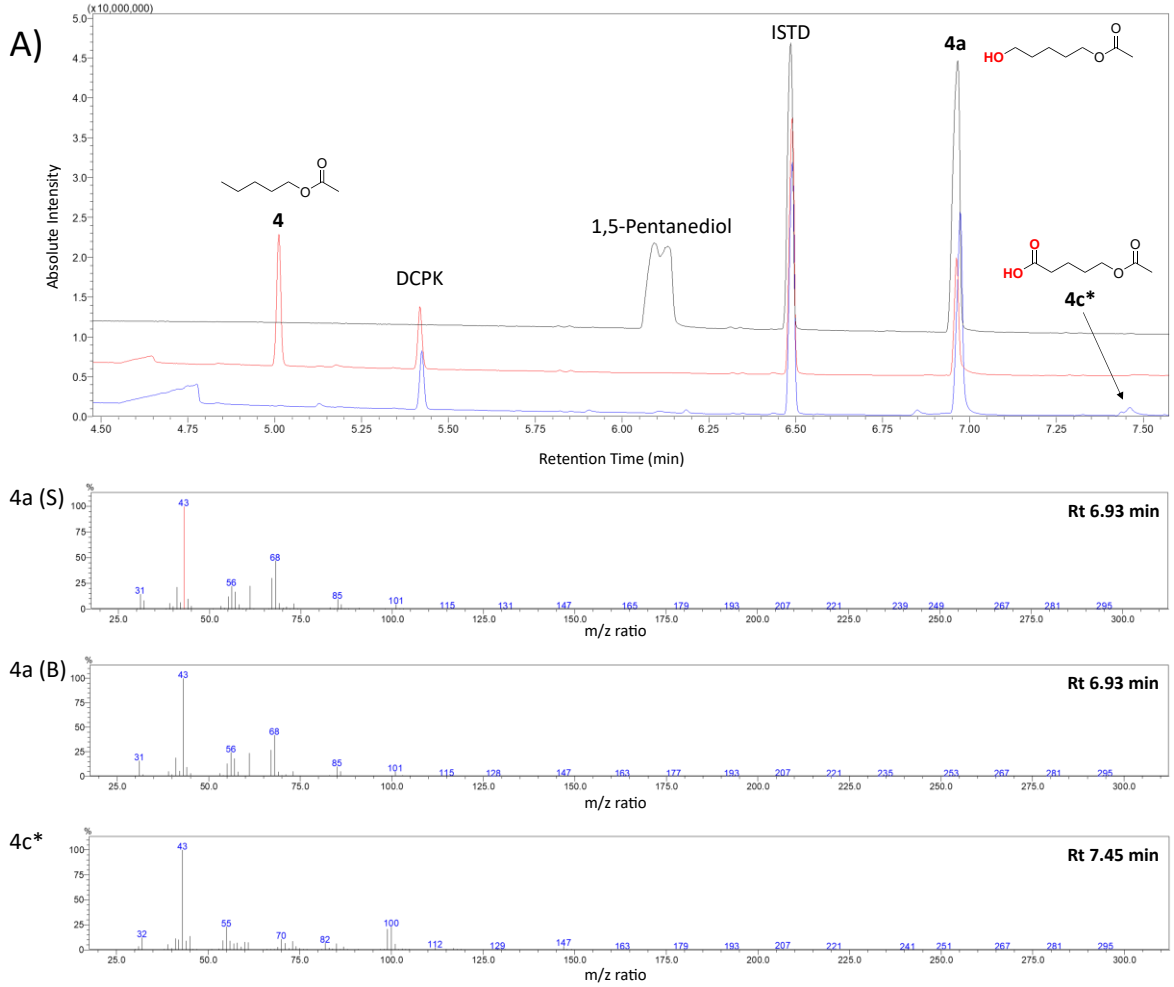

*Figure 40 – (A) Comparison between GCMS chromatograms of the synthesized standard **4a** (black) with samples from biotransformations of **4** with Msp AlkB wild type (+ AlkL), taken 1h (red) and 24 h (blue) after reaction start. (B1) Mass spectra are shown for the **4a** standard (S) and the biotransformation product (B), and the putative biotransformation product **4c***. Compounds marked by an asterisk (*) were preliminarily identified by mass spectrum analysis, but not confirmed by other means.*

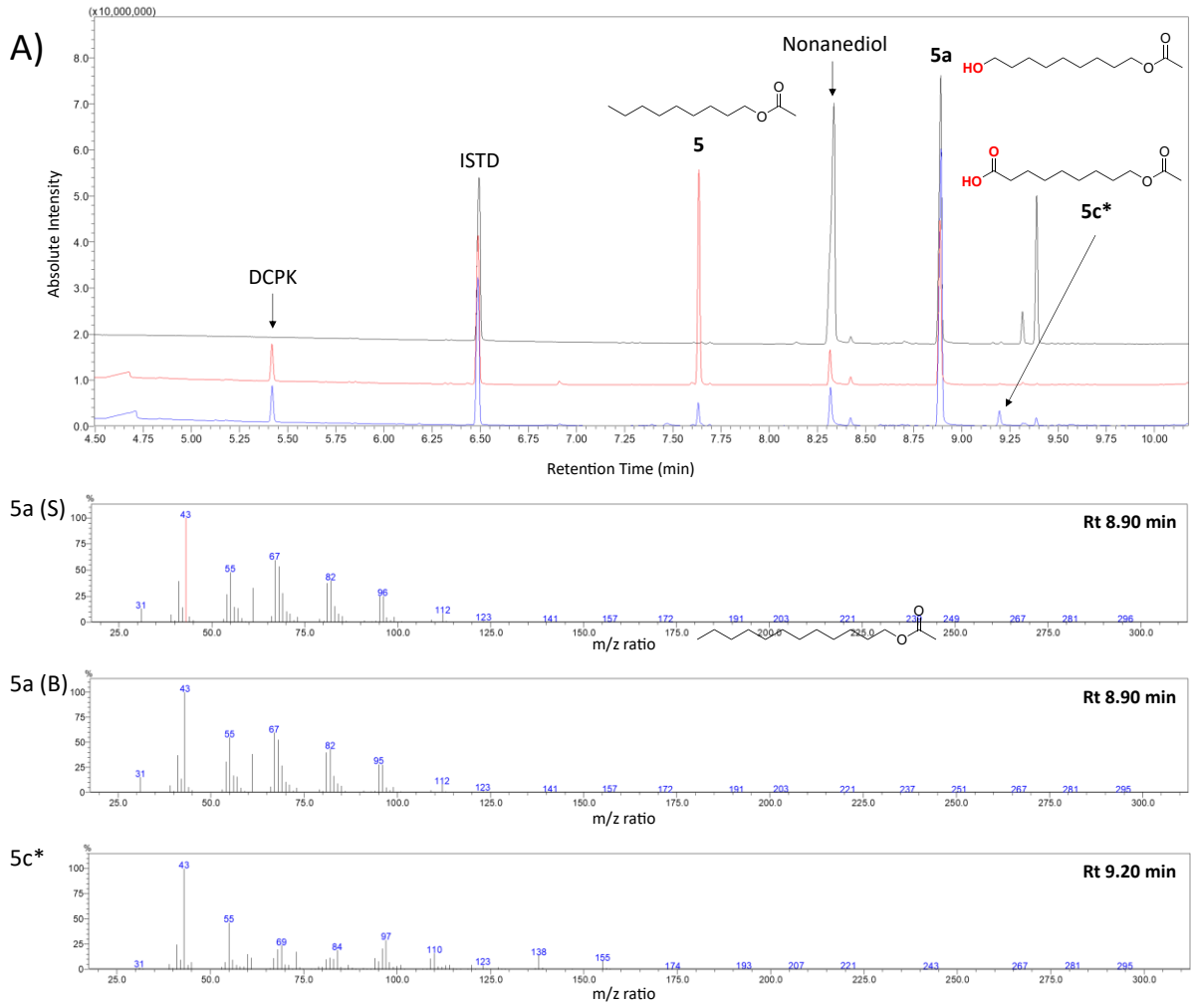

*Figure 41 – (A) Comparison between GCMS chromatograms of the synthesized standard **5a** (black) and of samples from biotransformations of **5** with Msp AlkB wild type (+ AlkL) taken 1h (red) and 24 h (blue) after reaction start Mass spectra are shown for the **5a** standard (S) and the biotransformation product (B), and the putative biotransformation product **5c***. Compounds marked by an asterisk (*) were preliminarily identified by mass spectrum analysis, but not confirmed by other means.*

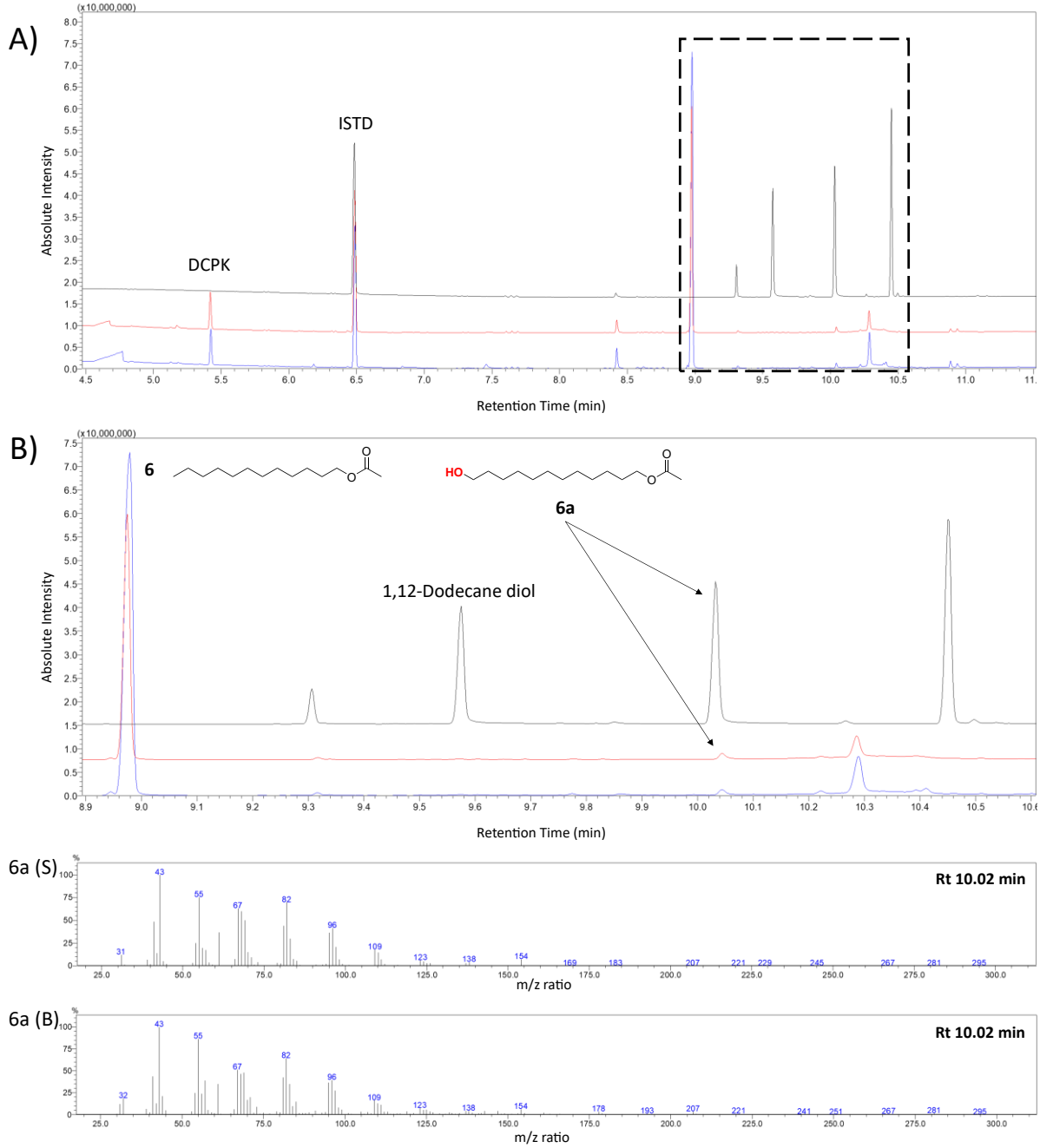

*Figure 42 – (A) Comparison between GCMS chromatograms of the synthesized standard **6a** (black) and of samples from biotransformations of **6** with Msp AlkB (+AlkL) wild type, taken 1h (red) and 24 h (blue) after reaction start. (B) Closer view of the upper chromatogram showing the small product peak overlapping with the standard. At 10.3 min the unknown side product can be seen. Mass spectra are shown for the **6a** standard (S) and the biotransformation product (B).*

7.5.4 Preliminary biotransformation tests

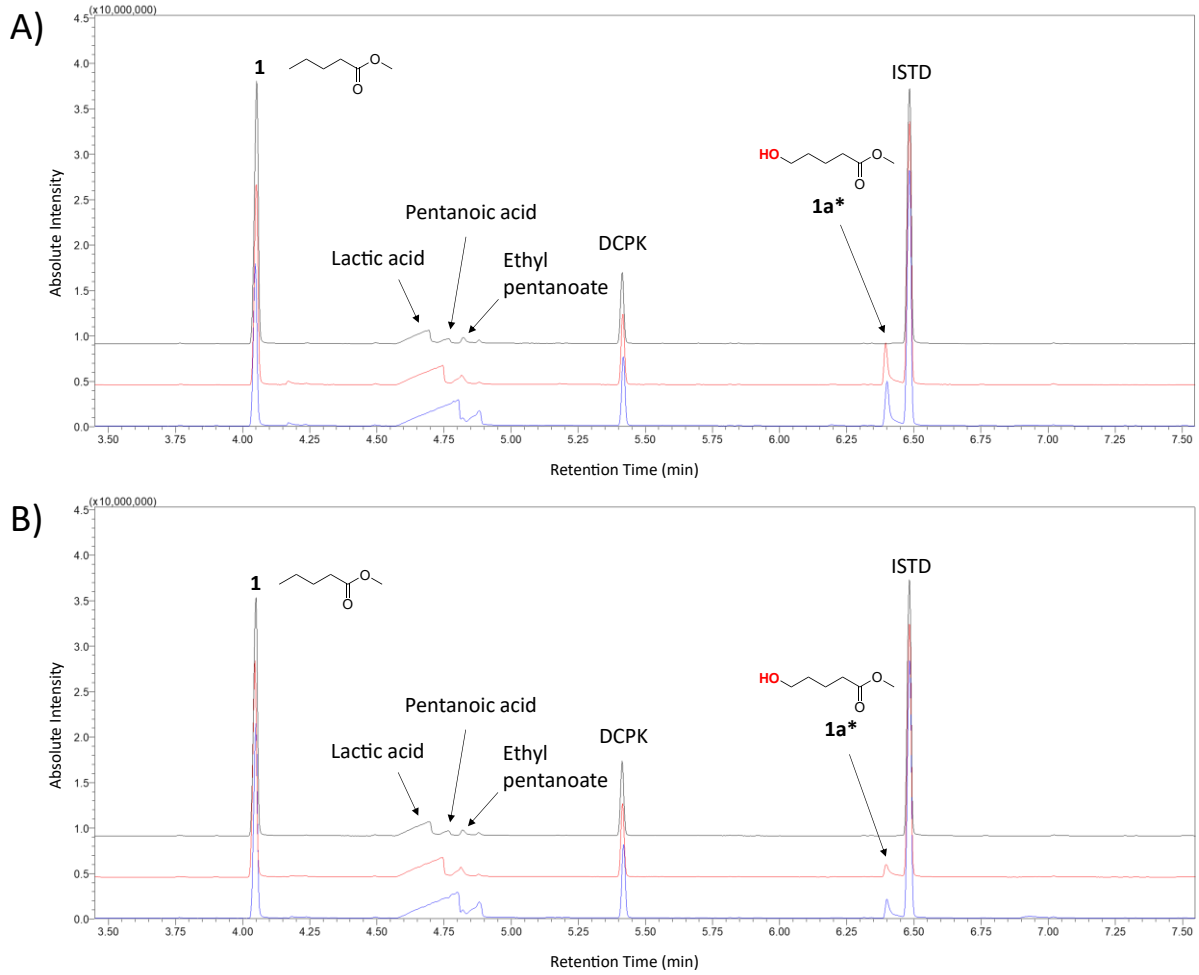

*Figure 43 – GC-MS chromatogram of samples from biotransformation of **1** with Pp GPo1 AlkB wild type. (A) Msp AlkB wild type (-AlkL). B) Msp AlkB wild type (+AlkL). Colours indicate the sampling timepoints: t0 (black), t1 (red) and t24 (blue). Compounds marked by an asterisk (*) were preliminarily identified by mass spectrum analysis, but not confirmed by other means.*

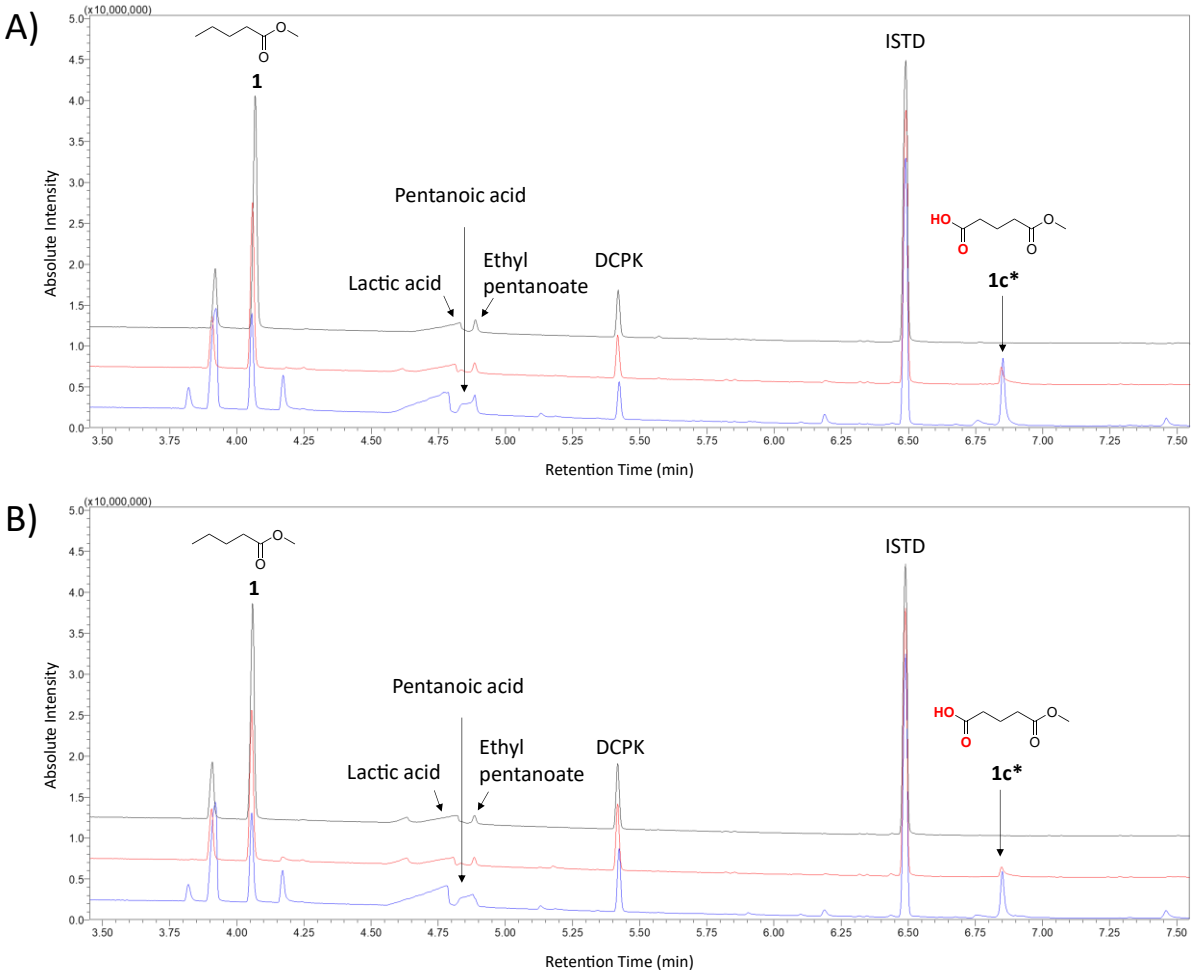

*Figure 44 – GC-MS chromatogram of samples from biotransformation of **1** with Msp AlkB wild type. (A) Msp AlkB wild type (-AlkL). B) Msp AlkB wild type (+AlkL). Colours indicate the sampling timepoints: t0 (black), t1 (red) and t24 (blue). Compounds marked by an asterisk (*) were preliminarily identified by mass spectrum analysis, but not confirmed by other means.*

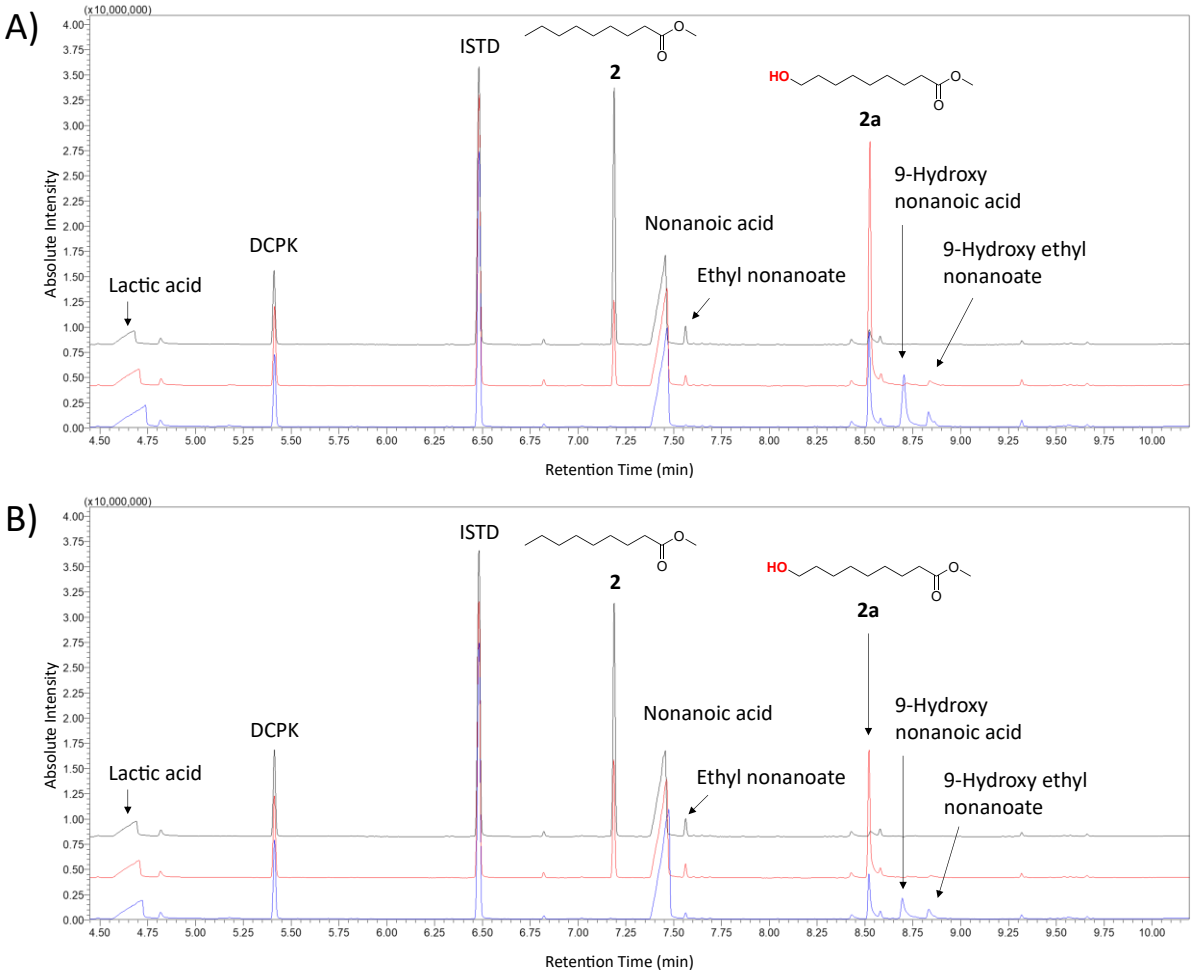

*Figure 45 – GC-MS chromatogram of samples from biotransformation of **2** with Pp GPo1 AlkB wild type. (A) Msp AlkB wild type (-AlkL). B) Msp AlkB wild type (+AlkL). Colours indicate the sampling timepoints: t0 (black), t1 (red) and t24 (blue).*

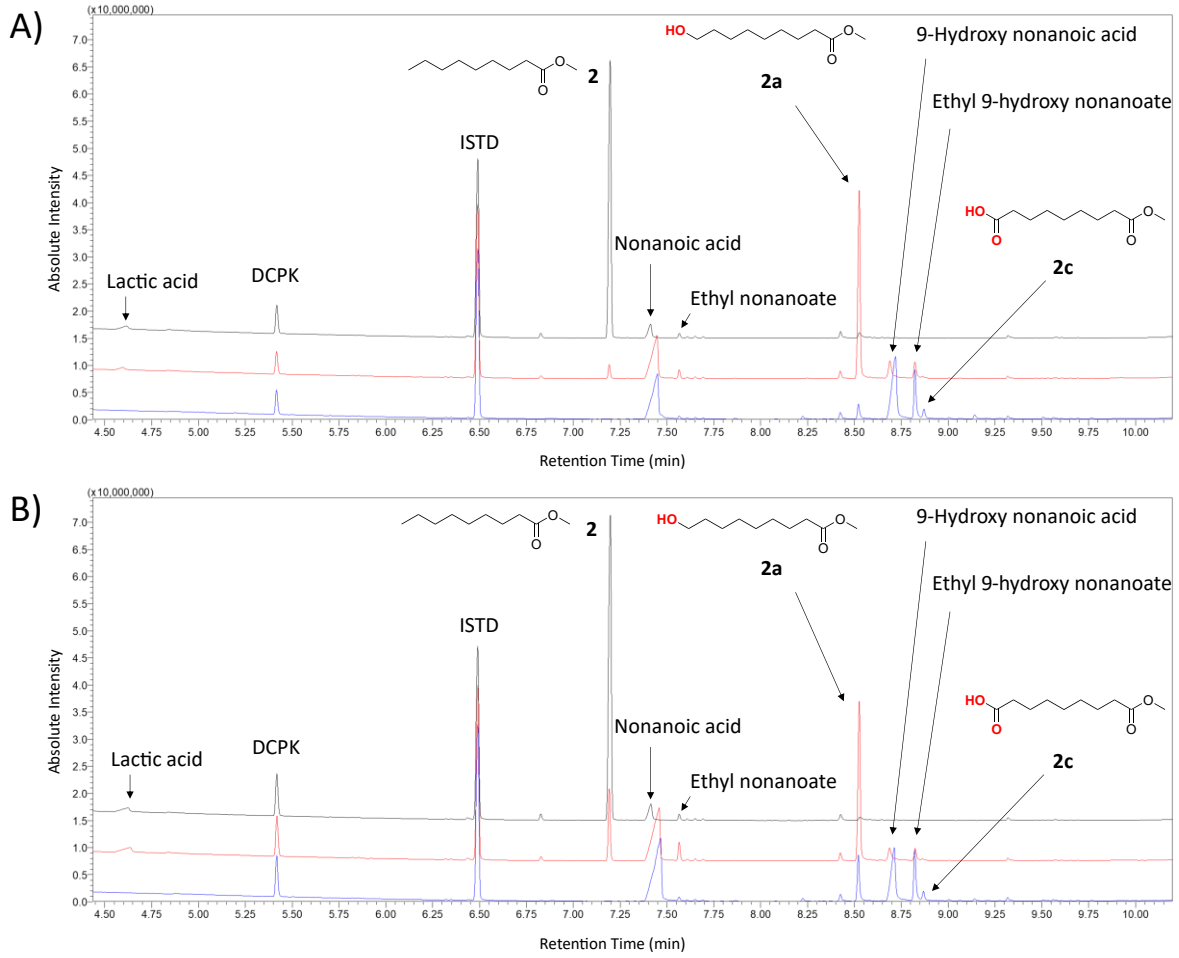

*Figure 46 – GC-MS chromatogram of samples from biotransformation of **2** with Msp AlkB wild type. (A) Msp AlkB wild type (-AlkL). B) Msp AlkB wild type (+AlkL). Colours indicate the sampling timepoints: t0 (black), t1 (red) and t24 (blue).*

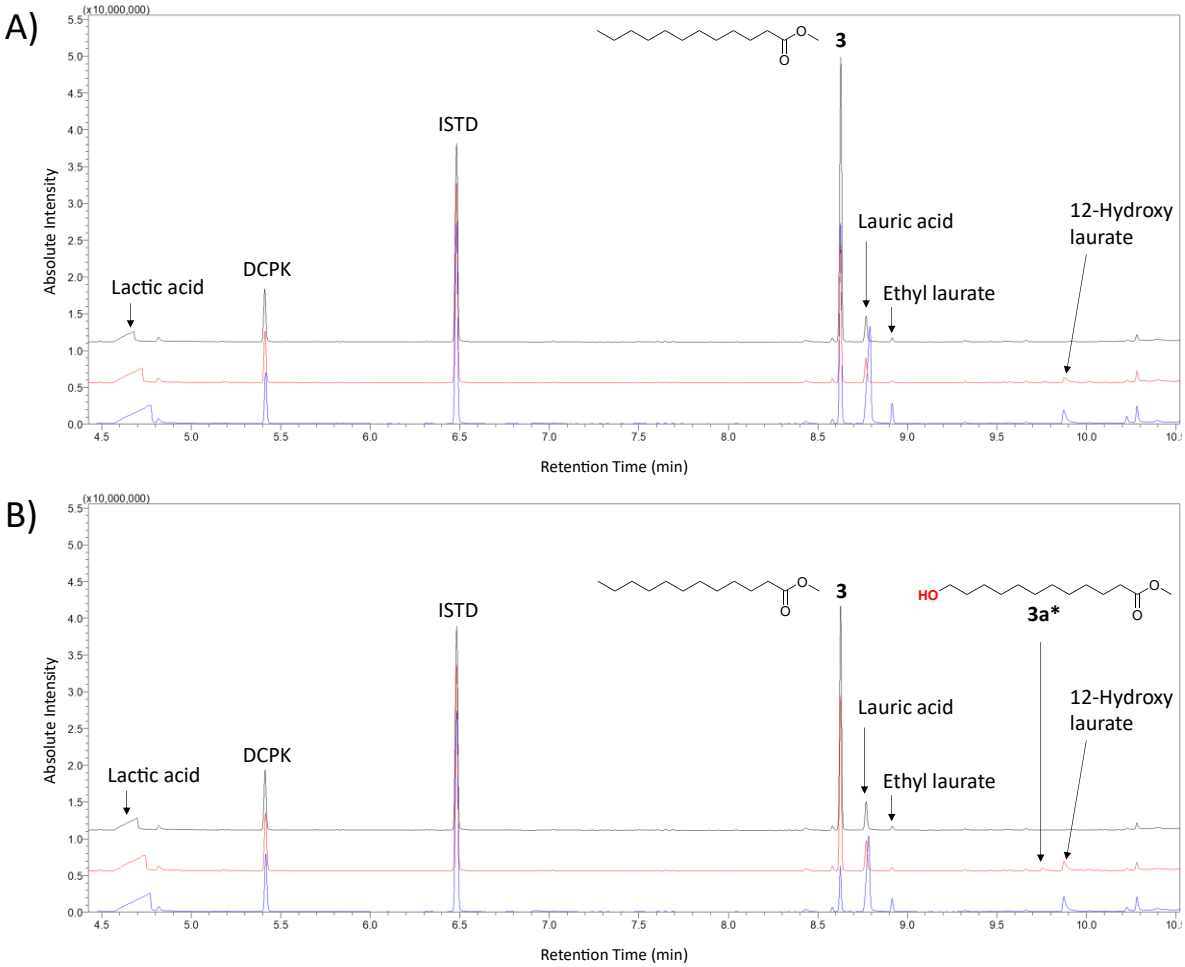

*Figure 47 – GC-MS chromatogram of samples from biotransformation of **3** with Pp GPo1 AlkB wild type. (A) Msp AlkB wild type (-AlkL). B) Msp AlkB wild type (+AlkL). Colours indicate the sampling timepoints: t0 (black), t1 (red) and t24 (blue). Compounds marked by an asterisk (*) were preliminarily identified by mass spectrum analysis, but not confirmed by other means.*

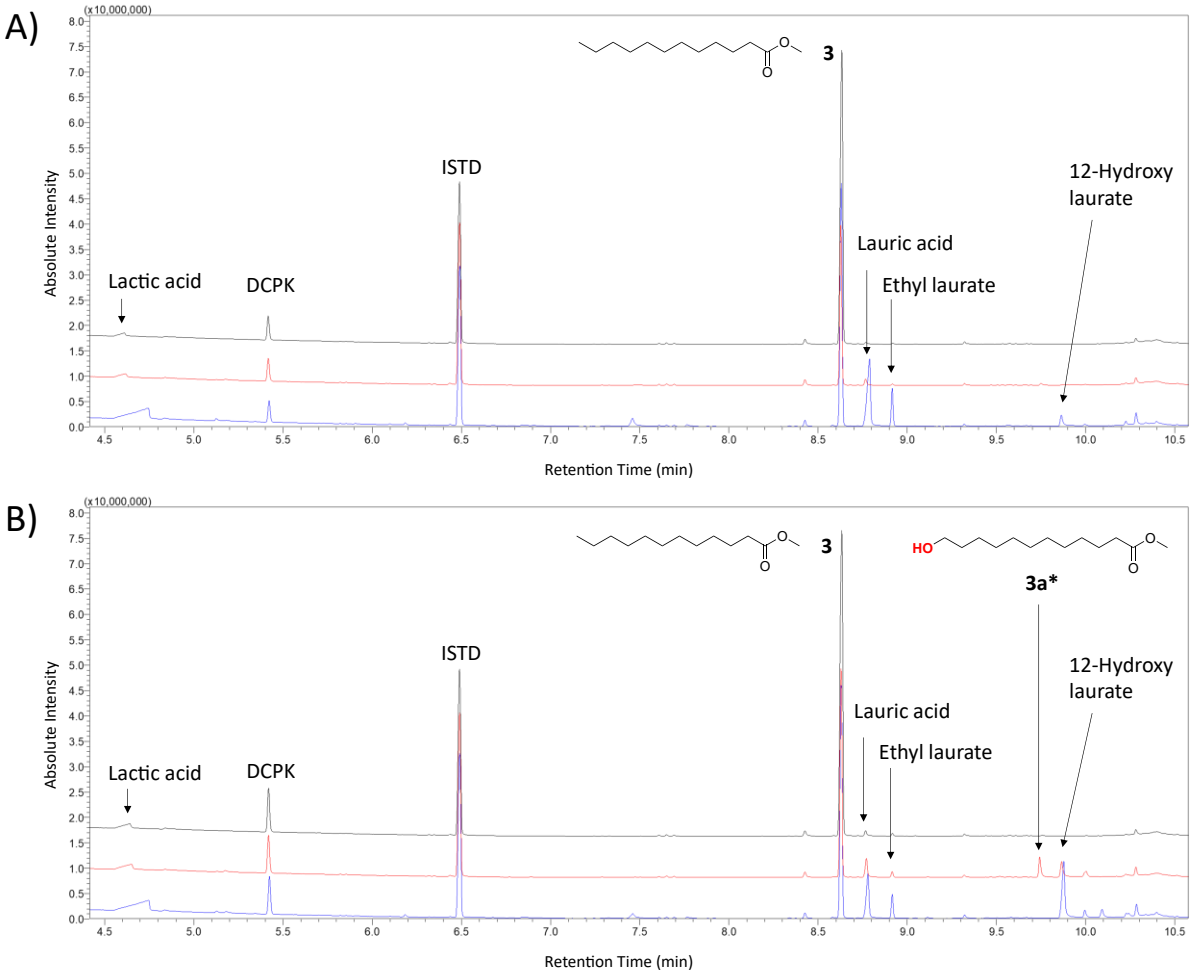

*Figure 48 – GC-MS chromatogram of samples from biotransformation of **3** with Msp AlkB wild type. (A) Msp AlkB wild type (-AlkL). B) Msp AlkB wild type (+AlkL). Colours indicate the sampling timepoints: t0 (black), t1 (red) and t24 (blue). Compounds marked by an asterisk (*) were preliminarily identified by mass spectrum analysis, but not confirmed by other means.*

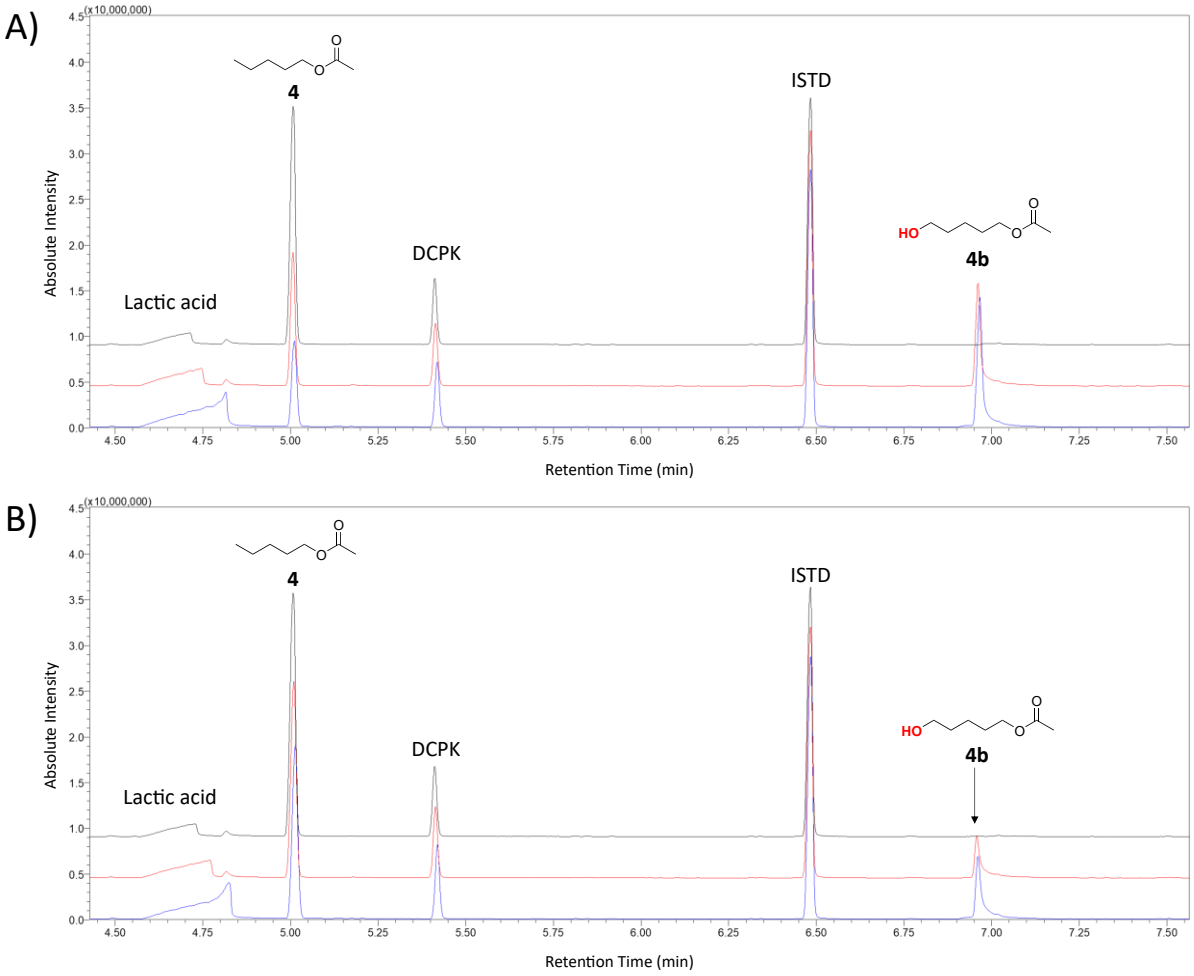

*Figure 49 – GC-MS chromatogram of samples from biotransformation of **4** with Pp GPo1 AlkB wild type. (A) Msp AlkB wild type (-AlkL). B) Msp AlkB wild type (+AlkL). Colours indicate the sampling timepoints: t0 (black), t1 (red) and t24 (blue).*

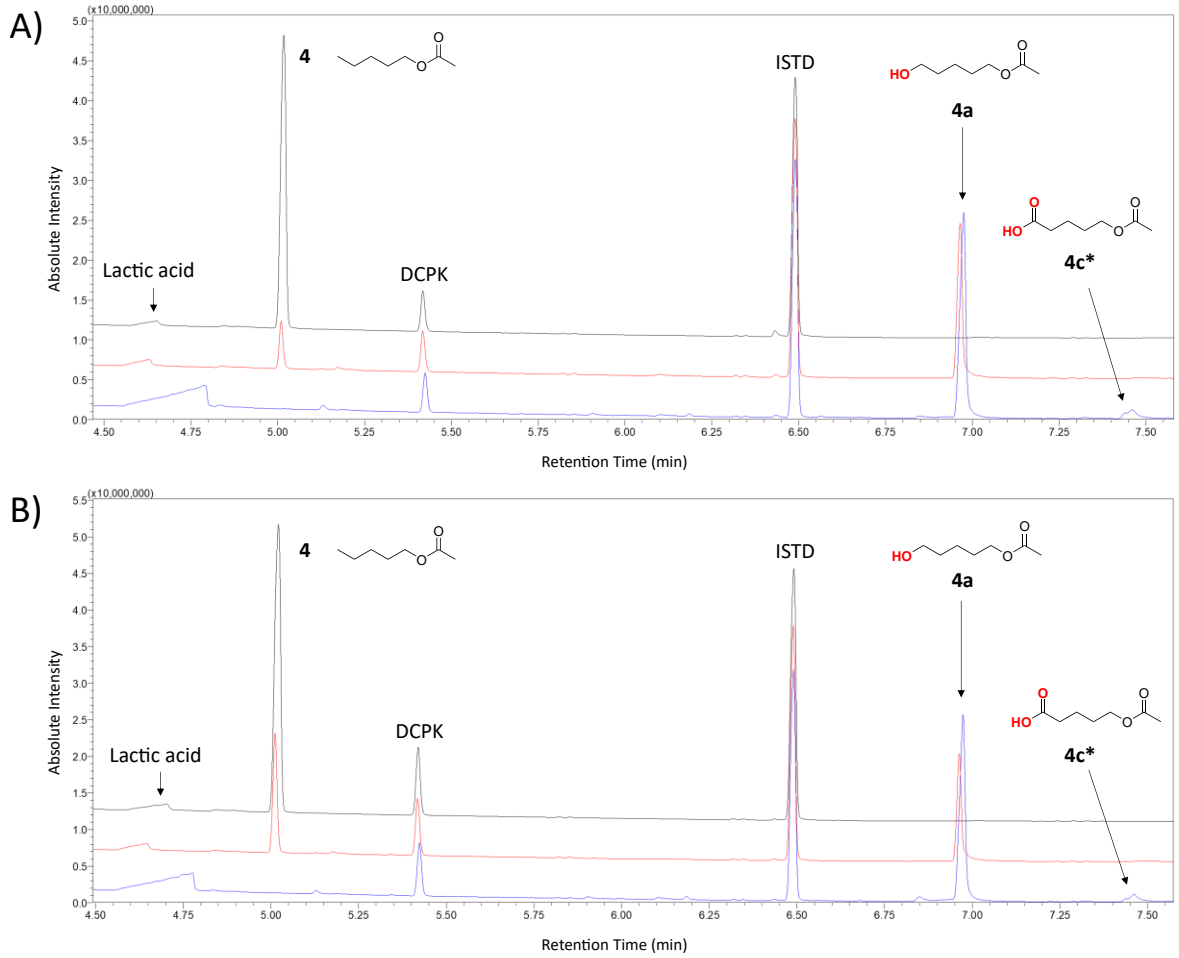

*Figure 50 – GC-MS chromatogram of samples from biotransformation of **4** with Msp AlkB wild type. (A) Msp AlkB wild type (-AlkL). B) Msp AlkB wild type (+AlkL). Colours indicate the sampling timepoints: t0 (black), t1 (red) and t24 (blue). Compounds marked by an asterisk (*) were preliminarily identified by mass spectrum analysis, but not confirmed by other means.*

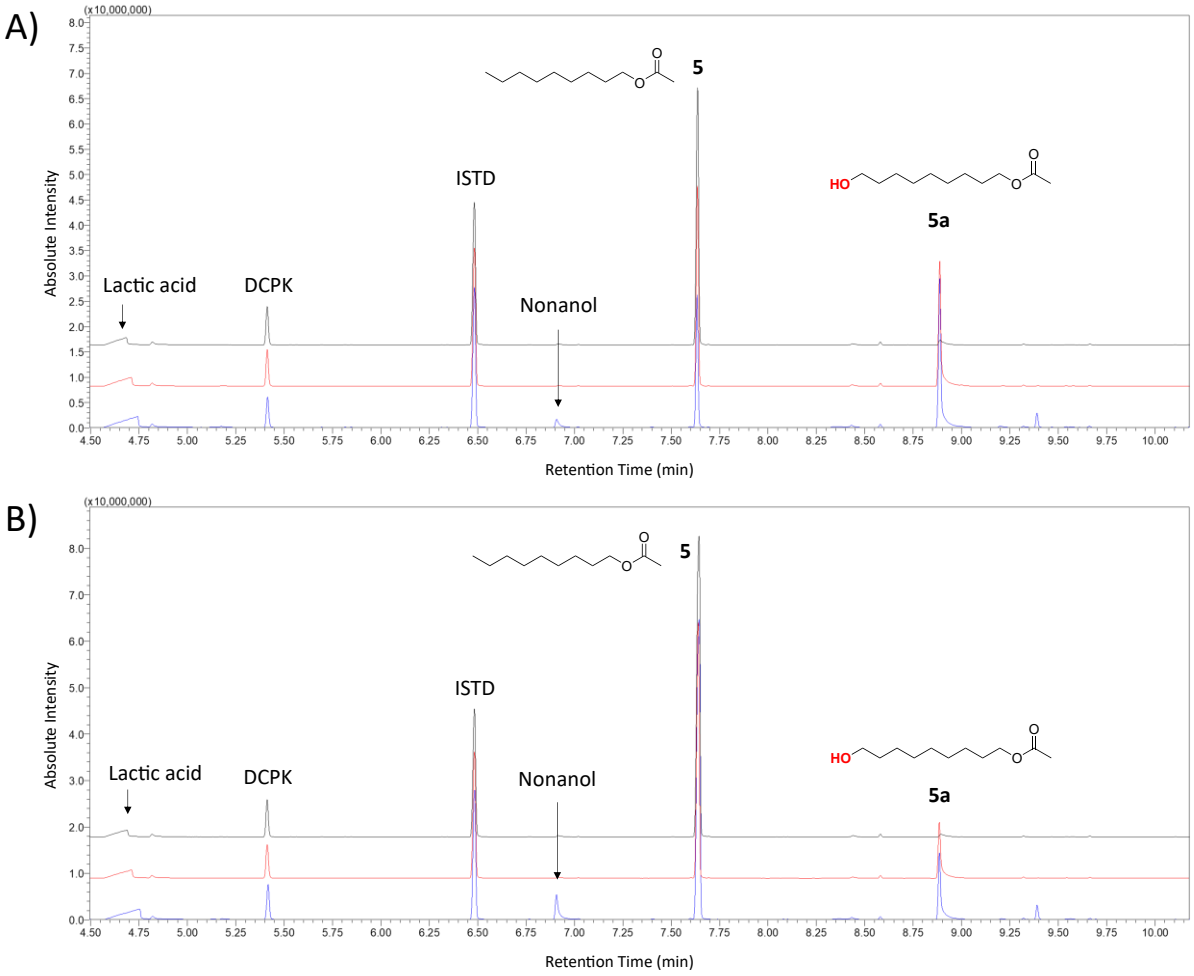

*Figure 51 – GC-MS chromatogram of samples from biotransformation of **5** with Pp GPo1 AlkB wild type. (A) Msp AlkB wild type (-AlkL). B) Msp AlkB wild type (+AlkL). Colours indicate the sampling timepoints: t0 (black), t1 (red) and t24 (blue).*

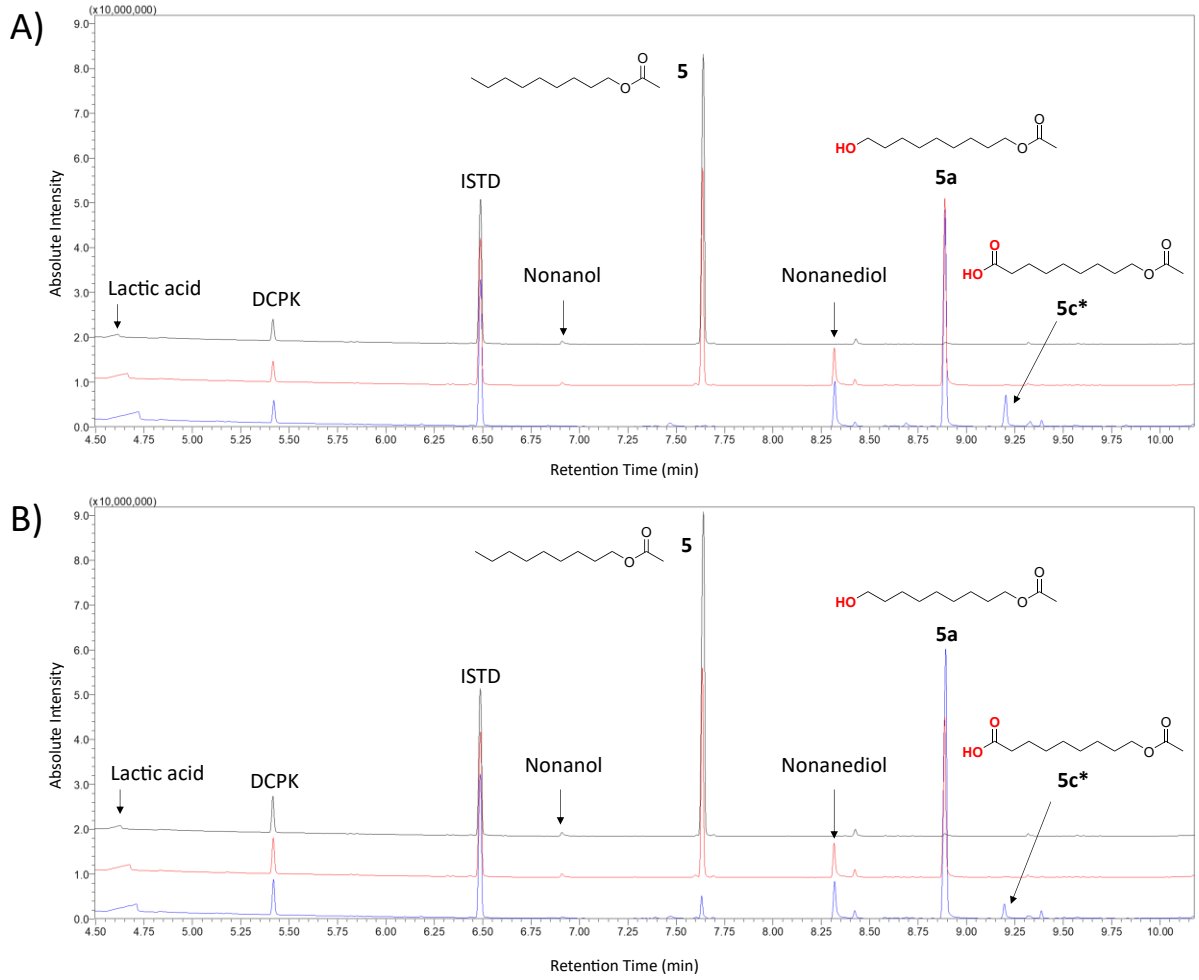

*Figure 52 – GC-MS chromatogram of samples from biotransformation of **5** with Msp AlkB wild type. (A) Msp AlkB wild type (-AlkL). B) Msp AlkB wild type (+AlkL). Colours indicate the sampling timepoints: t0 (black), t1 (red) and t24 (blue). Compounds marked by an asterisk (*) were preliminarily identified by mass spectrum analysis, but not confirmed by other means.*

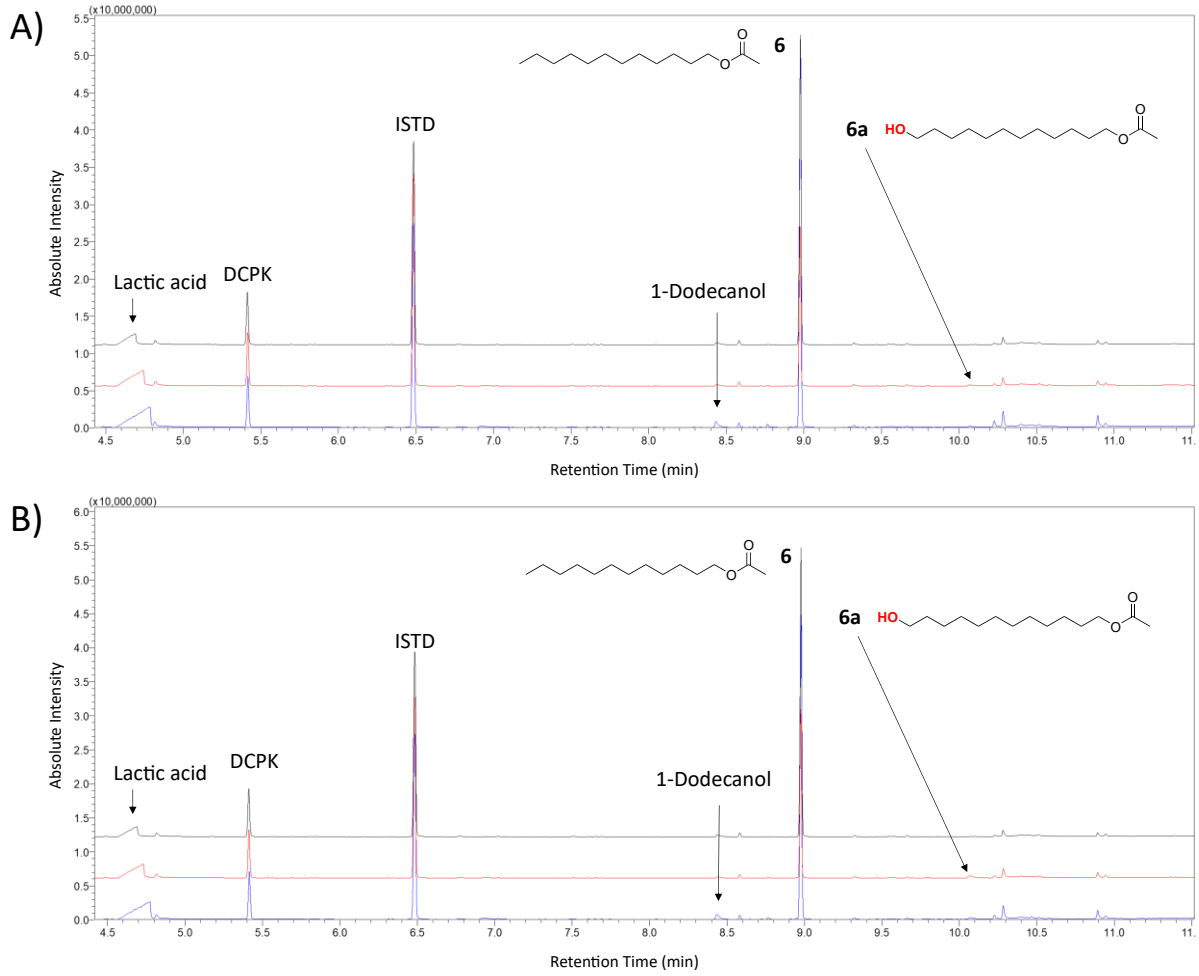

*Figure 53 – GC-MS chromatogram of samples from biotransformation of **6** with Pp GPo1 AlkB wild type. (A) Msp AlkB wild type (-AlkL). B) Msp AlkB wild type (+AlkL). Colours indicate the sampling timepoints: t0 (black), t1 (red) and t24 (blue).*

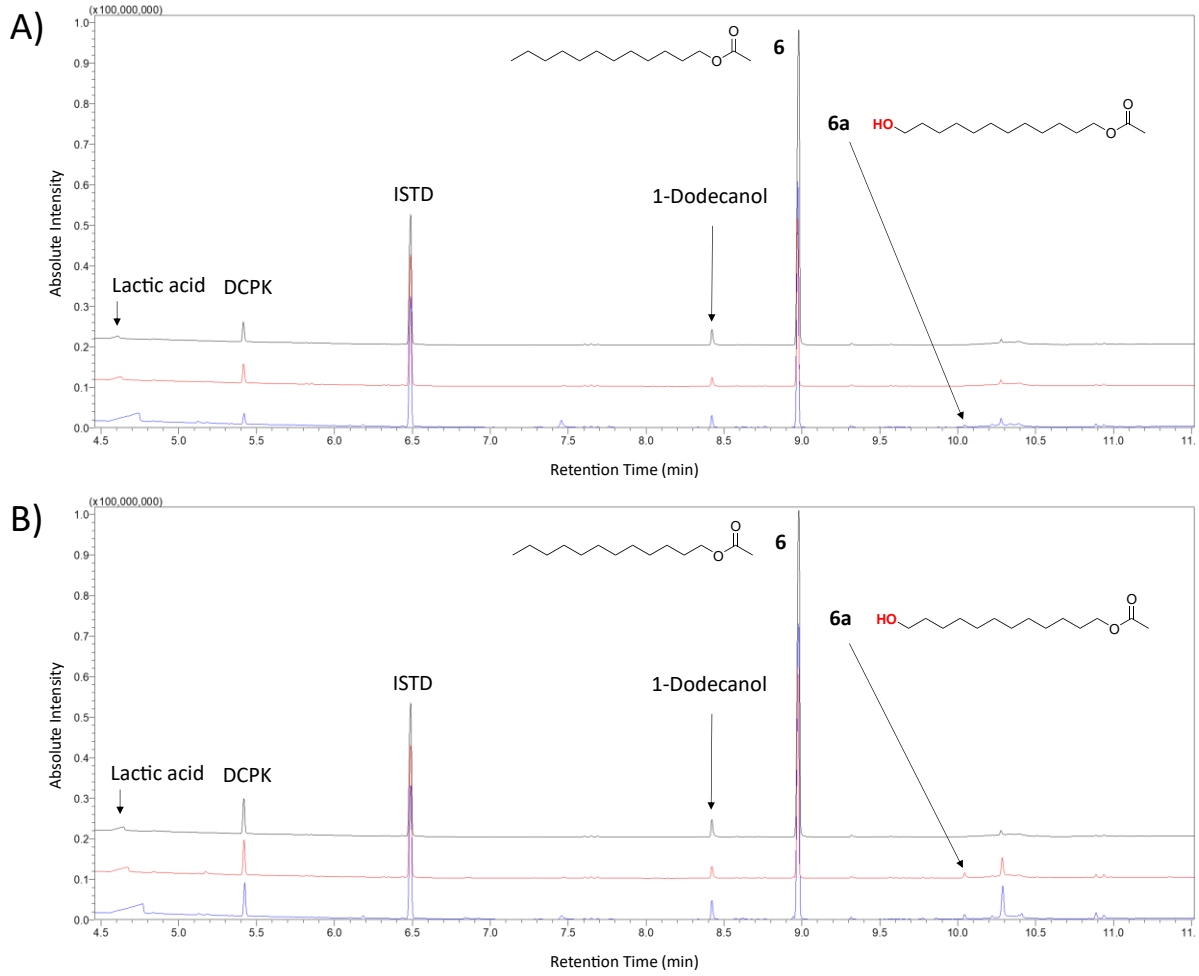

*Figure 54 – GC-MS chromatogram of samples from biotransformation of **6** with Msp AlkB wild type. (A) Msp AlkB wild type (-AlkL). B) Msp AlkB wild type (+AlkL). Colours indicate the sampling timepoints: t0 (black), t1 (red) and t24 (blue).*

7.5.5 Biotransformations with mutants

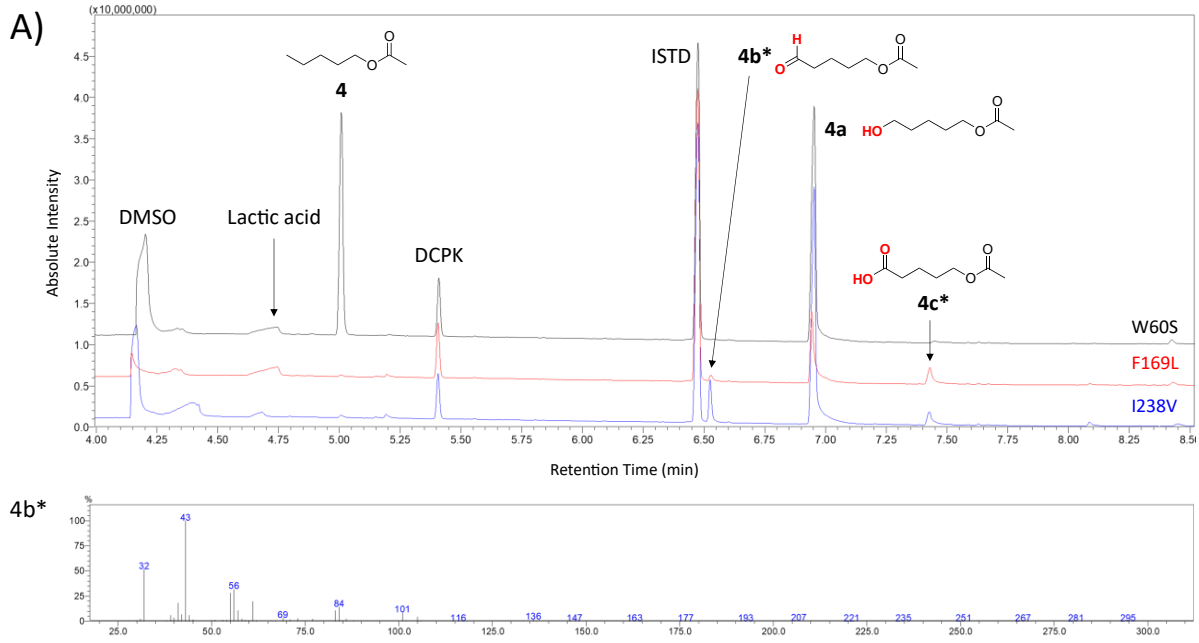

*Figure 55 – GC-MS chromatograms of samples from biotransformation of **4** with Msp AlkB (+ AlkL) mutants W60S, F169L, I238V, taken 1 hour after reaction start. Mass spectrum is shown for the putative biotransformation product **4b***. Compounds marked by an asterisk (*) were preliminarily identified by mass spectrum analysis, but not confirmed by other means.*

7.5.6 Negative controls

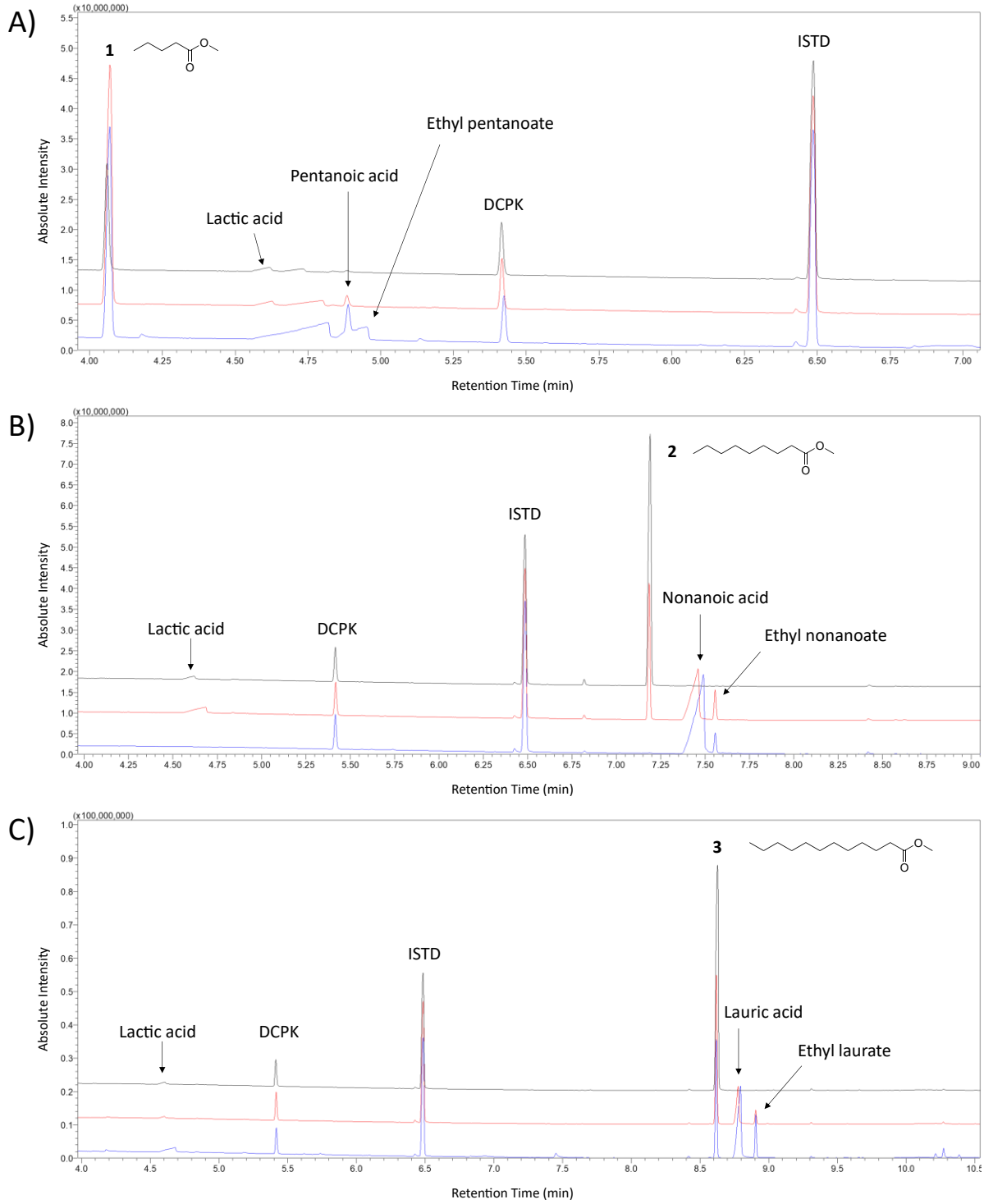

Figure 56 – Negative controls with inactive variant Msp AlkB (H278A) and methyl esters in ethanol.

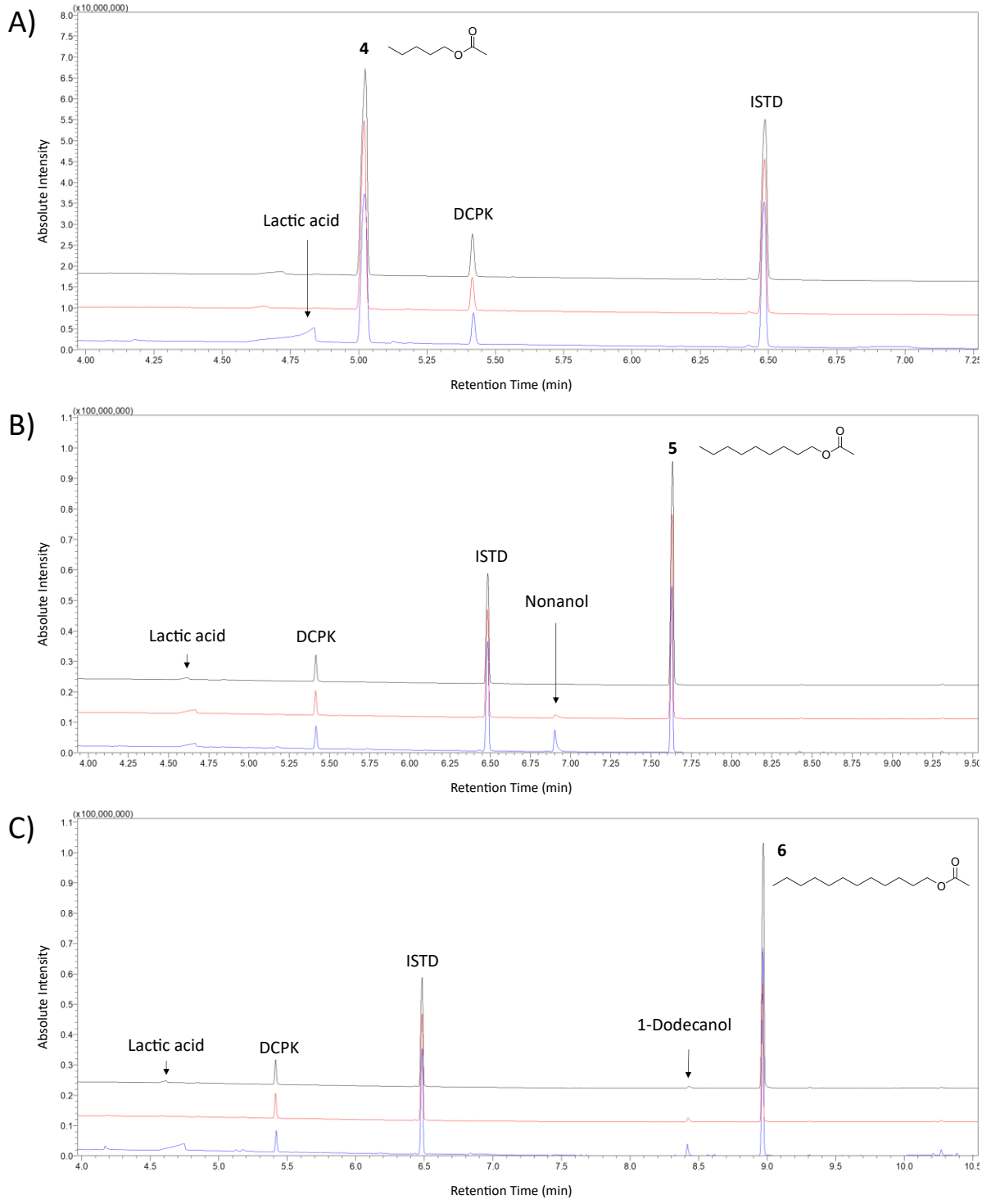

Figure 57 – Negative controls with inactive variant Msp AlkB (H278A) and acetate esters in ethanol.

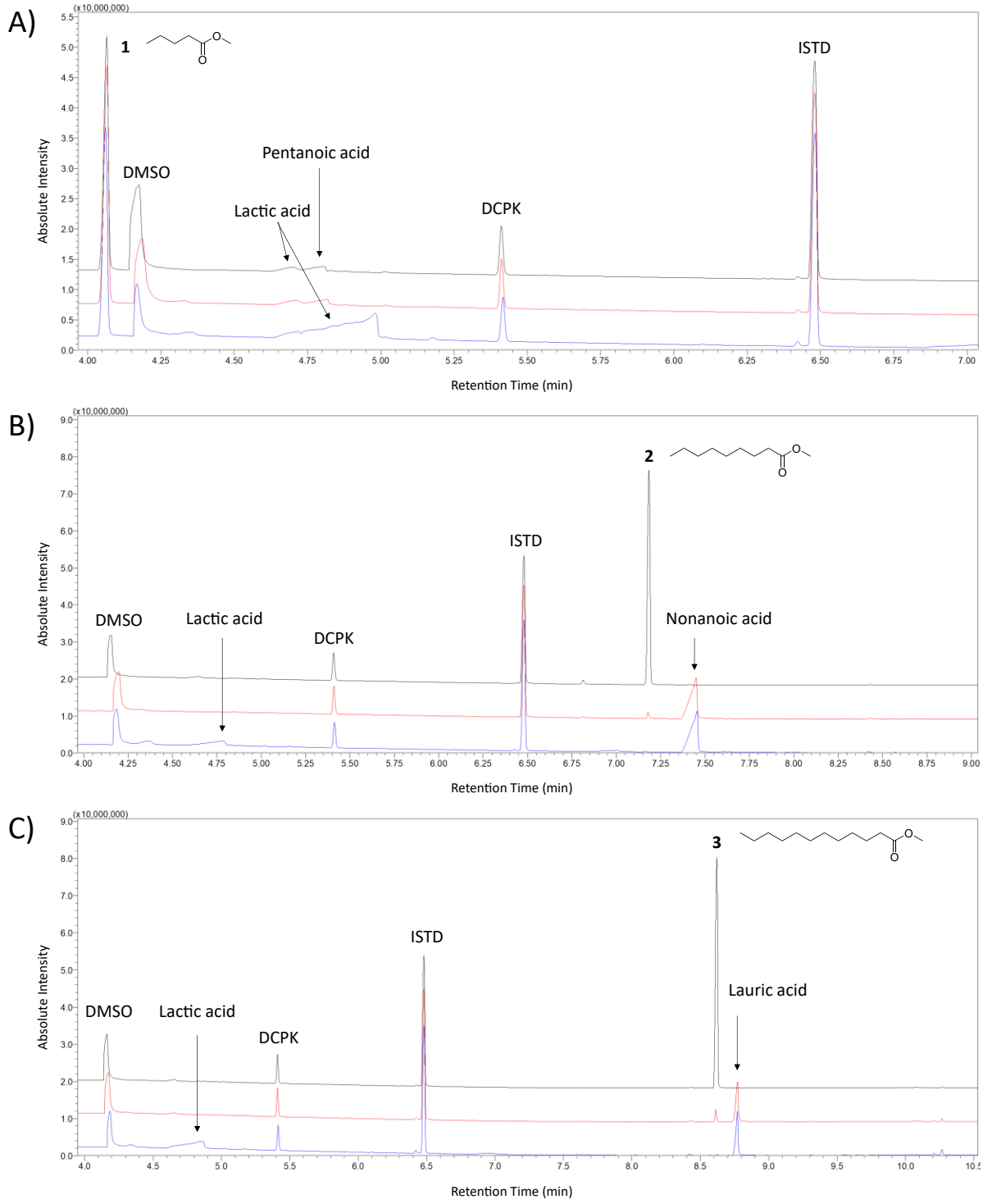

Figure 58 – Negative controls with inactive variant Msp AlkB (H278A) and FAMEs in DMSO.

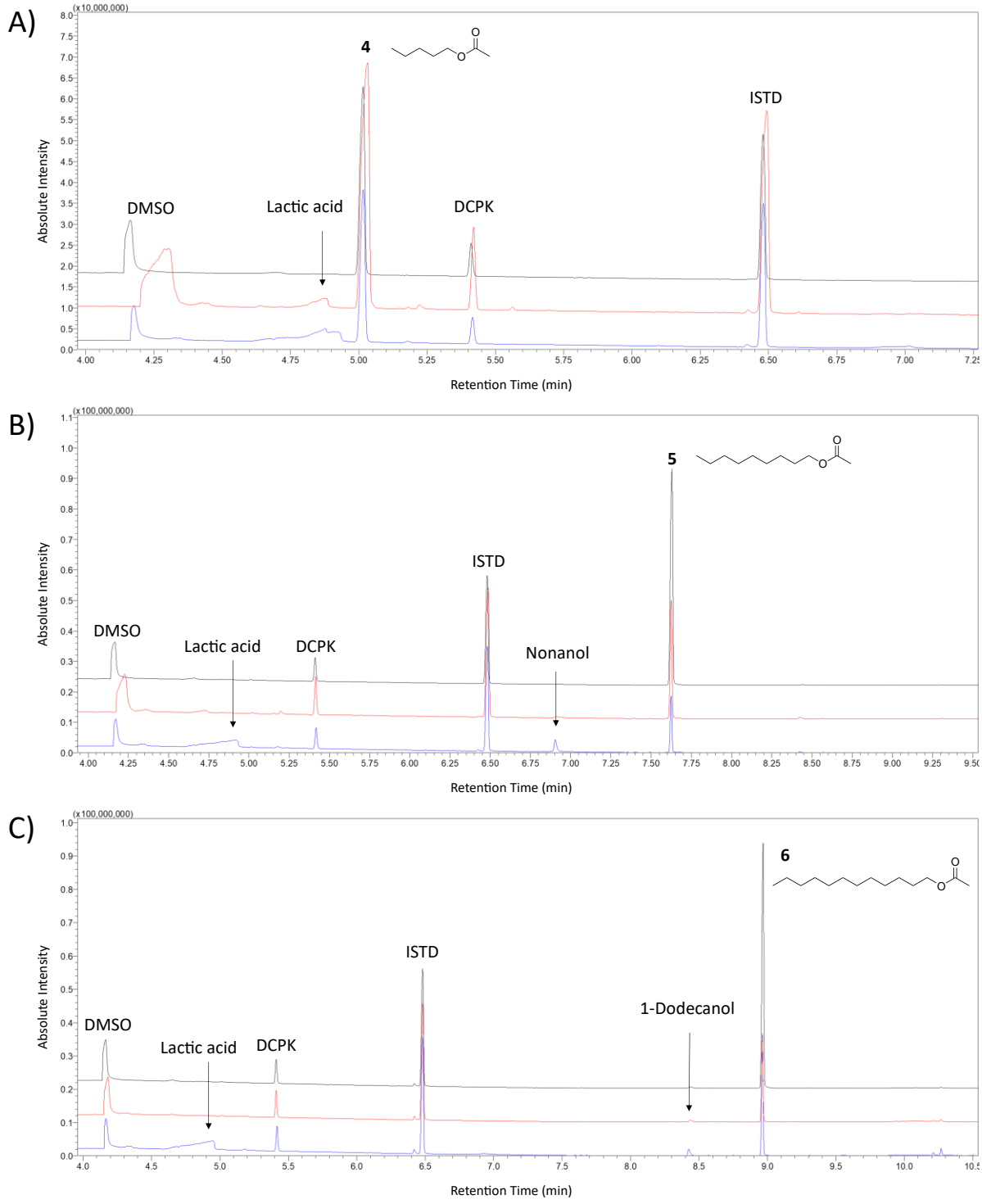

Figure 59 – Negative controls with inactive variant Msp AlkB (H278A) and AAs in DMSO.

8 Raw data

8.1 Methyl nonanoate (2)

*Table 16 – Summary of the data from biotransformations of **2** with Msp AlkB wild type at 1 g_{CDW} L^{-1}. The average concentrations of the substrate, (side-)products and the corresponding standard deviations listed were derived from triplicates.*

	t [min]	2		Nonanoic acid		2a		2c	
		Mean [mM]	Std. Dev. [+/-]	Mean [mM]	Std. Dev. [+/-]	Mean [mM]	Std. Dev. [+/-]	Mean [mM]	Std. Dev. [+/-]
***Msp AlkB* wildtype**	0	2.05	0.08	0.00	0.00	0.00	0.00	n.d.	
	15	0.45	0.04	0.05	0.01	0.09	0.01		
	30	0.42	0.05	0.09	0.02	0.19	0.04		
	45	0.43	0.04	0.12	0.02	0.26	0.04		
	60	0.49	0.09	0.16	0.02	0.35	0.05		
	120	0.32	0.02	0.32	0.04	0.61	0.12		
	240	0.00	0.00	0.45	0.01	0.81	0.03	0.11	0.00

*Table 17 – Summary of the data from biotransformations of **2** with Msp AlkB W60S at 1 g_{CDW} L^{-1}. The average concentrations of the substrate, (side-)products and the corresponding standard deviations listed were derived from triplicates.*

	t [min]	2		Nonanoic acid		2a		2c	
		Mean [mM]	Std. Dev. [+/-]	Mean [mM]	Std. Dev. [+/-]	Mean [mM]	Std. Dev. [+/-]	Mean [mM]	Std. Dev. [+/-]
***Msp AlkB* W60S**	0	1.48	0.43	0.00	0.00	0.00	0.00	n.d.	
	15	0.32	0.06	0.04	0.01	0.04	0.01		
	30	0.30	0.03	0.08	0.02	0.11	0.03		
	45	0.30	0.03	0.12	0.04	0.15	0.04		
	60	0.30	0.06	0.16	0.05	0.21	0.05		
	120	0.21	0.16	0.32	0.08	0.36	0.07	0.01	0.02
	240	0.03	0.03	0.44	0.10	0.41	0.13	0.04	0.05

*Table 18 – Summary of the data from biotransformations of **2** with Msp AlkB F169L at 1 g_{CDW} L^{-1}. The average concentrations of the substrate, (side-)products and the corresponding standard deviations listed were derived from triplicates.*

	t [min]	2		Nonanoic acid		2a		2c	
		Mean [mM]	Std. Dev. [+/-]	Mean [mM]	Std. Dev. [+/-]	Mean [mM]	Std. Dev. [+/-]	Mean [mM]	Std. Dev. [+/-]
***Msp AlkB* F169L**	0	1.84	0.38	0.00	0.00	0.00	0.00	n. d.	
	15	0.41	0.03	0.04	0.01	0.15	0.01		
	30	0.39	0.03	0.09	0.01	0.34	0.01		
	45	0.39	0.02	0.12	0.01	0.45	0.02		
	60	0.33	0.10	0.17	0.00	0.62	0.01		
	120	0.04	0.01	0.29	0.02	0.83	0.15		
	240	0.00	0.00	0.33	0.02	0.74	0.14	0.10	0.07

*Table 19 – Summary of the data from biotransformations of **2** with Msp AlkB I238V at 1 g_{CDW} L^{-1}. The average concentrations of the substrate, (side-)products and the corresponding standard deviations listed were derived from triplicates.*

	t [min]	2		Nonanoic acid		2a		2c	
		Mean [mM]	Std. Dev. [+/-]	Mean [mM]	Std. Dev. [+/-]	Mean [mM]	Std. Dev. [+/-]	Mean [mM]	Std. Dev. [+/-]
***Msp AlkB* I238V**	0	2.16	0.06	0.00	0.00	0.00	0.00	n. d.	
	15	0.41	0.05	0.05	0.01	0.16	0.03		
	30	0.39	0.02	0.09	0.01	0.30	0.04		
	45	0.42	0.02	0.13	0.01	0.45	0.04		
	60	0.45	0.02	0.17	0.01	0.57	0.05		
	120	0.15	0.02	0.32	0.02	0.92	0.13		
	240	0.00	0.00	0.38	0.00	0.95	0.01	0.14	0.00

*Table 20 – Data from biotransformations of **2** with Msp AlkB wild type at a cell density of 1 g_{CDW} L^{-1} and an initial substrate concentration of 5 mM. The average concentrations of the substrate, (side-)products and the corresponding standard deviations listed were derived from a single replicate.*

	t [min]	2 [mM]	Nonanoic acid [mM]	2a [mM]	2c [mM]
***Msp AlkB* WT**	0	4.57	0.00	0.00	n.d.
	15	0.48	0.04	0.08	
	30	0.63	0.08	0.18	
	45	0.46	0.12	0.28	
	60	0.44	0.16	0.37	
	120	0.61	0.32	0.68	
	240	0.72	0.54	0.95	0.03
	1440	0.00	0.94	0.94	0.18

*Table 21 – Data from biotransformations of **2** with Msp AlkB I238V at a cell density of 1 g_{CDW} L^{-1} and an initial substrate concentration of 5 mM. The average concentrations of the substrate, (side-)products and the corresponding standard deviations listed were derived from a single replicate.*

	t [min]	2 [mM]	Nonanoic acid [mM]	2a [mM]	2c [mM]
***Msp AlkB* I238V**	0	3.33	0.00	0.00	n.d.
	15	0.41	0.04	0.12	
	30	0.41	0.09	0.30	
	45	0.43	0.13	0.41	
	60	0.45	0.17	0.54	
	120	0.53	0.34	0.94	0.05
	240	0.13	0.56	1.27	0.14
	1440	0.00	0.49	0.69	0.41

*Table 22 – Data from biotransformations of **2** with Msp AlkB F169I. The average concentrations of the substrate, (side-)products and the corresponding standard deviations listed were derived from a single replicate.*

	t [min]	2 [mM]	Nonanoic acid [mM]	2a [mM]	2c [mM]
***Msp AlkB* F169I**	0	2.65	0.00	0.00	0.00
	15	0.65	0.02	0.06	0.05
	30	0.50	0.06	0.13	0.07
	45	0.49	0.09	0.18	0.08
	60	0.51	0.14	0.24	0.10
	120	0.53	0.30	0.35	0.11
	240	0.25	0.58	0.44	0.17

*Table 23 – Data from biotransformations of **2** with Msp AlkB F169V. The average concentrations of the substrate, (side-)products and the corresponding standard deviations listed were derived from a single replicate.*

	t [min]	2 [mM]	Nonanoic acid [mM]	2a [mM]	2c [mM]
***Msp AlkB* F169V**	0	2.64	0.00	0.00	0.00
	15	0.71	0.05	0.09	0.05
	30	0.62	0.09	0.14	0.08
	45	0.64	0.16	0.15	0.11
	60	0.64	0.21	0.15	0.12
	120	0.60	0.46	0.17	0.29
	240	0.06	0.70	0.09	0.56

*Table 24 – Data from biotransformations of **2** with Msp AlkB* F169L/I238V*. The average concentrations of the substrate, (side-)products and the corresponding standard deviations listed were derived from a single replicate.*

	t [min]	2 [mM]	Nonanoic acid [mM]	2a [mM]	2c [mM]
***Msp AlkB* F169L/I238V**	0	2.48	0.00	0.00	n.d.
	15	0.57	0.03	0.15	
	30	0.48	0.08	0.32	
	45	0.51	0.13	0.47	
	60	0.46	0.18	0.61	
	120	0.12	0.33	0.97	0.09
	240	0.00	0.38	0.79	0.11

*Table 25 – Data from biotransformations of **2** with Msp AlkB T141A. The average concentrations of the substrate, (side-)products and the corresponding standard deviations listed were derived from a single replicate.*

	t [min]	2 [mM]	Nonanoic acid [mM]	2a [mM]	2c [mM]
***Msp AlkB* T141A**	0	2.17	0.00	0.00	n.d.
	15	0.59	0.03	0.13	
	30	0.45	0.07	0.20	
	45	0.45	0.12	0.31	
	60	0.47	0.16	0.40	
	120	0.25	0.33	0.78	0.06
	240	0.00	0.44	0.78	0.14

*Table 26 – Data from the biotransformation of **2** with Msp AlkB wild type at a cell density of 2.2 g_{CDW} L^{-1}. The average concentrations of the substrate, (side-)products and the corresponding standard deviations listed were derived from a single replicate.*

	t [min]	2 [mM]	Nonanoic acid [mM]	2a [mM]	2c [mM]
***Msp AlkB* WT**	0	2.22	0.00	0.00	n.d.
	15	0.47	0.06	0.13	
	30	0.49	0.13	0.28	
	45	0.53	0.20	0.44	
	60	0.45	0.28	0.58	
	120	0.03	0.42	0.66	

*Table 27 - Data from the biotransformation of **2** with Msp AlkB I238V at a cell density of 2.2 g_{CDW} L^{-1}. The average concentrations of the substrate, (side-)products and the corresponding standard deviations listed were derived from a single replicate.*

	t [min]	2 [mM]	Nonanoic acid [mM]	2a [mM]	2c [mM]
***Msp AlkB* I238V**	0	2.27	0.00	0.00	n.d.
	15	0.48	0.08	0.27	
	30	0.48	0.15	0.54	
	45	0.35	0.22	0.79	
	60	0.10	0.28	0.96	
	120	0.00	0.33	0.79	0.03

*Table 28 – Data from the biotransformation of **2** with Msp AlkB wild type at a cell density of 3.1 g_{CDW} L^{-1}. The average concentrations of the substrate, (side-)products and the corresponding standard deviations listed were derived from a single replicate.*

	t [min]	2 [mM]	Nonanoic acid [mM]	2a [mM]	2c [mM]
***Msp AlkB* WT**	0	2.18	0.00	0.00	n.d.
	15	0.70	0.11	0.20	
	30	0.55	0.22	0.45	
	45	0.22	0.31	0.67	
	60	0.11	0.36	0.71	
	120	0.00	0.43	0.55	
	1440	0.00	0.41	0.12	0.09

*Table 29 – Data from the biotransformation of **2** with Msp AlkB W60S at a cell density of 3.1 g_{CDW} L^{-1}. The average concentrations of the substrate, (side-)products and the corresponding standard deviations listed were derived from a single replicate.*

	t [min]	2 [mM]	Nonanoic acid [mM]	2a [mM]	2c [mM]
***Msp AlkB* W60S**	0	2.13	0.00	0.00	n.d.
	15	0.45	0.12	0.16	
	30	0.35	0.22	0.32	
	45	0.09	0.30	0.41	
	60	0.04	0.37	0.42	
	120	0.00	0.37	0.27	0.11
	1440	0.00	0.02	0.00	0.20

*Table 30 – Data from the biotransformation of **2** with Msp AlkB F169L at a cell density of 3.1 g_{CDW} L^{-1}. The average concentrations of the substrate, (side-)products and the corresponding standard deviations listed were derived from a single replicate.*

	t [min]	2 [mM]	Nonanoic acid [mM]	2a [mM]	2c [mM]
***Msp AlkB* F169L**	0	2.17	0.00	0.00	n.d.
	15	0.50	0.43	0.14	
	30	0.08	0.19	0.67	
	45	0.00	0.22	0.63	0.04
	60	0.00	0.22	0.52	0.07
	120	0.00	0.23	0.26	0.27
	1440	0.00	0.00	0.00	0.18

*Table 31 – Data from the biotransformation of **2** with Msp AlkB I238V at a cell density of 3.1 g_{CDW} L^{-1}. The average concentrations of the substrate, (side-)products and the corresponding standard deviations listed were derived from a single replicate.*

	t [min]	2 [mM]	Nonanoic acid [mM]	2a [mM]	2c [mM]
***Msp AlkB* I238V**	0	2.42	0.00	0.00	n.d.
	15	0.64	0.13	0.38	
	30	0.18	0.22	0.73	
	45	0.01	0.26	0.77	
	60	0.00	0.27	0.71	
	120	0.00	0.27	0.42	0.18
	1440	0.00	0.00	0.00	0.19

8.2 Pentyl acetate (**4**)

*Table 32 – Summary of the data from biotransformations of **4** with Msp AlkB wild type at 1 g_{CDW} L^{-1}. The average concentrations of the substrate, products and the corresponding standard deviations listed were derived from triplicates.*

	t [min]	4		4a		4c	
		Mean [mM]	Std. Dev. [+/-]	Mean [mM]	Std. Dev. [+/-]	Mean [mM]	Std. Dev. [+/-]
***Msp AlkB* wildtype**	0	2.18	0.27	0.00	0.00		
	15	1.79	0.22	0.01	0.01		
	30	1.65	0.23	0.08	0.03		
	45	1.55	0.21	0.12	0.03	n.d.	
	60	1.42	0.18	0.17	0.03		
	120	0.96	0.12	0.32	0.04		
	240	0.42	0.10	0.70	0.01		

*Table 33 – Summary of the data from biotransformations of **4** with Msp AlkB W60S at 1 g_{CDW} L^{-1}. The average concentrations of the substrate, products and the corresponding standard deviations listed were derived from triplicates.*

	t [min]	4		4a		4c	
		Mean [mM]	Std. Dev. [+/-]	Mean [mM]	Std. Dev. [+/-]	Mean [mM]	Std. Dev. [+/-]
***Msp AlkB* W60S**	0	2.27	0.06	0.00	0.00		
	15	1.97	0.06	0.04	0.01		
	30	1.82	0.06	0.09	0.01		
	45	1.68	0.06	0.14	0.02	n.d.	
	60	1.58	0.04	0.20	0.01		
	120	1.02	0.02	0.38	0.07		
	240	0.42	0.07	0.76	0.06		

*Table 34 – Summary of the data from biotransformations of **4** with Msp AlkB F169L at 1 g_{CDW} L^{-1}. The average concentrations of the substrate, products and the corresponding standard deviations listed were derived from triplicates.*

	t [min]	4		4a		4c	
		Mean [mM]	Std. Dev. [+/-]	Mean [mM]	Std. Dev. [+/-]	Mean [mM]	Std. Dev. [+/-]
***Msp AlkB* F169L**	0	1.97	0.13	0.00	0.00		
	15	1.69	0.02	0.06	0.00		
	30	1.40	0.11	0.13	0.01		
	45	1.27	0.13	0.20	0.01	n.d.	
	60	1.12	0.06	0.29	0.02		
	120	0.47	0.08	0.59	0.01		
	240	0.63	0.44	0.76	0.15		

*Table 35 – Summary of the data from biotransformations of **4** with Msp AlkB I238V at 1 g_{CDW} L^{-1}. The average concentrations of the substrate, products and the corresponding standard deviations listed were derived from triplicates.*

	t [min]	4		4a		4c	
		Mean [mM]	Std. Dev. [+/-]	Mean [mM]	Std. Dev. [+/-]	Mean [mM]	Std. Dev. [+/-]
***Msp AlkB* I238V**	0	1.95	0.10	0.00	0.00	n.d.	
	15	1.68	0.07	0.04	0.01		
	30	1.45	0.12	0.10	0.01		
	45	1.26	0.26	0.16	0.02		
	60	1.23	0.19	0.23	0.04		
	120	0.69	0.28	0.51	0.09		
	240	0.67	0.29	0.75	0.06		

*Table 36 – Data from the biotransformation of **4** with Msp AlkB wild type at a cell density of 2.2 g_{CDW} L^{-1}. The average concentrations of the substrate, products and the corresponding standard deviations listed were derived from a single replicate.*

	t [min]	4 [mM]	4a [mM]	4c [mM]
***Msp AlkB* WT**	0	1.95	0.00	n.d.
	15	1.25	0.05	
	30	1.26	0.11	
	45	1.05	0.18	
	60	1.03	0.27	
	120	0.34	0.61	

*Table 37 – Data from the biotransformation of **4** with Msp AlkB I238V at a cell density of 2.2 g_{CDW} L^{-1}. The average concentrations of the substrate, products and the corresponding standard deviations listed were derived from a single replicate.*

	t [min]	4 [mM]	4a [mM]	4c [mM]
***Msp AlkB* I238V**	0	1.71	0.00	n.d.
	15	1.41	0.08	
	30	1.11	0.19	
	45	0.85	0.32	
	60	0.56	0.45	
	120	0.00	0.59	

*Table 38 – Data from the biotransformation of **4** with Msp AlkB wild type at a cell density of 3.1 g_{CDW} L^{-1}. The average concentrations of the substrate, products and the corresponding standard deviations listed were derived from a single replicate.*

	t [min]	4 [mM]	4a [mM]	4c [mM]
***Msp AlkB* wildtype**	0	1.10	0.00	n.d.
	15	3.38	0.19	
	30	1.10	0.36	
	45	0.00	0.47	
	60	3.79	0.58	
	120	0.00	0.71	
	1440	0.00	0.22	0.24

*Table 39 – Data from the biotransformation of **4** with Msp AlkB W60S at a cell density of 3.1 g_{CDW} L^{-1}. The average concentrations of the substrate, products and the corresponding standard deviations listed were derived from a single replicate.*

	t [min]	4 [mM]	4a [mM]	4c [mM]
***Msp AlkB* W60S**	0	2.47	0.00	n.d.
	15	2.45	0.22	
	30	1.27	0.40	
	45	1.09	0.56	
	60	0.70	0.64	
	120	0.06	0.90	
	1440	0.00	1.01	0.10

*Table 40 – Data from the biotransformation of **4** with Msp AlkB F169L at a cell density of 3.1 g_{CDW} L^{-1}. The average concentrations of the substrate, products and the corresponding standard deviations listed were derived from a single replicate.*

	t [min]	4 [mM]	4a [mM]	4c [mM]
***Msp AlkB* F169L**	0	0.58	0.00	n.d.
	15	8.84	0.20	
	30	3.34	0.45	
	45	0.15	0.54	
	60	0.00	0.21	0.07
	120	0.02	0.00	0.19
	1440	0.00	0.11	0.22

*Table 41 – Data from the biotransformation of **4** with Msp AlkB I238V at a cell density of 3.1 g_{CDW} L^{-1}. The average concentrations of the substrate, products and the corresponding standard deviations listed were derived from a single replicate.*

	t [min]	4 [mM]	4a [mM]	4c [mM]
***Msp AlkB* I238V**	0	2.01	0.00	n.d.
	15	1.53	0.41	
	30	2.82	0.73	
	45	0.78	1.07	
	60	0.00	0.66	
	120	0.00	0.33	0.41
	1440	0.00	0.29	0.62

8.3 Nonyl acetate (5)

*Table 42 – Summary of the data from biotransformations of **5** with Msp AlkB wild type at 1 g_{CDW} L^{-1}. The average concentrations of the substrate, products and the corresponding standard deviations listed were derived from triplicates.*

	t [min]	5		5a		5c	
		Mean [mM]	Std. Dev. [+/-]	Mean [mM]	Std. Dev. [+/-]	Mean [mM]	Std. Dev. [+/-]
***Msp AlkB* wild type**	0	1.93	0.38	0.00	0.00		
	15	0.29	0.03	0.07	0.02		
	30	0.17	0.02	0.14	0.03		
	45	0.17	0.01	0.22	0.02	n.d.	
	60	0.18	0.01	0.29	0.03		
	120	0.22	0.01	0.56	0.07		
	240	0.19	0.12	0.90	0.06		

*Table 43 – Summary of the data from biotransformations of **5** with Msp AlkB W60S at 1 g_{CDW} L^{-1}. The average concentrations of the substrate, products and the corresponding standard deviations listed were derived from triplicates.*

	t [min]	5		5a		5c	
		Mean [mM]	Std. Dev. [+/-]	Mean [mM]	Std. Dev. [+/-]	Mean [mM]	Std. Dev. [+/-]
***Msp AlkB* W60S**	0	1.50	0.56	0.00	0.00		
	15	0.25	0.07	0.03	0.00		
	30	0.13	0.04	0.06	0.01		
	45	0.12	0.04	0.10	0.02	n.d.	
	60	0.09	0.01	0.13	0.03		
	120	0.10	0.01	0.25	0.06		
	240	0.14	0.10	0.47	0.06		

*Table 44 – Summary of the data from biotransformations of **5** with Msp AlkB F169I at 1 g_{CDW} L^{-1}. The average concentrations of the substrate, products and the corresponding standard deviations listed were derived from triplicates.*

	t [min]	5		5a		5c	
		Mean [mM]	Std. Dev. [+/-]	Mean [mM]	Std. Dev. [+/-]	Mean [mM]	Std. Dev. [+/-]
***Msp AlkB* F169L**	0	1.81	0.49	0.00	0.00		
	15	0.28	0.05	0.10	0.00		
	30	0.17	0.04	0.19	0.01		
	45	0.15	0.01	0.27	0.01	n.d.	
	60	0.16	0.02	0.35	0.03		
	120	0.18	0.08	0.63	0.03		
	240	0.09	0.07	0.86	0.16		

*Table 45 – Summary of the data from biotransformations of **5** with Msp AlkB I238V at 1 g_{CDW} L^{-1}. The average concentrations of the substrate, products and the corresponding standard deviations listed were derived from triplicates.*

	t [min]	5		5a		5c	
		Mean [mM]	Std. Dev. [+/-]	Mean [mM]	Std. Dev. [+/-]	Mean [mM]	Std. Dev. [+/-]
***Msp AlkB* I238V**	0	1.66	0.53	0.00	0.00	n.d.	
	15	0.32	0.11	0.09	0.01		
	30	0.18	0.03	0.17	0.02		
	45	0.15	0.01	0.24	0.04		
	60	0.17	0.01	0.33	0.07		
	120	0.17	0.09	0.67	0.14		
	240	0.10	0.14	0.92	0.21		

*Table 46 – Data from the biotransformation of **5** with Msp AlkB wild type at a cell density of 3.1 g_{CDW} L^{-1}. The average concentrations of the substrate, products and the corresponding standard deviations listed were derived from a single replicate.*

	t (min)	5 [mM]	5a [mM]	5c [mM]
***Msp AlkB* wildtype**	0	1.65	0.00	n.d.
	15	0.27	0.28	
	30	0.32	0.46	
	45	0.22	0.60	
	60	0.27	0.82	
	120	0.03	0.79	0.03
	1440	0.00	0.66	0.05

*Table 47 – Data from the biotransformation of **5** with Msp AlkB W60S at a cell density of 3.1 g_{CDW} L^{-1}. The average concentrations of the substrate, products and the corresponding standard deviations listed were derived from a single replicate.*

	t (min)	5 [mM]	5a [mM]	5c [mM]
***Msp AlkB* W60S**	0	0.92	0.00	n.d.
	15	0.16	0.15	
	30	0.27	0.32	
	45	0.12	0.43	
	60	0.05	0.47	
	120	0.00	0.64	0.08
	1440	0.06	1.00	0.10

*Table 48 – Data from the biotransformation of **5** with Msp AlkB F169L at a cell density of 3.1 g_{CDW} L^{-1}. The average concentrations of the substrate, products and the corresponding standard deviations listed were derived from a single replicate.*

	t (min)	5 [mM]	5a [mM]	5c [mM]
***Msp AlkB* F169L**	0	2.27	0.00	n.d.
	15	0.22	0.30	
	30	0.32	0.45	
	45	0.33	0.62	0.04
	60	0.21	0.68	0.07
	120	0.03	0.60	0.13
	1440	0.00	0.55	0.22

*Table 49 – Data from the biotransformation of **5** with Msp AlkB I238V at a cell density of 3.1 g_{CDW} L^{-1}. The average concentrations of the substrate, products and the corresponding standard deviations listed were derived from a single replicate.*

	t (min)	5 [mM]	5a [mM]	5c [mM]
***Msp AlkB* I238V**	0	2.29	0.00	n.d.
	15	0.24	0.42	
	30	0.25	0.80	
	45	0.11	0.86	
	60	0.06	0.92	
	120	0.00	0.91	0.06
	1440	0.00	0.39	0.20

8.4 Dodecyl acetate (6)

*Table 50 – Data from the biotransformation of **6** with Msp AlkB W60S at a cell density of 3.1 g_{CDW} L^{-1}. The average concentrations of the substrate, products and the corresponding standard deviations listed were derived from three replicates.*

		6		6a	
	t (min)	**Mean [mM]**	**Std. Dev. [+/-]**	**Mean [mM]**	**Std. Dev. [+/-]**
Msp AlkB W60S	0	1.45	0.06	0.00	0.00
	15	0.13	0.07	0.05	0.01
	30	0.05	0.02	0.06	0.01
	45	0.03	0.01	0.06	0.01
	60	0.08	0.05	0.09	0.03
	120	0.16	0.07	0.26	0.08
	240	0.29	0.03	0.29	0.01

8.5 Negative controls

*Table 51 – Results from the negative control for **2** incubated with cells expressing the inactive variant H278A for 24 hours. Also, the substrate loss and hydrolysis to nonanoic acid quantified in percent are shown.*

	2		**Nonanoic acid**	
Time [h]	**Mean [mM]**	**Std. Dev. [+/-]**	**Mean [mM]**	**Std. Dev. [+/-]**
0	1.54	0.12	0.00	0.00
1	0.02	0.01	0.43	0.02
24	0.00	0.00	0.44	0.05
Loss [%]	99%		-	

*Table 52 – Results from the negative control for **4** incubated with cells expressing the inactive variant H278A for 24 hours. Also, the substrate loss quantified in percent is shown.*

	4	
Time	**Mean [mM]**	**Std. Dev. [+/-]**
0	2.28	0.13
1	2.02	0.05
24	1.76	0.14
Loss [%]	11%	

*Table 53 – Results from the negative control for **5** incubated with cells expressing the inactive variant H278A for 24 hours. Also, the substrate loss quantified in percent is shown.*

	5	
Time	**Mean [mM]**	**Std. Dev. [+/-]**
0	1.42	0.07
1	0.21	0.04
24	0.19	0.05
Loss [%]	86%	

*Table 54 – Results from the negative control for **6** incubated with cells expressing the inactive variant H278A for 24 hours. Also, the substrate loss quantified in percent is shown.*

	6	
Time	**Mean [mM]**	**Std. Dev. [+/-]**
0	0.93	0.12
1	0.19	0.01
24	0.25	0.03
Loss [%]	80%	

*Table 55 – Results from the negative control for **2** incubated in reaction buffer without cells for 4 hours. Also, the substrate loss quantified in percent is shown.*

	2	
Time [h]	**Mean [mM]**	**Std. Dev. [+/-]**
0	0.66	0.31
1	0.13	0.01
24	0.12	0.01
Loss [%]	81%	

*Table 56 – Results from the negative control for **4** incubated in reaction buffer without cells for 4 hours. Also, the substrate loss quantified in percent is shown.*

	4	
Time [h]	**Mean [mM]**	**Std. Dev. [+/-]**
0	2.40	0.03
1	2.06	0.02
24	1.75	0.19
Loss [%]	14%	

*Table 57 – Results from the negative control for **5** incubated in reaction buffer without cells for 4 hours. Also, the substrate loss quantified in percent is shown.*

	5	
Time [h]	**Mean [mM]**	**Std. Dev. [+/-]**
0	0.87	0.21
1	0.05	0.01
24	0.06	0.02
Loss [%]	**94%**	

*Table 58 – Results from the negative control for **6** incubated in reaction buffer without cells for 4 hours. Also, the substrate loss quantified in percent is shown.*

	6	
Time [h]	**Mean [mM]**	**Std. Dev. [+/-]**
0	1.00	0.12
1	0.06	0.03
24	0.03	0.01
Loss [%]	94%	